2002

Estuarine suspended aggregate dynamics and characteristics

David C. Fugate
College of William and Mary - Virginia Institute of Marine Science

ESTUARINE SUSPENDED AGGREGATE DYNAMICS AND CHARACTERISTICS

A Dissertation

Presented to

The Faculty of the School of Marine Science

The College of William and Mary in Virginia

In Partial Fulfillment

Of the Requirements for the Degree of

Doctor of Philosophy

by David C. Fugate

2002

APPROVAL SHEET

This dissertation is submitted in partial fulfillment of

the requirements for the degree of

Doctor of Philosophy

David C. Fugate

Approved, March 2002

Carl T. Friedrichs
Committee Chairman/Advisor

John M. Brubaker

Steven A. Kuehl

Walter I. Priest

Patricia L. Wiberg
University of Virginia
Charlottesville, Virginia

TABLE OF CONTENTS

ACKNOWLEDGEMENTS

This manuscript benefited from critical review by the dissertation committee members, Pat Wiberg, John Brubaker, Steve Kuehl, and Walter Priest, and especially from the support and guidance from my advisor, Carl Friedrichs. Field work was coordinated by Grace Battisto and aided by Wayne Reisner, Charles Madchen, Todd Nelson, and Bob Gammisch. Tom Chisholm also provided invaluable assistance. I am very grateful to all of these people for their help.

Funding for data collection was provided by the Office of Naval Research through the Harbor Processes Program (grant N00014-93-1-0986). Additional funding for data analysis was provided by the EPA through the Chesapeake Bay Environmental Effects Committee and by the National Science Foundation Division of Ocean Sciences (grant OCE-9984941 and grant OCE-0002529).

I would also like to thank my wife, Alayde Barbosa, for her forbearance.

LIST OF TABLES

LIST OF FIGURES

ABSTRACT

The research presented in this study is motivated by the need to improve prediction of sediment transport in estuaries. A novel application of the Acoustic Doppler Velocimeter (ADV) in the lower Chesapeake Bay is shown to estimate in-situ particle fall velocity at a single point without affecting the ambient turbulence. Acoustic backscatter from the ADV proved to be the best estimator of mass concentrations due to its apparent insensitivity to the size or density of muddy aggregates. Fall velocities are estimated analytically from a balance of settling and diffusive flux gradients using two methods, one employing Reynolds concentration flux, and the other estimating eddy diffusivity using the von-Karman Prandtl equation. Single elevation estimates of fall velocity using the ADV to estimate Reynolds concentration flux produced the best estimates of fall velocity, which are on the order of 1 mm/s.

A novel method is presented to measure TKE production using a profiling ADV instrument that has been contaminated by boat motion. The relative importance of physical processes that determine particle size distributions differs in three mid-Atlantic U.S.A. estuaries (York R., Elizabeth R., Chesapeake Bay) with different hydrodynamics and benthic characteristics as well as in different depth regimes within each estuary. Surface particle size dynamics in all of the estuaries are affected by irregular advection events. Middepth regions in the energetic estuaries are controlled tidally by the combined processes of TKE production decreasing particle size and differential settling increasing particle size. Middepth regions in the low energy estuary are controlled by irregular resuspension and trapping at the pycnocline of large low density particles. Bottom regions in all estuaries are most strongly influenced by resuspension, tidally in the energetic estuaries and irregularly in the low energy estuary.

The interrelationships between metal concentrations, particle size, percent fixed solids (PFS), chlorophyll a, and molar Carbon to Nitrogen (C/N) ratios of suspended sediment are investigated in a heavily industrialized and polluted estuary, the Elizabeth R., VA. The relationship between PFS, C/N and aggregate size are also investigated in a relatively energetic, high concentration, and undisturbed estuary, the York. R., VA. Standard paradigms of contaminant concentration relationships with particle size and particle constituents were not supported in the low energy, low concentration suspended sediments of the Elizabeth R. Chlorophyll a values varied seasonally, but were not related to grain size or metal concentrations. Chlorophyll a values tended to be higher at the surface and upstream from the study site. C/N was vertically homogenous and varied significantly over timescales longer than the tidal period. C/N was not related to grain size, metal concentrations, PFS or chlorophyll a values. C/N is lower downstream of the study site, suggesting that the source of the higher organic constituent material downstream is not marine phytoplankton. Metal concentrations were not related to median grain sizes, nor to tidally varying hydrodynamics, but showed a strong tendency to be high at surface and middepth during stratified conditions. It is speculated that most net transport of trace metals in the Elizabeth R. occurs in the dissolved or colloidal phase and ultimately depends on the hydrodynamics of the system. In contrast to the Elizabeth R., measures of organic content from PFS levels and C/N in the York R. were related to aggregate size, consistent with standard paradigms. Lower PFS levels and C/N were associated with larger size aggregates.

ESTUARINE SUSPENDED AGGREGATE DYNAMICS AND CHARACTERISTICS

GENERAL INTRODUCTION

The research presented in this study is motivated by the need to improve prediction of sediment transport in estuaries. Understanding and predicting sediment transport is important to numerous societal and scientific issues. Many contaminants such as PCB's, PAH's, and heavy metals have a high affinity for suspended particles in estuaries. Smaller particles are more efficient at scavenging contaminants than larger particles, and particles with a high degree of organic matter may also be better scavengers. Understanding the particle size distributions, constituents, and transport of the particles helps understand the fate and transport of the contaminants. Prediction of sediment transport is crucial to many waterways engineering projects, from choosing dredge spoil locations to developing marinas. Sediment transport also affects the ecology in an estuary, over large spatial scales as well as in localized regions such as the estuarine turbidity maximum. Deposition patterns and processes interact with benthic flora and fauna to help determine the benthic environment of the estuary. Patterns of deposition also determine the stratigraphy of a region, and understanding contemporary sedimentation processes helps decipher from sediment cores the paleo processes and environments that may have existed in a region.

A simple along-channel equation for predicting sediment transport is:

$$\frac{\partial C}{\partial t} + \frac{\partial (uC)}{\partial x} - w_s \frac{\partial C}{\partial z} - \frac{\partial}{\partial z}\left(A_z \frac{\partial u}{\partial z} \right) = 0$$

where u is the along channel velocity, C is the concentration, w_s is the settling velocity of the particles, and A_z is the eddy diffusivity. Hydrodynamic models can predict u, and

reasonable estimates of the eddy diffusivity can be made. But development of successful sediment transport models in estuaries is most often hampered by a lack of knowledge of the settling velocity of the particles. The settling velocity of particles is often estimated by Stoke's law:

$$w_s = \frac{1}{18}\frac{(\rho'-\rho)gD^2}{\mu}$$

where ρ' is the density of the particle and D is the particle diameter. The other parameters in the equation (g is gravity, ρ is the water density, and μ is viscosity) are more or less constant. There is an inverse relationship between an estuarine particle's size and density. As aggregate particles grow, the constituent particles become more loosely bound to each other, and the overall aggregate becomes less dense; the opposite happens as the particles disaggregate. This aggregation and disaggregation of the particles may occur over very short time scales.

The difficulty in measuring the density and size of estuarine aggregates lies not only in the short timescales in which they change, but also in their fragility. Aggregates collected in a water bottle are likely to change size as they are removed from the ambient hydrodynamic conditions. Consequently, aggregates are best measured with instruments deployed in situ.

The first chapter of this thesis is focused on methods to measure the characteristics of suspended sediment in estuaries. It explores the use and response of acoustic, optic, and laser instruments deployed in situ. Each of these instruments respond to different characteristics of the particles and measure different parameters. The responses of the different instruments are compared and evaluated with regard to their ability to measure suspended sediment mass concentration and particle size. In addition, an indirect method of estimating the settling velocity of aggregates is presented.

The second chapter examines in detail the processes that affect aggregation and disaggregation in partially mixed estuaries. Three estuaries that have different levels of hydrodynamic energy and different benthic habitats are compared. The first estuary is the York R. VA, which is an energetic estuary with a reduced benthic faunal community.

The second study site is in the lower Chesapeake Bay at the Cherrystone Flats region. This area is moderately energetic but has a rich benthic community. The last study site to be considered is the Elizabeth R., VA. This estuary is a very low energy system, and because of its high levels of toxins and regular dredging routine has very little benthic fauna. It will be seen that the physical and biological environments of these estuaries help determine the aggregation processes and the particle size distributions. In addition, within each estuary, variations in the dominant processes occur within different depth regimes.

The last chapter examines the constituents of estuarine aggregates and their relationship to particle size. Specifically, the factors that cause the quality and quantity of organic matter in the aggregates to vary are examined. In the highly contaminated Elizabeth R., variations in particulate trace metal concentrations are examined. These results will show that factors that are traditionally considered important in undisturbed well mixed estuaries are different in the low energy partially mixed environment of the heavily developed Elizabeth R.

Chapter 1. Determining Concentration and Fall Velocity of Estuarine Particle Populations Using ADV, OBS and LISST

This chapter has been accepted for publication by Continental Shelf Research with authors D. C. Fugate and C. T. Friedrichs

ABSTRACT

In describing suspended sediment conditions in the lower Chesapeake Bay, Virginia, U.S.A., this paper reports and develops methods for distinguishing multiple particle populations in the bottom boundary layer of estuaries in general. In addition, a novel application of the Acoustic Doppler Velocimeter (ADV) is shown to estimate in situ particle fall velocity at a single point without affecting the ambient turbulence. In situ estimates of suspended sediment concentration from ADV, Optical Backscatter (OBS), and Laser In Situ Scattering and Transmissometry (LISST) instruments are compared with gravimetrically determined mass concentrations from pumped water samples. In this environment, acoustic backscatter from the ADV proved to be the best estimator of mass concentrations due to its apparent insensitivity to the size or density of muddy aggregates. The concentration estimates and the relative sensitivities of the instruments to particle size and density combined with size distribution information from the LISST reveal the characteristics of multiple particle populations in the bottom boundary layer. Two rapidly settling sediment populations are suggested with similar fall velocities but distinct critical erosion stresses. A slowly settling background population is also identified whose concentration varies over meteorological time scales. Fall velocities are estimated analytically from a balance of settling and diffusive flux gradients using two methods, one employing Reynolds concentration flux, and the other estimating eddy diffusivity using the von-Karman Prandtl equation. Comparison of the local change and advective terms in the solute transport equation to the magnitude of the settling term suggests that a balance between the settling and resuspension term is a good first order approximation at this site, validating the indirect method for estimating settling velocity. Single elevation estimates of fall velocity using the ADV to estimate Reynolds concentration flux produced the best estimates of fall velocity which are on the order of 1 mm/s.

INTRODUCTION

A thorough understanding of sediment transport in estuaries is crucial to the management of multiple societal issues ranging from commercial fisheries to contaminant transport and harbor maintenance (Canuel and Zimmerman, 1999; Latimer et al., 1999, Manning and Dyer, 1999). While the general form of the equations for suspended sediment transport might be well described, key inputs to these equations remain elusive, including the temporally varying, population dependent particle fall velocity (Lynch et al., 1994; Hill et al., 1998). Estuarine particles are complicated aggregates of mineral and organic materials of different sizes, densities, porosities and degrees of stickiness (Eisma et al., 1991, Fettweis et al., 1998; Jago and Bull, 2000). Equations for sediment transport are typically applied to specific size classes or other classes of particle characteristics such as density (Lynch et al., 1994; Manning and Dyer, 1999). Although suspended sediment concentrations in estuaries are indeed composed of multiple populations of size classes and constituents, these populations are difficult to distinguish in practice. Not only are fragile flocculants in the water column difficult to measure, but their characteristics potentially change on short time scales with changes in turbulence in the water column and also on longer time scales as the dominant source and type of primary particles change (van Leussen, 1994; Eisma et al., 1997; Fettweis et al., 1998). In describing suspended sediment conditions in the lower Chesapeake Bay, Virginia, U.S.A., this paper reports and develops methods for distinguishing multiple particle populations in the bottom boundary layer of estuaries in general, using estimates of particle size, concentration and fall velocity. In addition, a novel application of the Acoustic Doppler Velocimeter (ADV) is shown to estimate in-situ particle fall velocity without affecting the ambient turbulence.

The difficulties of measuring the fall velocity of fragile flocs whose densities may change with their changing diameter are well documented (e.g. Eisma et al., 1991; Dyer

et al., 1996; Manning and Dyer, 1999; Van Leussen, 1999). Most attempts to directly measure the settling velocities of estuarine particles use either Owen tube type calculations (e.g., Van Leussen, 1999; Jones and Jago, 1996) or in situ, on board, or laboratory settling chambers in conjunction with a still (Syvitski et al 1995; Knowles and Wells, 1996) or video camera (Sternberg et al., 1996; Manning and Dyer, 1999). Methods which isolate particles in settling tubes alter the turbulence which may change the particle size and fall velocity due to enhanced flocculation. However, settling velocities of particles may also be estimated indirectly through analytical techniques (e.g. Kawanisi, 1997, Lynch and Agrawal, 1991). The method applied here has advantages over previous applications of the diffusion-settling balance because it measures vertical turbulent sediment flux directly rather than relying on a separate estimate of eddy diffusivity.

INSTRUMENTATION FOR MEASURING SUSPENDED SEDIMENT CONCENTRATION

Optical Backscatter and Transmission

Optical instruments such as optical back scatter (OBS) sensors and transmissometers have been used to measure suspended sediment concentrations in situ for many years. During that time their sensitivity to the size distribution of the sediment has been demonstrated theoretically as well as empirically (e.g. Baker and Lavell, 1984; Ludwig and Hanes, 1990; Wells and Kim, 1991; Gibbs and Wolansky, 1992; Green and Boon, 1993; Battisto et al., 1999; Lynch and Agrawal, 1991). Transmissometers measure the attenuation of a transmitted light beam along a fixed path length. Optical backscatter sensors work by emitting a light beam and registering the amount which is scattered back to a light sensor mounted adjacent to the transmitter. At moderate concentrations, the aggregate cross-sectional area of the suspended particles directly governs how much light will be transmitted or backscattered. Thus in quantifying turbidity, both of these instruments effectively measure total grain cross-sectional area per unit area (A) rather than mass concentration, where backscatter is proportional to A and transmission is proportional to 1-A. At sufficiently high concentrations, one must also account for varying degrees of multiple scattering and absorption (Kineke and Sternberg, 1992).

To lowest order, the total cross-sectional area of suspended sediment particles per unit volume scales as

$$A = \sum_n A_n \sim \sum_n N_n (d_n)^2 \qquad (1)$$

where N is the number of particles, d is diameter and n indicates size class. The volume concentration in each size class (C_{Vn}) scales as

$$C_{Vn} \sim N_n (d_n)^3 \tag{2}$$

Eliminating N, we then have

$$A \sim \sum_n \frac{C_{Vn}}{d_n} \tag{3}$$

and it can be seen that the response of transmissometer and OBS are both directly proportional to the particle volume concentration and inversely proportional to the particle diameter. This dependence on size distribution has resulted in poor calibration relationships between optical instrument outputs and field obtained gravimetric analyses when the size distribution varies over time, a condition which is common in estuarine environments.

Acoustic Backscatter

In the last decade much work has been done to apply acoustic backscatter in measuring particle concentrations (e.g., Hay and Sheng, 1992; Thorne et al., 1993; Thevenot and Kraus, 1993; Lynch et al., 1994; Vincent and Downing, 1994; Kawanise and Yokosi, 1997). These instruments transmit pulses of sound which are scattered back by particles in the water column. This acoustic backscatter is then registered by a pressure sensor. In a manner somewhat analogous to backscatter of light, the intensity of the backscattered pressure due to suspended particles is given by (Vincent and Downing, 1994)

$$I \sim \sum_n \frac{C_n f_n}{d_n} \tag{4}$$

where f_n is a "form factor" which describes the backscattering strength of the nth size class and is a complex function of grain size, shape, elasticity and density. At relatively low concentrations and a fixed distance from the transducer, attenuation and spreading can be assumed constant and multiple scattering can be neglected. d_n again appears in the denominator because backscatter is proportional to a summation of individual particle cross-sections. In this case, however, the presence of d_n in the denominator of Eq. (4) is overwhelmed by the sensitivity of f_n to d_n. The sensitivity of f_n to d_n results from the relatively large wavelength of sound relative to the diameter of the particles. (This is not an issue for backscatter or transmission of light because the wavelength of light is small compared to the aggregated diameter of most estuarine particles.) The behavior of f_n^2/d_n for naturally aggregated silts and clays is unknown, although laboratory investigation of disaggregated irregularly shaped particles suggests f_n^2/d_n is an increasing function of d_n over the range of 1 to 100 microns (Sheng and Hay,1988; Lynch et al., 1994). Given the present uncertainties, however, a reasonable approach in applying acoustic backscatter to estuarine particles is to infer f_n^2/d_n based on in situ calibration. Reasonable success has been achieved by others who have applied acoustic backscatter to muddy environments utilizing similarly empirical calibrations (Thevenot and Kraus, 1993; Kawanisi and Yokosi, 1997; Lynch et al., 1994).

Laser diffraction

Laser diffraction technology has been used and evaluated in various instruments to measure the size spectra of suspended particles (Bale et al., 1989, 1996; Agrawal and Pottsmith, 1994, 2000; Lynch et al., 1994; Phillips et al., 1998; Beuselinck et al., 1999; Traykovski, 1999). The LISST 100 (Laser In Situ Scattering and Transmissometry) instrument developed by Sequoia Scientific Inc. measures volume concentrations and size spectra using laser diffraction as well as measuring beam transmission. It works by measuring the intensity of scattered laser light at different angles with a series of concentric ring detectors. The intensities of light gathered by the ring detectors are inverted to estimate the particle area concentrations for 8 multiple size categories ranging from 5 to 500 μm in the version of the model 100 used in this study. These estimates,

along with an empirically determined volume calibration constant, then provide a volume concentration spectrum over this same size range. The LISST's transmissometer detector is located in the center of the ring detectors and measures the light which is not scattered or absorbed. Extensive descriptions of the instrument and its operation principles can be found in Agrawal and Pottsmith (1994, 2000).

The LISST works well in resolving unimodal silicate particle distributions (Traykovski et al., 1999; Agrawal and Pottsmith, 2000; Battisto, 2000). Traykovski et al. (1999) also found that the LISST resolved multiple narrow peaks in suspended sand distributions which were separated by 1 phi or more. More recent tests by Agrawal and Pottsmith (2000) with an improved inversion algorithm have shown higher resolution of multimodal distributions of glass spheres. However, the primary particle populations and loose aggregates found in biologically productive estuaries are more complex than sand particles with respect to their refractive indices and size distributions, which may be multimodal with wide and narrow peaks or may be uniform (Krank et al., 1996). The inversion approach is an inherently underdetermined problem, so the resulting size distribution is approximate. Multiple peaks in the actual size distribution may be blurred and single peaks in the real distribution can produce non-existent aliases (Mikkelson, 2000). The presence of particles finer and coarser than the measured size range also affect the estimated size distributions from the LISST (Traykovski, 1999; Mikkelsen, 2000). An additional complication to estimating volume concentrations in estuaries with the LISST is the difficulty of determining the volume calibration constant for estuarine particles because of their size-density dependence and fragility. Accurate measurements of aggregate sizes in estuarine environments may still best be made with video and still photographic techniques, while results from the LISST may be more successfully interpreted in a qualitative sense by examining relative changes in the size distributions and volume concentrations rather than relying on the exact values obtained from the instrument and the inversion results.

FIELD EXPERIMENT SITE AND METHODS

The field experiment reported here took place in August 1996 at the Cherrystone site in the southern Chesapeake Bay (Fig. 1-1). This site and the nearby Wolftrap site have been extensively studied with regard to benthic biology, and bed characteristics (e.g. Wright et al., 1987, 1992, 1997; Schaffner, 1990; Lee, 1995; Thompson ,2000; Thompson and Schaffner, 2000). The mean depth of the study site is 14 meters, mean tidal range is 0.6 meters, and salinities typically range from 17-23 ppt. The bed is soft and composed of fine sand and mud; disaggregated grain sizes from the top 5 mm collected in May 1994 were: very fine sand (50%), silt (33%), and clay (17%) (Lee, 1995). Seasonally, benthic organisms such as *Chaetopteris pergamentaceus* and *Euclymene zonalis* vigorously bioturbate the sediment. These organisms also provide the dominant bottom roughness (2-3 cm.) in the form of small hummocks and worm tubes (Wright et al., 1987). Lee (1995) studied bed erosion parameters at the Cherrystone site in May 1994. His field experiments employing an annular flume to determine critical shear stress (τ_{cr}) of the bottom sediment at the Cherrystone site were complicated by the surficial "fluff" layer, and were not conclusive, but appeared to give τ_{cr} between 0.10 and 0.12 Pa. In addition, there appeared to be sub-layers of the bed with lower τ_{cr} than overlying layers, instead of an expected monotonous increasing τ_{cr} with depth.

From August 26-28, 1996, two instrument pods were located along channel at the Cherrystone site. For a more detailed physical description of the instrument pod see Kim et al. (2000). Pod A was located at 37 degrees 13.98 mins N, and 76 degrees 5.01 mins West, and Pod B was located 650 meters seaward at 37 13.80 N 76 4.71 W. The pods contained a suite of Sontek acoustic Doppler velocimeters (ADV's), Marsh-McBirney electromagnetic current meters (EMCM's), Downing optical backscatter sensors

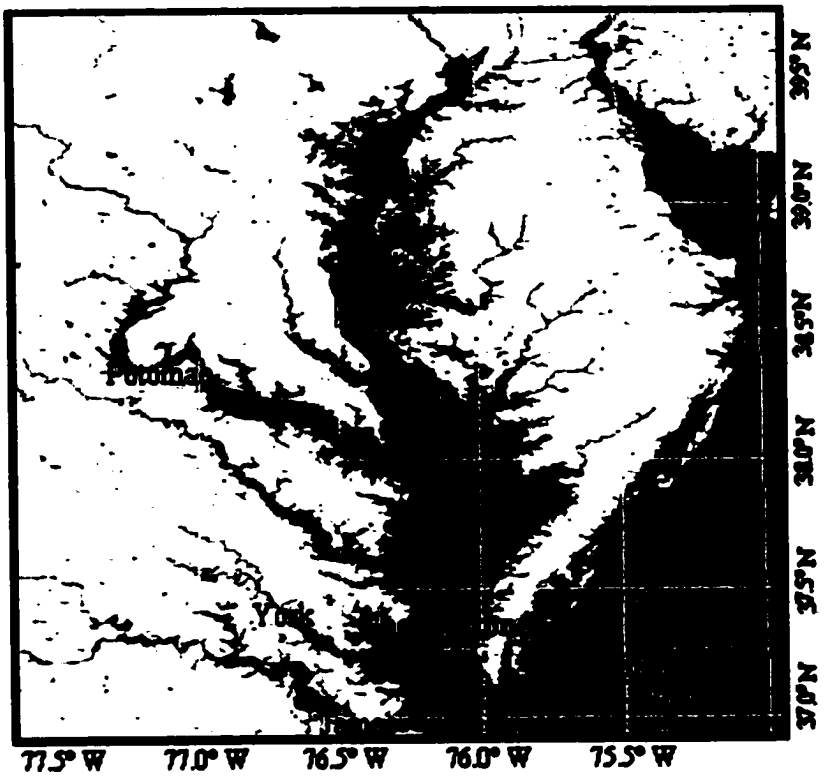

Fig. 1-1. Cherrystone study site location in the Southern Chesapeake Bay, VA, U.S.A.

(OBS's), and submersible pump intakes whose elevations and sampling intervals are presented in Table 1. Within 50 meters of Pod A, a profiler containing a Sequoia Science LISST 100 and an Applied Microsystems Laboratories STD 12plus was deployed about every 2 hours from the anchored R/V Langley. Hoses of 1.8 cm internal diameter led from the R/V Langley to the pump mounted on the profiler as well as the three pumps mounted on Pod A. These hoses were about 30 meters long and pumped at the rate of about 1 meter/s. Two liter bulk water samples were collected from each of the four hoses about every two hours. The shear in the hose and its length promote mixing within the hose and a more representative sample than would have been achieved by taking a two liter sample instantaneously in-situ, such as with a bottle sampler. Nevertheless, there is an unknown source of error related to temporal variation of suspended solids in the water column. Total suspended solids (TSS) were analyzed by passing a measured subsample through a 0.8 poresize glass fiber filter, followed by drying and weighing.

Table 1-1. Instrumentation

Pod A

Instrument	Elevation above bed (cm)	Sampling Interval
ADV	3	10 min. burst every 15 min.
ADV	23	
OBS	7	10 min. burst every 15 min.
	23	
	38	
	36	
	64	
Water pump	10	~ 2 hours
	25	
	40	

Pod B

Marsh McBirney	8	10 min. burst every 15 min.
	38	
	68	
	98	
OBS	8	10 min. burst every 15 min.
	21	
	34	
	65	
	94	

Profiler

LISST	10	~ 2 hours
Water pump	10	~ 2 hours
	200	

RESULTS AND DISCUSSION

Physical Environment

The along and cross channel current at 3 and 23 cm. above the bed (cmab) at the Cherrystone site are presented in Fig. 1-2a, with landward along channel defined as positive x. Currents from the ADV are rotated so that there is a minimum variance in the cross channel direction. Maximum along channel current speed at 23 cmab was about 30 cm/s on both flood and ebb. There was also a significant cross channel component to the current, especially during the transition from ebb to flood, with a maximum westward speed of 15.8 cm/s. Residual currents at 23 cmab over 5 tidal cycles were 0.4 cm/s landward along channel and 4.8 cm/s westward across channel.

The high frequency (5 Hz) velocity data from the ADV at two elevations can be used to estimate the friction velocity by several methods (Kim et al. 2000). Providing that the sensor is in the constant stress portion of the bottom boundary layer, a direct measure of the friction velocity at the bed can be determined using the near bed Reynolds stress:

$$u_* = \sqrt{-\overline{u'w'}}$$

where u' is the deviation from the burst averaged horizontal current and w' is the deviation from the burst averaged vertical component of the current. The horizontal velocity components for each 15 min burst were first rotated along the z axis so that minimum variance occurred in the cross channel dimension. The vertical and along channel components were then rotated along the y axis so that there was minimum variance in the vertical dimension.

Another common way to estimate u_* in the constant stress portion of a fully rough turbulent boundary layers is to use the von Karman-Prandtl equation:

$$\bar{u} = \frac{u_*}{\kappa} \ln\left(\frac{z}{z_0}\right)$$

where u bar is the mean horizontal current, κ is von Karman's constant = .41, z is the elevation above the bed, and z_0 is the hydraulic roughness. The "constant stress" log-layer is applicable in the portion of the bottom boundary layer where acceleration is much weaker than friction and stress is nearly equal to bottom stress. For a tidal boundary layer, the ratio of acceleration to friction scales as $\omega z^2/A_Z$, where $\omega \approx 1.4 \times 10^{-4}$ sec^{-1} is tidal radian frequency, A_Z is the eddy viscosity and z is elevation above the bed. A conservatively low estimate of A_Z for a partially stratified estuary is 10^{-3} m^2/s (e.g., Friedrichs and Hamrick, 1996). Thus friction is at least 10 times the magnitude of acceleration for heights above the bed lower than $z \approx sqrt(0.1A_Z/\omega) \approx 85$ cm. Even if A_Z were 10 times smaller, friction would still be 10 times the magnitude of acceleration at heights less than 27 cm. Assuming acceleration to be negligible, stress will be within 90% of bottom stress if measurements are made at a height above the bed no more than 1/10 of the total water depth, which at this location is a weaker constraint than that placed by acceleration. Best fit u_* was determined by a log profile for each of the 15 minute bursts using the burst averaged current speed from 3 and 23 cmab. Fig. 1-2b compares the time series of log profile and Reynolds stress estimates of u_*. Tidal straining of the density field favors enhanced stratification on ebb relative to flood, and consequently, a greater level of shear and higher stress is inferred by the log-profile method during ebb. However, the direct method of measuring shear stress with the Reynolds stress does not reflect this difference between tidal phases.

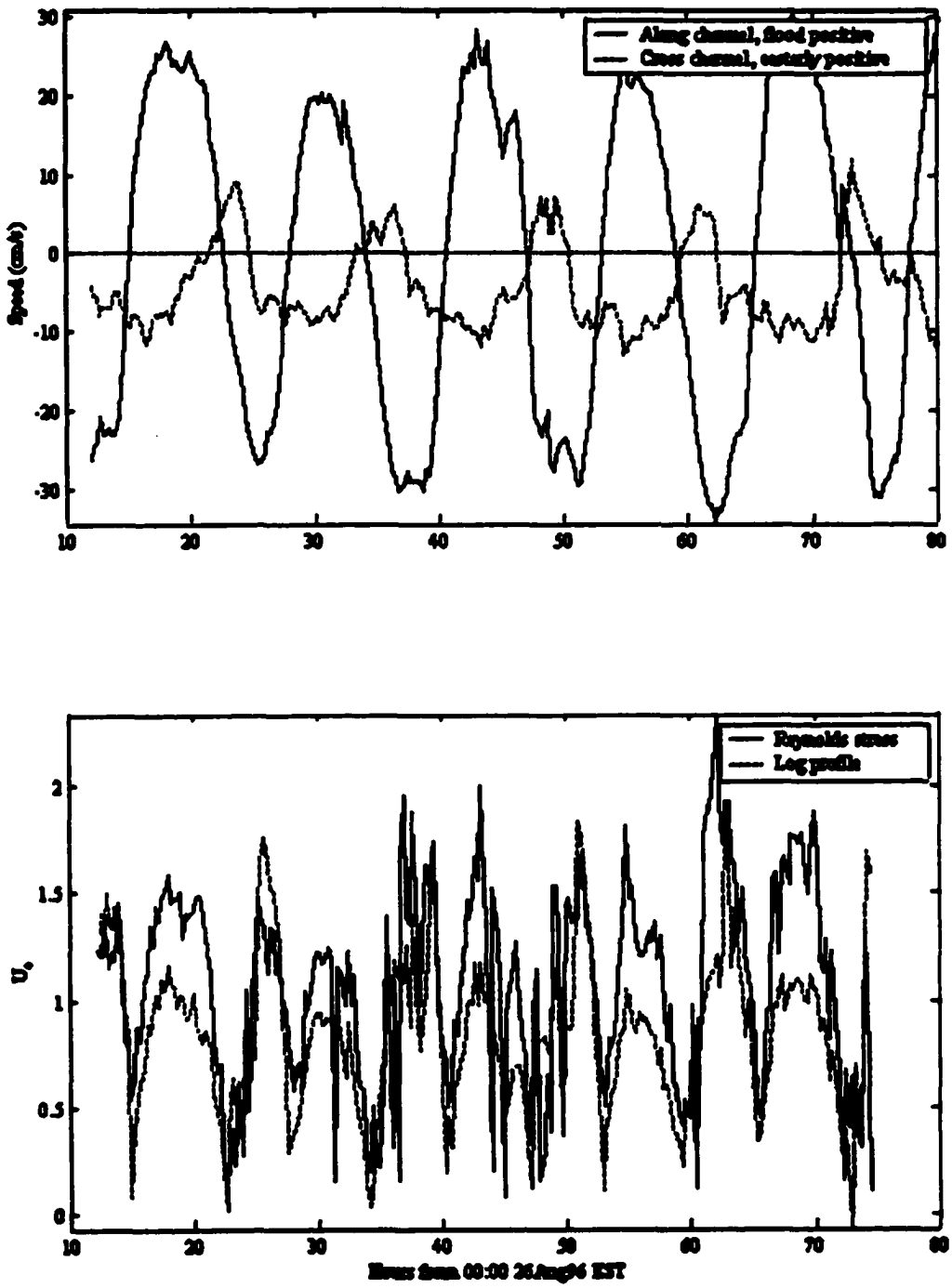

Fig. 1-2(a). Time series of current velocities at 23 cmab. Solid line is along channel current with flood positive, dashed line is across channel with easterly positive (b). Time series of friction velocity (u*) measured by the ADV. Solid line is Reynolds stress measured at 23 cmab, dashed line is from log profile at 3 and 23 cmab.

Suspended Sediment Concentration

Bulk Water Samples

Gravimetric analysis of bulk water samples collected from the tripod at depths of 10, 25 and 40 cmab yielded the total suspended sediment (TSS) concentrations shown in Fig. 1-3a. The mean standard error of the 4 duplicate split samples was 1.50 mg/l. Superimposed upon the regular tidal pattern of resuspension are higher peaks in concentration during the ebb/flood cycle between hours 35 and 44 (maximum of 72 mg/l at 10 cmab), and the ebb cycle around hour 62. During the peak concentrations of the first event, filters became clogged and some samples had to be discarded; some of the higher gravimetrically determined concentrations may be underestimated. A persistent minimum concentration of particles in the near-bed vertical profile, ranging from 15-22 mg/l during slack current periods, suggests the presence of a background population of particles which do not settle relative to the time scale of the tides. The regular tidal resuspension signal suggests a population of easily resuspendable benthic "fluff" with a very low critical shear stress. In addition to this easily resuspended population of sediment, the jump in concentration after hour 36 concomitant with the first high peak in friction velocity suggests the presence of a second population of rapidly settling sediment with an initial critical shear velocity for suspension of about 1.5 cm/s (equivalent to $\tau_{cr} \approx 0.23$ Pa).

Backscatter from ADV

Variations in the magnitude of the reflected sound pulse, or "backscatter" are recorded by the Sontek ADV in the form S_v (backscatter strength in dB.)$=10 \log_{10} (I/I_0)$ for each of the three receivers on each ADV, where I_0 is a receiver specific noise reference intensity. Since I_0 is an arbitrary sensor specific constant, we have adjusted I_0 for each sensor so that the minimum value of S_V is zero for each receiver. Fifteen minute burst averages of backscatter at 3 and 23 cmab from one of the receivers on each

Captions for Fig. 1-3. Time series of total suspended solids (TSS) and indirect measures of concentration (a) Total suspended solids measured from pumped samples at 10, 25 and 40 cmab. Dashed line is friction velocity measured by Reynolds stress at 23 cmab. (b) ADV backscatter from 3 and 23 cmab adjusted for minimum value (minimum value occurs outside of the time period shown).(c) OBS from 7, 23 and 36 cmab adjusted for minimum value. (d) Beam c measured by the transmissometer on the LISST at 10 and 200 cmab. after adjusting transmission for the maximum observed (e) Volume concentration as measured by the LISST, relative to the maximum observed concentration. (f) Total suspended solids pumped from 10 cmab by the profiler and the tripod. Dashed line is 1 to 1 correspondence between the two.

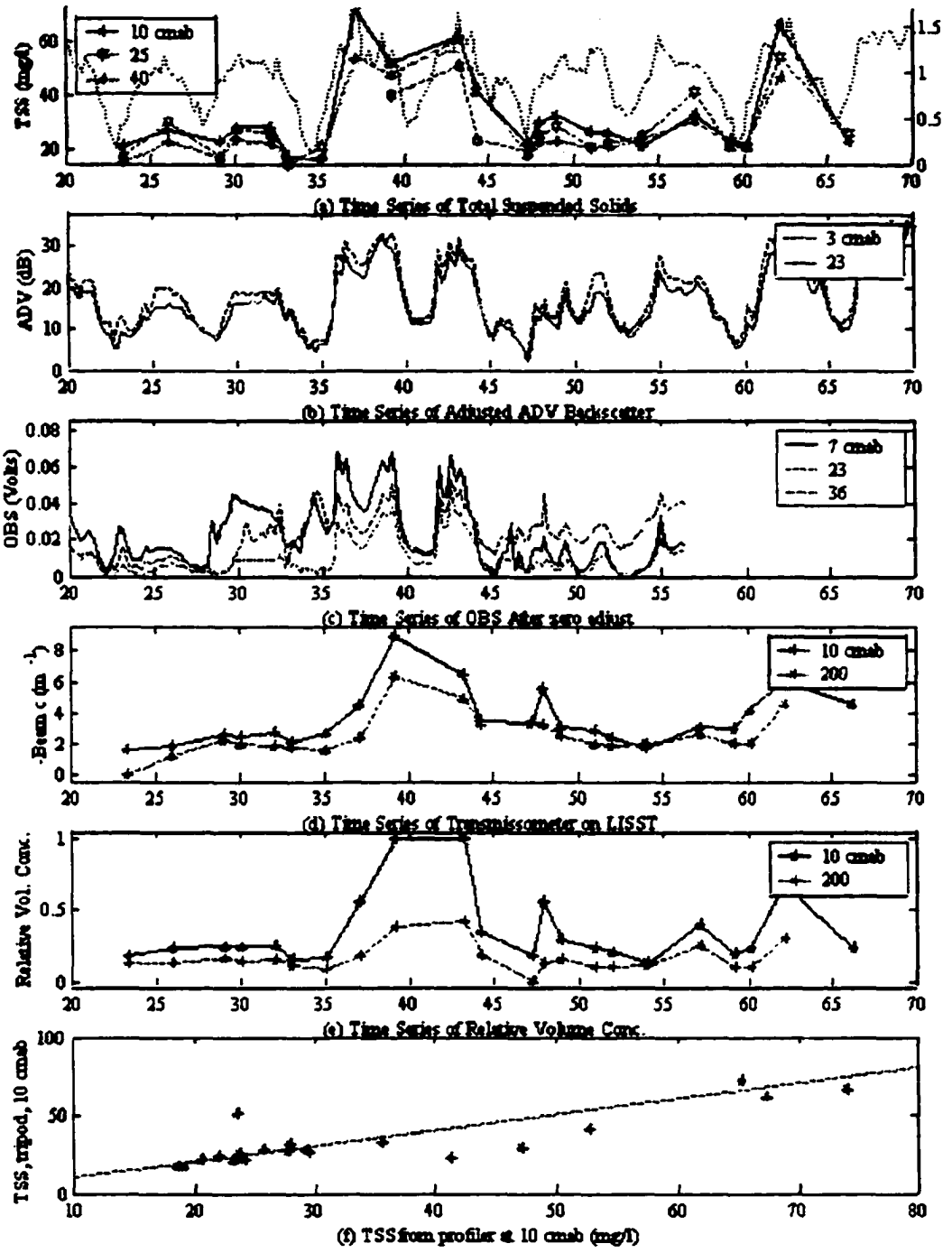

Fig. 1-3

ADV are shown in Fig. 1-3b (the adjusted responses from each of the three receivers on a given ADV are virtually identical). The receivers at the two depths track each other closely, duplicating even high resolution features. The r^2 between log(TSS) at 10 cmab and backscatter at 3 cmab is 0.77 (n=22). The r^2 between log(TSS) at 25 cmab and backscatter at 23 cmab is 0.72 (n=21, Fig. 1-4a)

OBS

Similar to the ADV, each OBS has its own sensor specific offset voltage at zero concentration. Therefore, the outputs of the OBS were also first adjusted by subtracting their minimum value over the course of the deployment. Examination of this adjusted output (Fig. 1-3c) shows that the sensor at 23 cmab experienced a gradual drift starting around hour 22. This drift at 23 cmab was corrected by applying a linear adjustment based on the outputs at hour 22 and hour 52.5, where minimum concentrations in all three sensors presumably should have occurred. Figure 1-4b shows TSS at 10 cm by OBS at 7 cm (r^2=0.40, n=17), TSS at 25 cmab and OBS at 23 cmab (r^2=0.46, n=16), and TSS at 40 cmab by OBS at 36 cmab (r^2=0.78, n=17), respectively. Both the optical and acoustic backscatter suggest that the minimum background concentration varies somewhat from one slack water to the next.

Transmissometer

The transmissometer on the LISST measures the attenuation of the intensity of the laser transmitted through 5 cm of water. Transmissivity values have been normalized to the maximum transmissivity at 200 cmab observed over the course of the deployment. The change between the transmitted and received intensity, T can be converted to a beam attenuation coefficient, or beam c (m^{-1}):

$$c = -\ln(T)/L$$

where L is the path length, and T is the beam transmission. The time series of beam c values at 10 and 200 cmab are shown in Fig. 1-3d. Comparisons of the indirect measures of concentration from the LISST, i.e. transmission and volume concentration, are compared with TSS values which were pumped from the profiler rather than from the tripod. Figure 1-3f shows the scatterplot of TSS values at 10 cmab from the profiler and the tripod at the closest corresponding sampling times (mean difference in corresponding sampling times is 0.3 hours, maximum is 1.45 hours). The values from the profiler tend to be slightly higher that those from the tripod, especially at higher concentrations. This may be due to slight resuspension by the profiler itself during these times. Nevertheless, there is good agreement (r^2=0.71, n=16) between these two measures, suggesting that there is not significant spatial or temporal variability at a scale of the order of 50 meters and 20 minutes at this site. Figure 1-4c shows TSS values from samples pumped at the profiler at 10 and 200 cmab and beam c for each respective elevation. The r^2 is 0.23 (n=21) at 10 cmab and 0.44 (n=16) at 200 cmab.

Total Volume Concentrations

The volume concentrations estimated by the LISST are initially obtained from estimates of areal concentrations. Unlike the OBS, however, the total volume estimates from the LISST are theoretically not sensitive to the grain size distribution of the suspended sediment since the inversion algorithm for area concentration explicitly weights for size classes. Volume concentrations at 10 and 200 cmab are shown in Fig. 1-3e, normalized to the maximum observed volume concentration. The two elevations show similar patterns, with more variation in the concentration at 10 cmab. The r^2 between the TSS values measured at the profiler at 10 cmab and the volume concentration at 10 cmab is 0.39 (n=21). If the two outliers at maximum volume concentrations are removed the r^2 rises to 0.80 (n=19). At 200 cmab the r^2 is 0.81 (n=16, Fig. 1-4d).

Captions for Fig. 1-4. Comparisons of total suspended solids (TSS) measured from pumped samples with indirect measures of concentration. Measured values at 3 and 7 cmab from the OBS and ADV respectively are matched with pumped samples from 10 cmab, measured values from 23 cmab from the OBS and ADV are matched with pumped samples from 25 cmab, and measured values of 36 cmab from the OBS are matched with pumped samples from 40 cmab. (a) TSS by adjusted ADV backscatter (b) TSS by adjusted OBS voltage (c) TSS by – (beam c) (d) TSS by volume concentration relative to the maximum observed

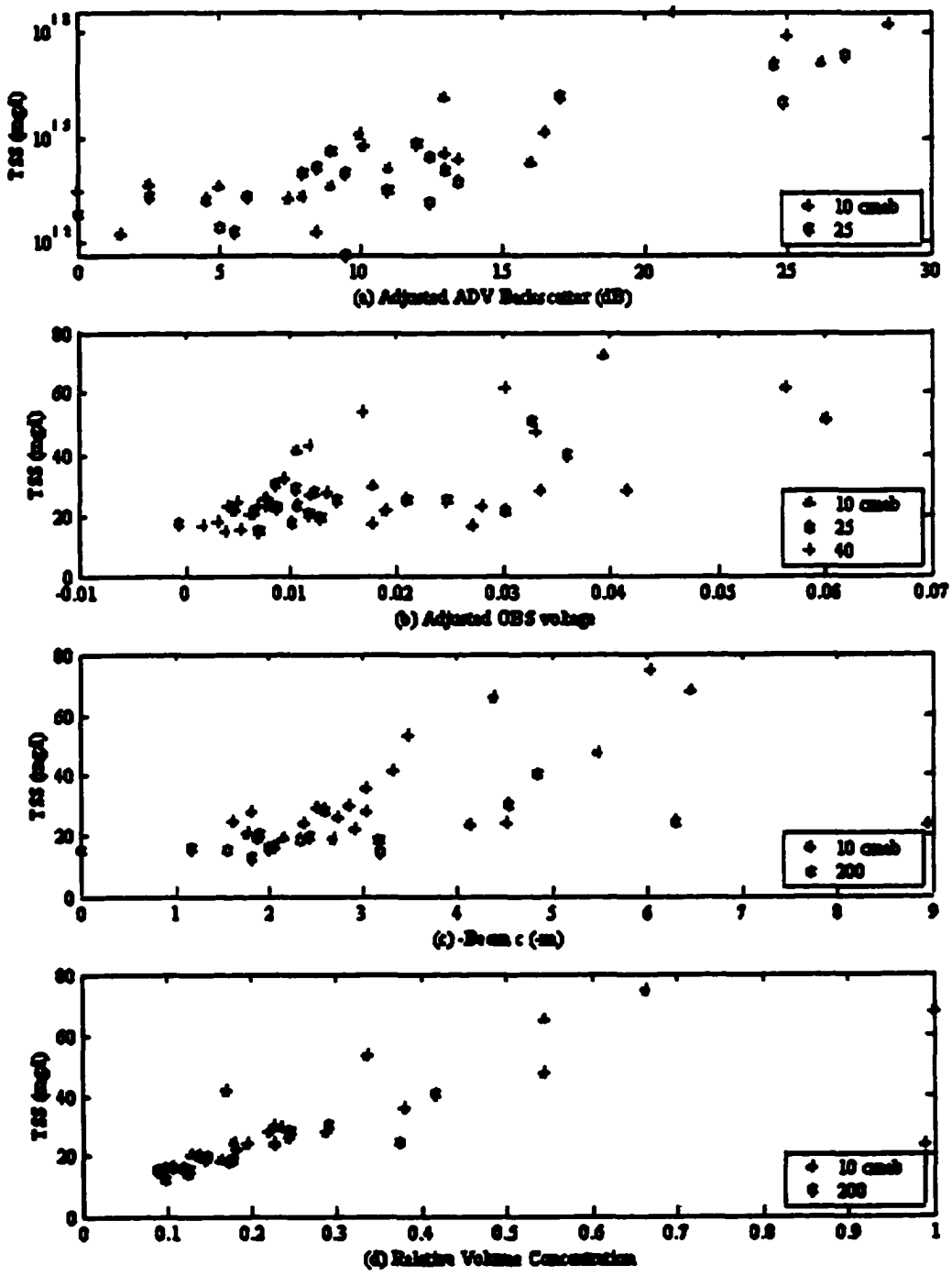

Fig. 1-4

Accounting for multiple particle populations

Two potentially coupled sources of particle variability may confound the direct conversion of backscatter or transmission to a simple representation of suspended sediment concentration. One is the presence of both rapidly settling and slowly settling (background) components and the second is the presence of multiple particle sizes within these two components. Two approaches which can be used to better infer sediment concentrations consisting of multiple subpopulations is to weight indirect measures of concentration by particle diameter and to separate measured concentrations associated with rapidly and weakly settling populations.

Estimates of mass concentration controlling for the size distribution

Information about grain size distributions as estimated by the LISST can be used to improve calibrations of the various in situ instruments. The grain size of the particles may affect the response of the instruments and confound the estimates of mass concentration, depending upon whether the instrument uses an optical or acoustic method, and the way in which the grain size is related to the density of the particles.

Optical methods such as the OBS and transmissometer measure the areal concentration of particles which is then used to estimate the mass concentration. From equation (3) it follows that:

$$TSS \sim d\,\rho(d)\,(V_{OBS}) \qquad (5)$$

where V_{OBS} is the OBS voltage, d is a characteristic particle diameter, and $\rho(d)$ is its density, which may vary with d. A given mass concentration of small size particles will produce a higher voltage response than the same concentration manifested in larger particles of the same density. A further effect on the calibration is a potential change in density with grain size. The density of fragile flocculants may decrease with increasing diameter. Conversely, fecal pellets or compressed bottom aggregates resuspended from

the bed may have increasing densities with larger grain size. Although the LISST, like the OBS, also uses an optical method to produce areal concentrations, the LISST takes into account the grain size distribution in its estimation of volume concentration. In this case:

$$TSS \sim \rho(d)\, C_V \qquad (6)$$

where C_V is the volume concentration, and there is still an interactive effect on the estimate of TSS by the grain size through its relationship to the density.

The variation in backscatter from acoustic instruments as a function of grain size depends mainly on the sensitivity of the form function ratio, f_n^2/d_n, to grain size. In particular, it depends on whether f_n^2/d_n responds to the characteristics of the aggregate as a whole or mainly to those of its constituent particles. If aggregates are loosely enough bound to scatter sound in a manner equivalent to an identical mass concentration of their constituent grains, then variations in the acoustic backscatter-mass concentration relation associated with aggregate size may be small. Alternatively, if aggregates scatter sound like single large grains or if large particles are actually sand, then variations in acoustic backscatter as a function of particle size will be strong.

The LISST particle size output provides data which can be used to test the utility of including grain size information in our calibrations of TSS based on OBS, ADV backscatter and laser transmission. Figure 1-5a displays the mean particle size distribution recorded by the LISST at 10 cmab over the course of the deployment. According to the LISST, the volume concentration is dominated by relatively large particles with a diameter on the order of 100 to 200 microns. The percentage of volume concentration greater than 89 microns (Fig. 1-5b) is used as an indicator of temporal variations in size distribution in multiple least square regression models to improve estimates of TSS from in situ instruments. The cutoff of 89 microns was chosen because it produced the maximum amount of variation in the size distribution variable. The

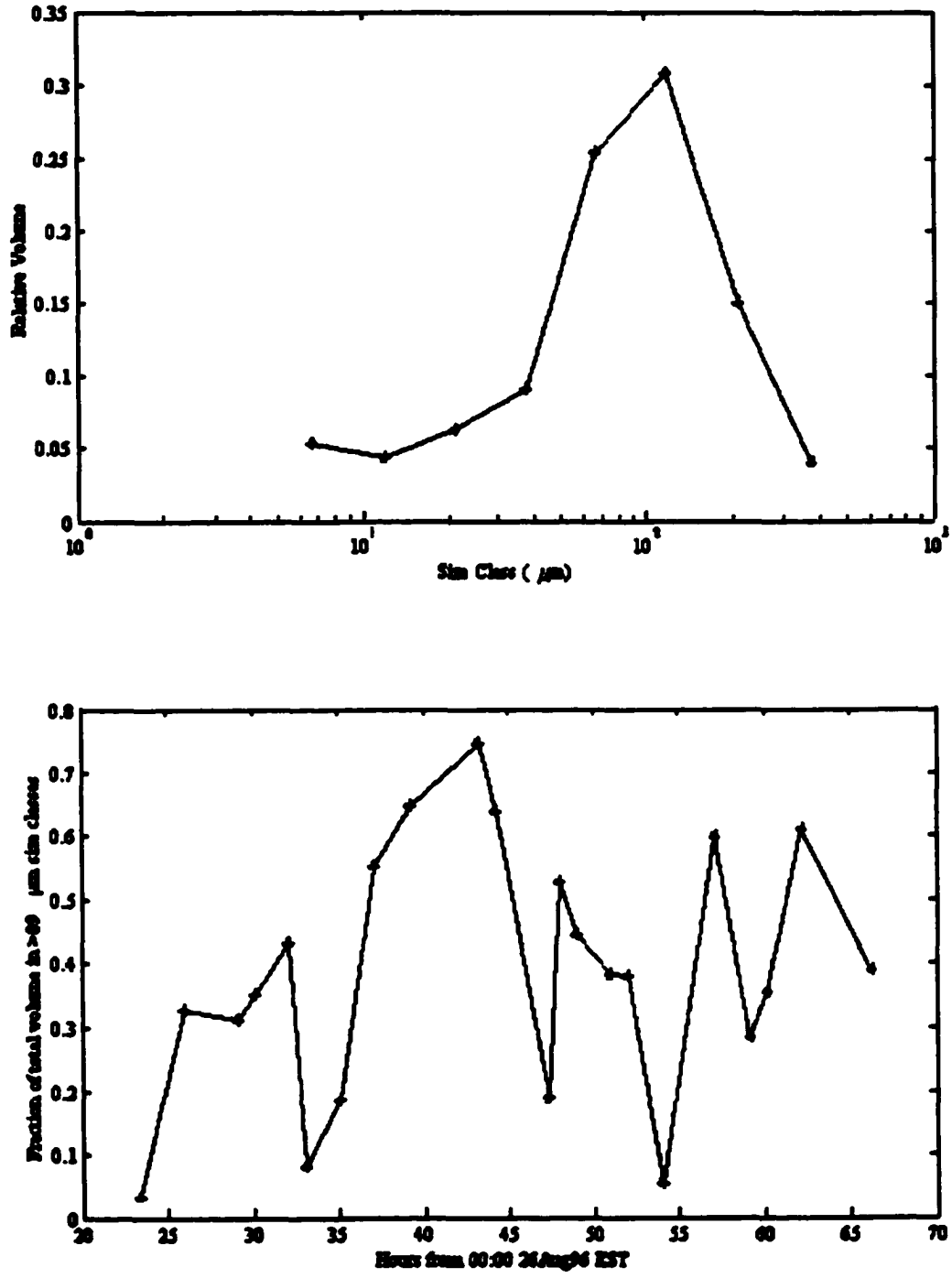

Fig. 1-5. Particle size data (a) Time averaged size distribution at 10 cmab (b) Size distribution variations as measured by the fraction of total volume contained in particles greater than 89 μm.

percent volume concentration greater than 89 microns is itself significantly correlated to TSS (r^2=0.58 at 10 cmab), suggesting that much of the temporal variability in TSS is associated with the presence or absence of large particles. The differences in variation explained (r^2) by the earlier calibration curves and alternate calibrations which include the percentage of volume concentration > 89 microns as a first order interactive effect are shown in Table 1-2.

Of the models excluding controls for size distribution, beam c at 10 cmab explained the least amount of variation in TSS, likely due to the confounding affect of changing grain size distribution. The OBS at 7 and 23 cmab also performed poorly. However, the OBS at 36 cmab performed well without size correction, suggesting that at this height above the bed particle size variation was less significant. In general, the ADV and LISST performed better than the simple optical instruments without correction for grain size. When corrections for grain size are included in the calibrations via multiple regression, the predictions of TSS by the optical sensors is greatly improved, most approaching r^2 values of 0.7 to 0.8. In contrast, there was little improvement in the LISST or ADV estimates of TSS when size distribution information was included.

These results support the following interpretation: (i) OBS and transmission are indeed highly sensitive to temporal changes in particle size in the field. This is suggested by the large improvement in r^2 for the near bed OBS and transmission when grain-size information is included. Conversely, the dramatic increase in r^2 by using size information from the LISST to improve predictions of an instrument which is known to be sensitive to size distribution suggests that, at least qualitatively, the LISST can be a useful instrument to gather information about aggregate sizes in estuarine environments. (ii) Particle size varies less at 40 cmab than at 10 or 25 cmab This is indicated by the initially large r^2 for OBS and smaller improvement in r^2 associated with particle size information at this height. (iii) The density of particles which dominate TSS variation at this location is a relatively weak function of grain size. This conclusion is based on the small improvement in the calibration of total volume concentration for TSS provided by adding particle size. (iv) Acoustic backscatter registered by ADV's is not sensitive to temporal changes in the particle size of near bed suspended aggregates in the southern Chesapeake Bay. This is suggested by the small improvement in r^2 for the acoustic

Table 1-2. Statistics for regressions of bulk water samples on in situ measures

Dependent	Independents	r^2	n
TSS @ 10 cmab	Beam c @ 10 cmab	0.23	21
	Beam c @ 10 cmab % Vol.Conc.>89μm	0.41	21
	LISST Total Vol. Conc.@ 10 cmab	0.39 (0.80)	21 (19)
	LISST Total Vol. Conc.@ 10 cmab % Vol.Conc.>89μm	0.41 (0.81)	21 (19)
	OBS @ 7 cmab	0.40	17
	OBS @ 7 cmab % Vol.Conc.>89μm	0.70	17
	ADV @ 3 cmab	0.77	22
	ADV @ 3 cmab % Vol.Conc.>89μm	0.84	22
TSS @ 25 cmab	OBS @ 23cmab	0.46	16
	OBS @ 23cmab % Vol.Conc.>89μm	0.75	16
	ADV @ 23cmab	0.72	21
	ADV @ 23cmab % Vol.Conc.>89μm	0.75	21
TSS @ 40 cmab	OBS @ 36cmab	0.78	17
	OBS @ 36cmab % Vol.Conc.>89μm	0.80	17
TSS @ 200 cmab	Beam c @ 200 cmab	0.44	16

Beam c @ 200 cmab % Vol.Conc.>89μm	0.59	16
LISST Total Vol. Conc.@ 200 cmab	0.81	16
LISST Total Vol. Conc.@ 10 cmab % Vol.Conc.>89μm	0.81	16

Table 2-1 cont.

backscatter calibrations and implies that large particles are not behaving acoustically as single grains. Rather, the acoustic backscatter-concentration relation of large aggregates is consistent with that of a similar mass concentration of smaller constituent grains. This is a significant advantage of acoustic backscatter over OBS in terms of remotely tracking TSS in muddy environments if one's aim is to determine time-varying mass concentration. If one were more concerned with the effectiveness with which muddy water blocks light, say in the context of light-limited primary production, then OBS may be more useful. Nonetheless, it is essential to recognize the different particle properties measured by the various sensors in order to best apply the resulting information.

Use of shear velocity to distinguish rapidly and slowly settling populations

The relationships between u_* and the concentration before and after the mid-experiment high concentration event (between hours 35.5 and 44) are fairly similar except that during the event, the concentrations are elevated by about 15 mg/l (Fig. 1-6). The slight difference in the shape of the curve for the time during the event may be evidence of the resuspension of a different density or type of particle. Geochemical analysis of the suspended particles (manuscript in prep.) during this high concentration event suggest that these particles are indeed different. More clearly, however, the relationship suggests that the increase in concentration during the event consists of a fairly constant increase in the background, very slowly settling, population.

Fall velocity of rapidly settling populations

The inherent intrusiveness of most direct measures of settling velocities and their ensuing vulnerabilities make indirect estimation appealing. Within a meter of the bed in marine boundary layers and at burst-averaged time-scales on the order of ten minutes, it is common to assume a lowest-order sediment concentration balance between

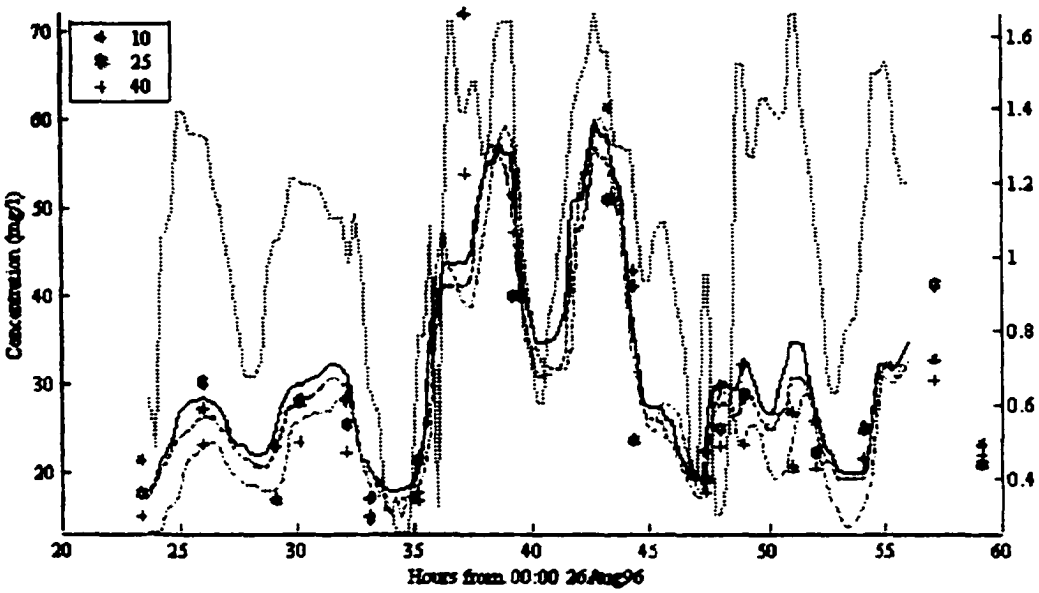

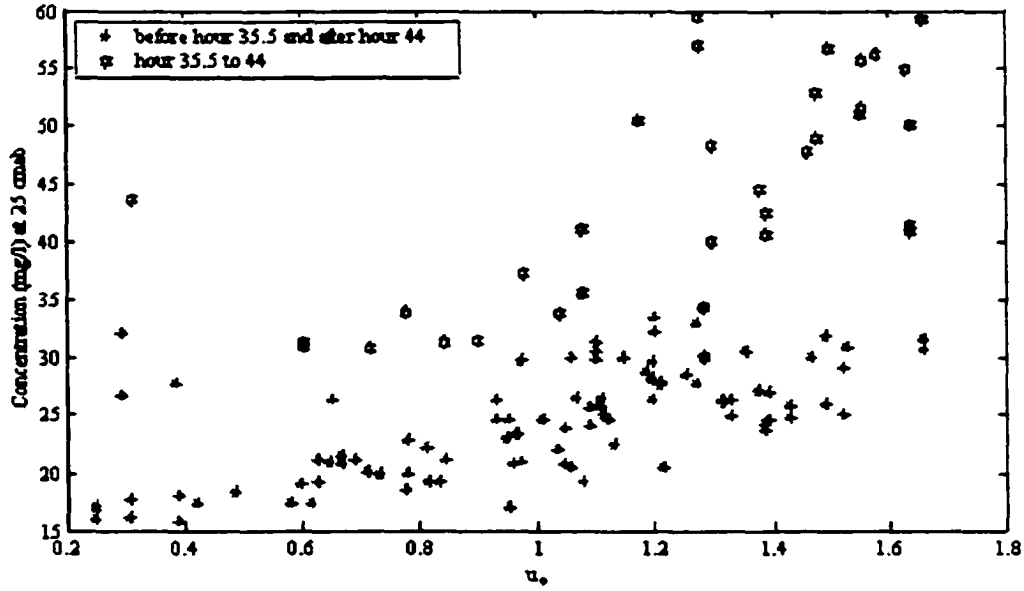

Fig. 1-6(a). Predicted mass concentrations from ADV at 10 and 25 cmab and OBS at 45 cmab. Dashed line is smoothed u_* from Reynolds stress. (b) Mass concentration predicted by the ADV at 25 cmab by friction velocity. '*' symbol represents measures before and after the high concentration event, and hexagons represent measures during the event.

gravitational settling and turbulent dispersion for each size class (e.g., Sleath, 1984; Glenn and Grant, 1989; Wiberg et al., 1994).

$$- w_{sn} C_n = K\, dC_n/dz \tag{7}$$

where w_{sn} is settling velocity of particle type n, C_n is the concentration of particle type n, and K is the eddy diffusivity. One can then solve for settling velocity simply by dividing both sides by C.

Estimation of vertical diffusive sediment flux

There are two independent ways that vertical diffusive flux can be estimated from the data set collect here: (i) direct measurement of turbulent diffusion using Reynolds flux, and (ii) estimation of the theoretical turbulent diffusion coefficient utilizing the law of the wall.

Separating concentration into mean and time oscillating components provides an alternative expression of turbulent diffusion via a Reynolds average:

$$K\, dC_n/dz = - \langle w'C_n' \rangle \tag{8}$$

Utilizing an ADV to measure turbulent fluctuations in both vertical velocity and backscatter, w' and C' are measured directly, and their correlation can be used to estimate the right-hand-side of eq. 7 without relying on an additional estimate of eddy diffusion. However, the ADV does not separately record concentrations associated with each individual size class.

Figures 1-7a and 1-7b display plots of $\langle w'C_{total}' \rangle$ vs. C_{total} with w_s determined from the slope of the best-fit regression. In each case, the x-axis intercept of the best fit regression at $\langle w'C_{total}' \rangle = 0$ is interpreted as the background concentration of the non-

settling component. The resulting slopes produce estimates of w_s = 0.69 mm/s +/- 0.03 at 3 cmab and w_s = 1.2 mm/s +/- 0.05 at 25 cmab with background concentrations of 13.0 +/- 1.5 mg/l and 16.0 +/- 1.3 mg/l, respectively. One might expect the to slope to increase with C as particles with larger settling velocities are suspended at higher velocities. Subsetting the data from 23 cmab into concentrations above 39 mg/l, which includes most of the values during the high concentration event, and concentrations below, which excludes most of the high concentration event, suggests a w_s of 1.1 mm/s for C <= 39 mg/l and 1.5 mm/s for C > 39 mg/l. Although these trends are consistent with expectations, the slopes are not statistically different.

The second way to estimate the right hand side of eq. 7 is via the law of the wall assumption (assuming equivalence between eddy diffusivity and eddy viscosity):

$$K = \kappa u_* z$$

where K is eddy diffusivity, κ is von Karman's constant set to 0.41, and z is the height above the bed. We have two independent methods for estimating u_*, one utilizing the Reynolds stress measured by the ADV, and one from a best-fit logarithmic velocity profile. Figures 1-7c and 1-7d display plots of $\kappa u_* z$ dC/dz vs. C at 25 cmab with w_s determined from the slope of the best-fit regression, and u_* determined from Reynolds averaging and log profile fit, respectively.

A limitation of this method for estimating w_s is that it requires accurate resolution of dC/dz as well as C. Because of problems with partially clogged filters during the high concentration event, an apparently homogeneous vertical profile was measured during this time. The calibrated in situ estimates reflect this relatively homogeneous vertical profile at high C and produce dC/dz values which are near zero or even of opposite sign. The regression for w_s based on all data points is affected by the poor resolution of dC/dz during the high concentration event, producing unrealistic overall estimates of the settling

Captions for Fig. 1-7. Settling velocity calculations (a) Reynolds concentration flux at 3 cmab by predicted concentration by the ADV at 3 cmab. (b) Reynolds concentration flux at 23 cmab by predicted concentration by the ADV at 23 cmab (c) $\kappa u_* z (dC)/(dz)$ by predicted concentration by the ADV at 23 cmab with u_* measured from Reynolds stress (d) $\kappa u_* z (dC)/(dz)$ by predicted concentration by the ADV at 23 cmab with u_* measured from log profile

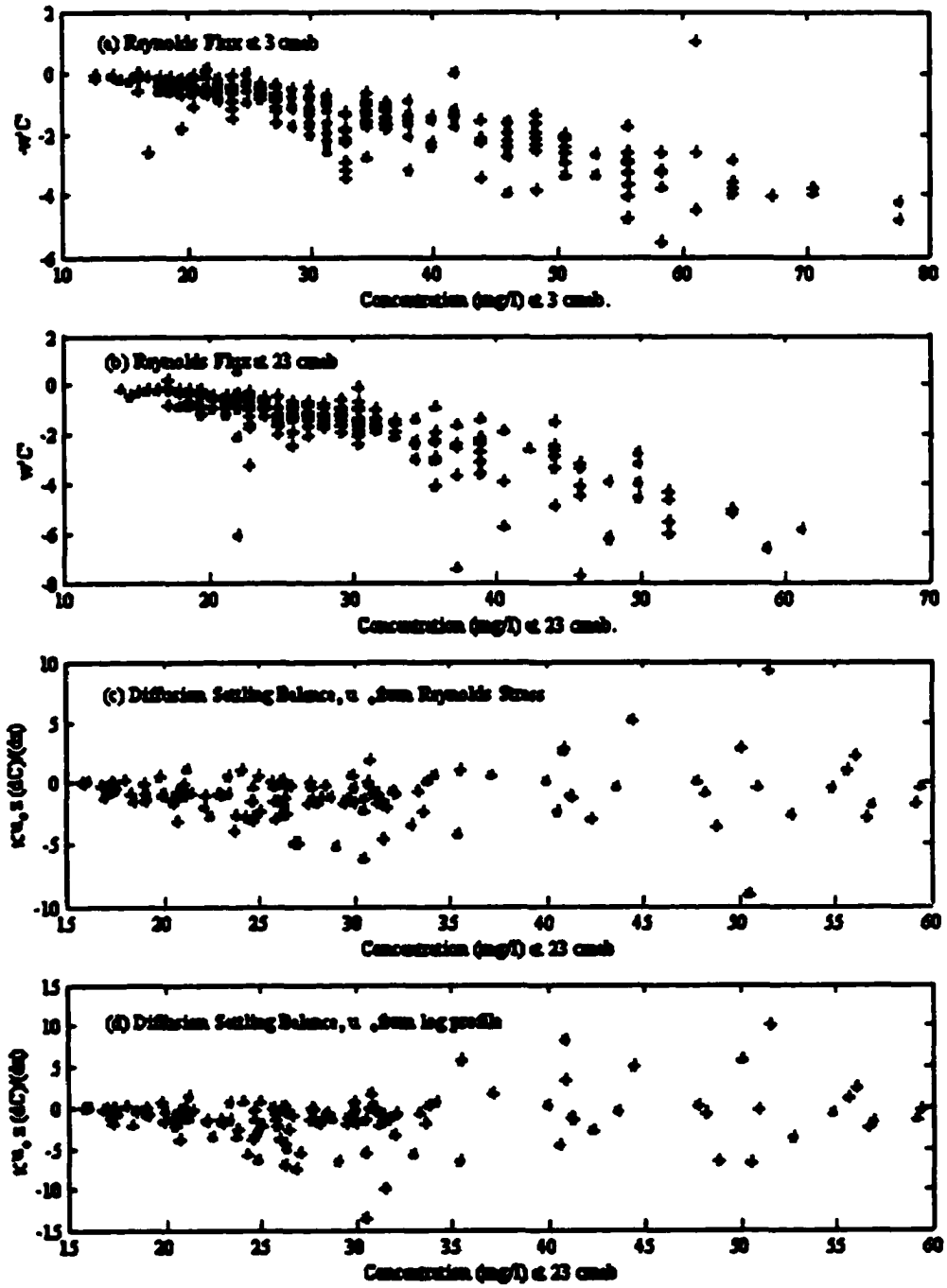

Fig. 1-7

velocity (-0.2 +/- 0.2 mm/s for Reynolds stress u_*, -0.4 mm/s +/- 0.2 for log-fit u_*, n=140). In contrast, the earlier estimates of w_s utilizing the ADV to directly measure Reynolds flux are much less sensitive to calibration errors among sensors, since errors in w_s based on Reynolds flux are proportional to percent errors in C rather than percent errors in dC/dz. When only data outside of this high concentration event are used to estimate dC/dz, more realistic values for the settling velocity are obtained: 0.72 +/- 0.3 mm/s using Reynolds stress u_*, and 1.3 +/- 0.5 mm/s using the log profile u_*.

Relative importance of local and advective changes in concentration

Neglecting across-channel and vertical advection, the sediment continuity equation may be approximated as:

$$\frac{\partial C}{\partial t} + \frac{\partial (uC)}{\partial x} + w_s \frac{\partial C}{\partial z} - \frac{\partial}{\partial z}\left(A_z \frac{\partial C}{\partial z} \right) = 0 \qquad (9)$$

where u is along channel velocity, C is concentration, and A_z is the eddy diffusivity. The methods we have applied for estimating w_s assume a lowest order balance between the last two terms in (9), gravitational settling and vertical mixing, respectively. As a consistency check, we now compare the size of the gravitational settling term to the first two terms in the sediment continuity equation, which we can independently estimate with some confidence, namely the local change and along-channel advection terms. It is possible to examine the size of the local advection term because a second tripod (Pod B) was deployed 650 m seaward from the main tripod (Pod A) along the axis of the estuary. The local change and along-channel advection terms relative to the settling term may be written as:

$$(\partial C/\partial t)/(w_s\, \partial C/\partial z) \qquad (10)$$

and

$$(u\ \partial C/\partial x + C\ \partial u/\partial x)/(w_s\ C/\partial z) \qquad (11)$$

Figure 1-8 displays time-series of the magnitude of these ratios along with time-series of u and C at the two tripods. As discussed earlier, clogged filters reduced our ability to accurately resolve time-variation in $\partial C/\partial z$, therefore, a single average value of $w_s = 1.2$ mm/s and $\partial C/\partial z = -0.15$ mg/cm^2 from Fig. 1-7 were used to estimate the order of magnitude of the settling term. The local change term, $\partial C/\partial t$, was evaluated by using the difference in concentrations between half hour intervals as estimated by the ADV at 23 cmab on Tripod A. Half hour intervals were chosen so that temporal and spatial scales in the estimates of the local and acceleration terms would match. Since the spatial interval, dx, is predetermined at the distance of 650 meters between pods and maximum tidal velocities are around 30 cm/s, an appropriate time interval, dt, is estimated at a half hour. Concentrations for $\partial C/\partial x$ are measured from the OBS sensors at 36 cmab on Pod A and B. The velocities to estimate $\partial u/\partial x$ are taken from the ADV sensor at 23 cmab for Pod A, and the velocities at Pod B are interpolated at 23 cmab from a log fit profile of EMCM sensors on Pod B at 8, 38, 68, and 98 cmab. Both the local concentration change and the advective term are generally between 1 and 3 orders of magnitude less than the scale of the settling term. These results suggest that even when the physical properties of suspended sediment populations change significantly with time as different populations are resuspended and/or advected into and out of the region, a local balance between the settling and resuspension term is still a good first order approximation.

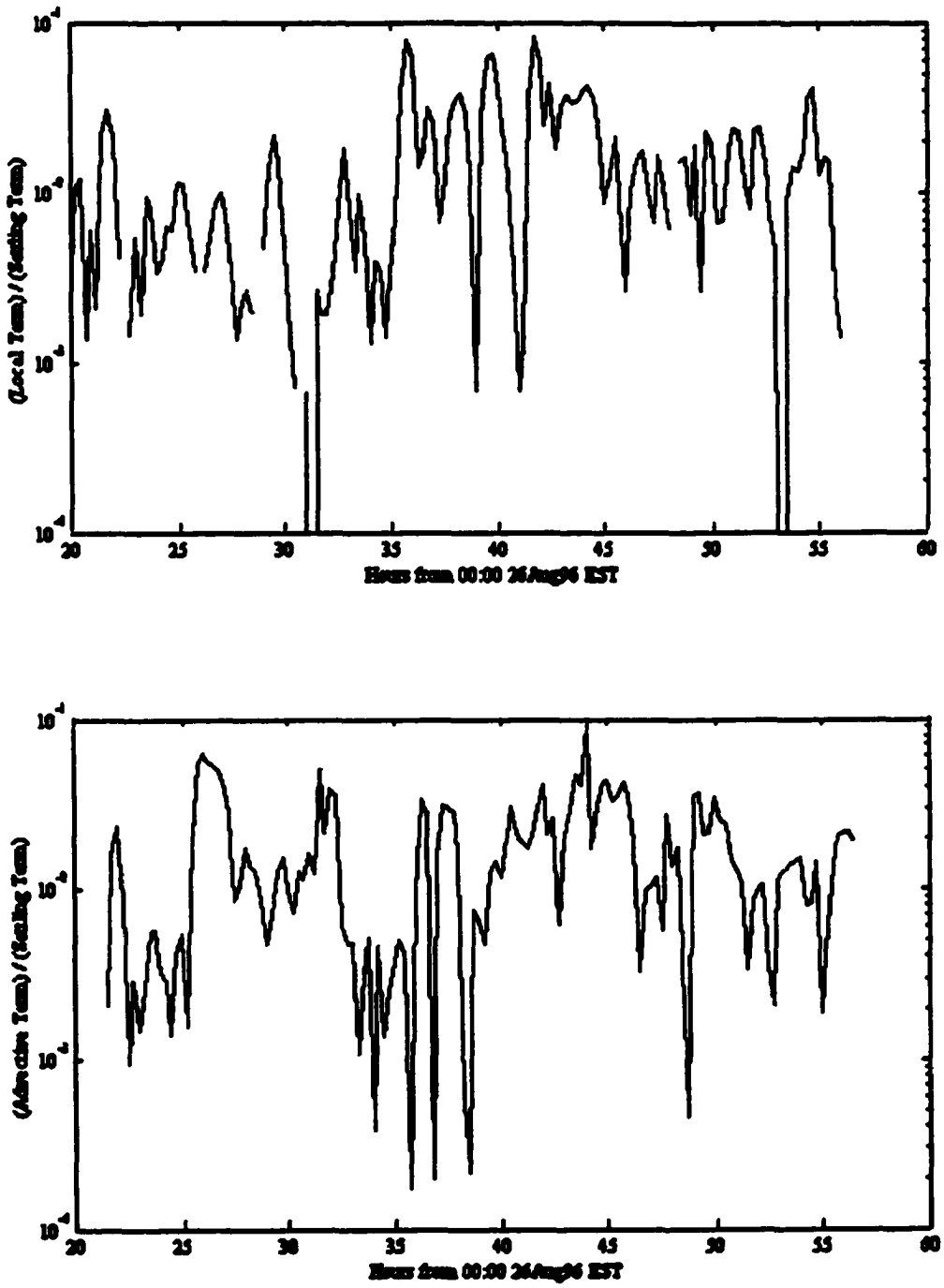

Fig. 1-8. Comparison of terms in the sediment transport equation (a) Time series of local term relative to settling term (b) Time series of advective term relative to settling term

SUMMARY AND CONCLUSIONS

The codeployment of several types of in situ optical and acoustical instruments including a LISST particle size analyzer has demonstrated their respective responses to changing size and density of multiple suspended particle populations and provided insight into the different suspended particle populations which are present in the near bed water column of the lower Chesapeake Bay. We have found at least three suspended particle subpopulations whose different characteristics are relevant to understanding sediment dynamics in the system. The first is a background population of small particles ranging from 15-22 mg/l in concentration which do not settle within the time scale of a tidal cycle. The second population is an easily resuspended "fluff" layer of somewhat larger particles with an estimated settling velocity of about 1 mm/s. A third population of fine very slowly settling particles may appear on a meteorological time scale and elevate concentration about 15 mg/l above the initial background level. In addition, a possible fourth population of aggregates with a density similar to their constituent particles is resuspended at bed friction velocities around 1.5 cm/s and may have a slightly larger settling velocity roughly estimated at about 1.5 mm/s.

The ADV proved to be a surprisingly versatile instrument for characterizing the suspended sediment dynamics. Acoustic backscatter from the ADV was relatively insensitive to grain size differences, thus producing the best estimates of mass concentration. The insensitivity of the ADV to particle size suggests that the acoustic form function for resuspended aggregates depends mostly on the size and shape of the constituent grains rather than the size or shape of the aggregate as a whole. In addition, the ability of the ADV to measure Reynolds bed stresses and vertical Reynolds flux of sediment allows estimation of critical shear velocities and the indirect analytical estimation of settling velocities of different particle types. This indirect method for estimating settling velocity has the advantage of not affecting the ambient turbulence and thus not altering the dynamics of flocculation. Furthermore, analytic estimation of fall

velocity using the ADV requires only a point measurement and is not sensitive to errors in estimation of the vertical concentration gradient. Comparison of the local change and advective terms in the solute transport equation to the magnitude of the settling term suggests that a balance between the settling and resuspension term is a good first order approximation at this site, validating the indirect method for estimating settling velocity.

One day prior to the study an independent experiment measured fall velocities at the site from a water sample taken by a diver at 1 meter above the bed using an Owen tube of height 32.7 cm and diameter of 10.2 cm. Median fall velocity was measured at 1.1 mm/s (Chisholm, unpubl. data). This direct independent measure of fall velocities produced values consistent with the analytical technique. In addition, the agreement between these measures suggests that the measured suspended particles were sturdy compressed aggregates which were not fundamentally altered by manipulations in the Owen tube as fragile flocculants might be. Other researchers have found similar values for aggregate settling velocities near bed and in the water column using a variety of techniques, invasive and indirect (e.g. ten Brinke, 1994, Syvitski et al., 1995, Dyer et al., 1996, Jago and Jones, 1998, Hill and McCave, 2001).We found OBS and optical transmission to be sensitive to changes in grain size very near the bed, as expected, but the OBS performed well at estimating mass concentrations further up at 36 cmab, suggesting that temporal variations in grain size were reduced at this height. Although acoustic backscatter outperformed these optical methods in measuring mass concentration, water quality applications concerned with how muddy sediment blocks light may be better served by OBS and/or optical transmission. The LISST combines attractive features of both the ADV and OBS in that it provides a measure of optical water clarity plus a size-corrected total volume concentration. It also proved to be a valuable tool for testing the sensitivity of concentration estimates to particle size. More importantly, the LISST provides unique insight into particle size distribution. The significant correlation between percent volume concentration greater that 89 microns and pumped mass concentration are consistent with a temporally variable rapidly settling population of aggregates with a diameter of a few hundred microns superimposed on a less rapidly varying background concentration of slowly settling particles with a diameter of few 10's of microns. Estimation of mass concentrations by the total volume

concentrations measured by the LISST are not improved by adding grain size distribution information, which suggests that for these near bed particles, density is not a strong function of grain size.

This study of sediment dynamics was limited to processes in the benthic boundary layer of the southern Chesapeake Bay, a location of moderate energy dissipation. Subpopulations of particles have been discovered using purely physical measurements of the suspended sediment and water column. Ongoing research will use geochemical data to further distinguish between suspended sediment populations. A promising approach may be to use statistical techniques such as principle components analysis to separate particle populations based on several characteristics at once. The dominant process affecting the rapidly settling near bed populations is resuspension by tidal currents. While these bottom processes are relevant to the benthic biota and to understanding the behavior of settled and resuspended contaminated particles, significant sediment transport in estuaries can also occur higher in the water column. Further analysis of this data set and similar data sets from estuaries with different energy regimes will more clearly reveal the relationship between particle size and turbulent shear near the bottom where compressed aggregates are resuspended and higher in the water column where more fragile flocs may dominate.

REFERENCES FOR CHAPTER 1

Agrawal, Y.C., Pottsmith, H.C., 1994. Laser diffraction particle sizing in STRESS. Continental Shelf Research 14(10-11), 1101-1121.

Agrawal, Y.C., Pottsmith, H.C., 2000. Instruments for particle size and settling velocity observations in sediment transport. Marine Geology 168, 89-114.

Baker, E.T., Lavell, J.W., 1984. The effect of particle size on the light attenuation coefficient of natural suspensions. Journal of Geophysical Research 89, 8197 - 8203.

Bale, A.J., 1996. In situ laser optical particle sizing. Journal of Sea Research 36(1-2), 31-36.

Bale, A.J., Barrett, C.D., West, J.R., Oduyemi, K.O.K., 1989. Use of in-situ laser diffraction particle sizing for particle transport studies in estuaries. In: McManus, J., Elliott, M. (Eds.), Developments in estuarine and coastal study techniques. pp. 133-138.

Battisto, G.M., Friedrichs, C.T., Miller, H.C., Resio, D.T., 1999. Response of OBS to mixed grain-size suspensions during Sandyduck '97. In: Kraus, NC and McDougal, WG (Eds.), Coastal Sediments '99: Proceedings of the 4th International Symposium on Coastal Engineering and Science of Coastal Sediment Processes, American Society of Civil Engineers.

Battisto, G.M., 2000. Field Measurement of mixed grain size suspension in the nearshore under waves. M.S. Thesis, School of Marine Science, College of William and Mary, Gloucester Point, VA, 87 pp.

Beuselinck, L., Govers, G., Poesen, J., 1999. Assessment of micro-aggregation using laser diffractometry. Earth Surface Processes and Landforms 24(1), 41-49.

Canuel, E.A., Zimmerman, A.R., 1999. Composition of particulate organic matter in

the southern Chesapeake Bay: Sources and Reactivity. Estuaries 22(4), 980-994.

Dyer, K.R. , 1989. Sediment processes in estuaries: Future research requirements. Journal of Geophysical Research 94, 14327-14339.

Dyer, K. R., Cornelisse, J., Dearnaley, M. P., Fennessy, M. J., Jones, S. E., Kappenberg, J., McCave, I. N., Pejrup, M., Puls, W.,Van Leussen, W., Wolfstein, K., 1996. A comparison of in situ techniques for estuarine floc settling velocity measurements, Journal of Sea Research 36(1/2) : 15-29, 1996.

Eisma, D., Bernard, P., Cadee, G.C., Ittekkot, V., Kalf, J., Laane, R., Martin, J.M., Mook, W.G., van Put, A., Schuhmacher, T., 1991. Suspended-matter particle size in some West-European Estuaries; Part II: A review on floc formation and break-up. Netherlands Journal of Sea Research 28(3), 215-220.

Eisma D., Dyer, K.R., van Leussen, W., 1997. The in situ determination of the settling velocities of suspended fine-grained sediment — a review. In: Burt, N. Parker, R., Watts, J. (Eds.), John Wiley & Sons, Chichester, pp 17-43.

Fettweis, M., Sas, M., Monbaliu, J., 1998. Seasonal, neap-spring and tidal variation of cohesive sediment concentration in the Scheldt Estuary, Belgium. Estuarine, Coastal and Shelf Science 47, 21-36.

Friedrichs, C.T., Hamrick, J.M., 1996. Effects of channel geometry on cross sectional variations in along channel velocity in partially stratified estuaries, Coastal and Estuarine Studies 53, 283-300.

Gibbs, R.J., Wolanski, E., 1992. The effect of flocs on optical backscattering measurements of suspended material concentration. Marine Geology 107(4), 289-291.

Glenn, S.M., Grant, W.D., 1987. A suspended sediment stratification correction for combined wave and current flow. Journal of Geophysical Research 92, 8244-8264.

Green, M.O., Boon, J.D. III., 1993. The measurement of constituent concentrations in nonhomogeneous sediment suspensions using optical backscatter sensors. Marine Geology 110, 73-81.

Hay, A.E., Sheng, J., 1992. Vertical profiles of suspended sand concentration and size from multifrequency acoustic backscatter. Journal of Geophysical Research 97(c10), 15661-15677.

Hill, P.S., Syvitski, J.P., Cowan, E.A., Powell, R.D., 1998. In situ observations of floc settling velocities in Glacier Bay, Alaska. Marine Geology 145, 85-94.

Hill, P.S., McCave, I.N., 2001. Suspended particle transport in benthic boundary layers. in: Boudreau,B.P., Jorgensen, B.B. (Eds.) The Benthic Boundary Layer: Transport Processes and Biogeochemistry. Oxford University Press 2001.

Jago, C.F., Jones, S.E., 1998. Observation and modelling of the dynamics of benthic fluff resuspended from a sandy bed in the southern North Sea. Continental Shelf Research 18, 1255-1282.

Jago, C.F., Bull, C.F.J., 2000. Quantification of errors in transmissometer-derived concentration of suspended particulate matter in the coastal zone: implications for flux determinations. Marine Geology 169, 273-286.

Jones, S.E., Jago, C.F., 1996. Determination of settling velocity in the Elbe estuary using quisset tubes, Journal of Sea Research 36(1/2):63-67.

Kawanisi, K., Yokosi, S., 1997. Characteristics of suspended sediment and turbulence in a tidal boundary layer, Continental Shelf Research 17(8), 859-875.

Kim, S.C., Friedrichs, C.T., Maa, J.P.Y., Wright, L.D., 2000. Estimating bottom stress in tidal boundary layer from acoustic doppler velocimeter data. Journal of Hydraulic Engineering , June 2000, 399-406.

Kinneke, G.C., Sternberg, R.W., 1992. Measurements of high concentration suspended sediments using the optical backscatterance sensor Marine Geology 108, 159 174.

Knowles, S.C., Wells, J.T., 1996. Suspended aggregate analysis using ISAAC, Elbe River, 9-10 June 1993. Journal of Sea Research 36(1/2), 69-75.

Kranck, K., Smith, P.C., Milligan, T.G., 1996. Grain-size characteristics of fine-grained unflocculated sediments I: 'one-round' distributions. Sedimentology 43, 589-596.

Latimer, J.S., Davis, W.R., Keith, D.J. 1999. Mobilization of PAHs and PCBs from in place contaminated marine sediments during simulated resuspension events. Estuarine, Coastal, and Shelf Science 49, 577-595.

Lee, C.-H., 1995. Resuspension behavior of natural estuarine sediments. Ph.D. Thesis, School of Marine Science, College of William and Mary, Gloucester Pt. VA.

Ludwig, K.A.,Hanes, D.M., 1990. A laboratory evaluation of optical backscatterance suspended solids sensors exposed to sand-mud mixtures, Marine Geology 94(1-2), 173-179.

van Leussen, W. 1994. Estuarine Macroflocs; their role in fine-grained sediment transport. CIP-Gegevens Koninklijke Bibliotheek, Den Haag., Utrecht, 488 pp.

van Leussen, W., 1999. The variability of settling velocities of suspended fine-grained sediment in the Ems estuary, Journal of Sea Research 41, 109-118.

Lynch, J.F., Agrawal, Y.C.. 1991. A model-dependent method for inverting vertical profiles of scattering to obain particle size spectra in boundary layers. Marine Geology 99, 387-401.

Lynch, J.F., Irish, J.D., Sherwood, C.R. Agrawal, Y.C., 1994. Determining suspended sediment particle size information from acoustical and optical backscatter measurements. Continental Shelf Research 14(10-11), 1139-1164.

Manning, A.J., Dyer, K.R., 1999. A laboratory examination of floc characteristics with regard to turbulent shearing, Marine Geology 160, 147-170.

Mikkelson, O.A., Pejrup, M., 2000. In situ particle size spectra and density of particle aggregates in a dredging plume. Marine Geology 170, 443-459.

Phillips, J.M., Walling, D.E., 1998. Calibration of a Par-Tec 200 laser back-scatter probe for in situ sizing fluvial suspended sediment. Hydrological Processes 12(2), 221-231.

Schaffner, L. C., 1990. Small-scale organism distributions and patterns of species diversity: evidence for positive interactions in an estuarine benthic community. Marine Ecology Progress Series 61, 107-117.

Sheng, J., Hay, A.E., 1988. An examination of the spherical scatterer approximation in aqueous suspensions of sand. Journal of the Acoustic Society of America 83(2), 598-610.

Sleath, J.F.A., 1984. Sea Bed Mechanics, John Wiley & Sons, New York, 355 pp.

Sternberg, R.W., Ogston, A., Johnson R., 1996. A video system for in-situ measurement of size and settling velocity of suspended particulates. Journal of Sea Research 36(1/2), 127-130.

Syvitski, J.PM., Asprey, K.W., Leblanc, K.W.G., 1995. In-situ characteristics of particles settling within a deep-water estuary. Deep-Sea Research II 42(1), 223-256.

ten Brinke, W.B.M., 1994. Settling velocities of mud aggregates in the Oosterschelde tidal basin (the Netherlands), determined by a submersible video system. Estuarine and Coastal Shelf Science 39, 549-564.

Thevenot, M.M., Kraus, N.C., 1993. Comparison of acoustical and optical measurements of suspended material in the Chesapeake Estuary. Journal of Marine Environmental Engineering 1, 65-79.

Thompson, M.L., 2000. Demographics, production, and benthic-pelagic coupling by the suspension feeding polychaete *Chaetopterus pergamentaceus* in the lower Chesapeake Bay, Ph.D. Thesis, School of Marine Science, College of William and Mary, Gloucester Pt., VA.

Thompson, M.L., Schaffner, L.C., 2000. Local demographics of the polychaete *Chaetopterus pergamentaceus* within the lower Chesapeake Bay and relationships to environmental gradients. Bulletin of Marine Science 67 .

Thorne, P.D., Hardcastle, P.J., Soulsly, R.L., 1993. Analysis of acoustic measurements of suspended sediments. Journal of Geophysical Research 98, 899-910.

Traykovski, P., Latter, R.J., Irish, J.D., 1999. A laboratory evaluation of the laser in situ scattering and transmissometry instrument using natural sediments. Marine Geology 159, 355-367.

Vincent, C.E., Downing, A., 1994. Variability of suspended sand concentrations, transport and eddy diffusivity under non-breaking waves on the shoreface, Continental Shelf Research 14(2/3), 223-250

Wells, J.T., Kim, S.-Y., 1991. The relationship between beam transmission and concentration of suspended particulate material in the Neuse River Estuary, North Carolina. Estuaries 14(4), 395-403.

Wiberg, P.L., Drake, D.E., Cacchione, D.A., 1994. Sediment suspension and bed armoring during high bottom stress events on the northern California inner continental shelf: measurements and predictions. Continental Shelf Research 14, 1191-1219.

Wright, L.D. Prior, D.B., Hobbs, C.H., Byrne, R.J., Boon, J.D., III, Schaffner, L.C., Green, M.O., 1987. Spatial variability of bottom types in the lower Chesapeake Bay and adjoining estuaries and inner shelf. Estuarine, Coastal and Shelf Science 24, 765-784.

Wright, L.D., Boon, J.D., Xu, J.P., Kim, S.C., 1992. The bottom boundary layer of the bay stem plains environment of Lower Chesapeake Bay. Estuarine, Coastal and Shelf Science 35, 17-36.

Wright, L.D., Schaffner, L.C., Maa, J.P.Y., 1997. Biological mediation of bottom boundary layer processes and sediment suspension in the lower Chesapeake Bay. Marine Geology 141, 27-50.

Chapter 2. Particle Aggregation Dynamics and Turbulent Kinetic Energy Production in Partially Mixed Estuaries

Submitted to Estuarine Coastal and Shelf Sciences with authors

D.C. Fugate and C.T. Friedrichs

ABSTRACT

Knowledge of aggregate size in estuaries is important to determining the fate and transport of suspended sediment and particle adherent contaminants. Their fragility necessitates the use of in situ instruments to measure them. We have used a combination of an upward looking Acoustic Doppler Profiler (ADP) and a suite of in situ instruments deployed together on an instrument profiler. These instruments include a CTD, acoustic doppler velocimeter (ADV), an optical backscatterer (OBS), a laser in situ scatterer and transmissometer (LISST) as well as pump intakes to collect bulk water samples. Physical processes that are usually invoked to explain aggregate size dynamics include sediment concentration, turbulent shear, differential settling and organic content. Variation in turbulent shear can be measured by turbulent kinetic energy (TKE) production. A novel method is presented to measure TKE production using a profiling ADV instrument that has been contaminated by boat motion. The relative importance of each of the physical processes differs in three mid-Atlantic U.S.A. estuaries with different hydrodynamics and benthic characteristics as well as in different depth regimes within each estuary. The York R. and Chesapeake Bay estuaries are hydrodynamically energetic. The former has a bottom dominated by physical mixing and the bottom of the latter is dominated by bioturbation. The Elizabeth R. estuary is a low energy, low concentration, polluted urban estuary. Surface particle size dynamics in all of the estuaries are affected by irregular advection events. Middepth regions in the energetic estuaries are controlled tidally by the combined processes of TKE production decreasing particle size and differential settling increasing particle size. Middepth regions in the low energy estuary are controlled by irregular resuspension and trapping at the pycnocline of large low density particles. Bottom regions in all estuaries are most strongly influenced by resuspension, tidally in the energetic estuaries and irregularly in the low energy estuary. Near bed particle size distributions are controlled by both TKE production and the distribution of particles in the bed. Just above the bed, large porous particles survive resuspension in the low energy estuary, high TKE production causes smaller dense particles to be found in the energetic estuary dominated by physical reworking, and biological aggregation causes large dense particles to resist turbulent breakup in the energetic estuary with a more active benthic community. The net result just above the bed is that particle size and settling velocity are positively correlated to TKE production and sediment concentration in the biologically dominated energetic estuary, negatively correlated in the physically dominated energetic estuary, and poorly correlated in the low energy estuary.

INTRODUCTION

One of the major obstacles to predicting the fate and transport of sediment and particle adherent contaminants in estuaries is the determination of the size and settling velocity of particles. The settling velocity of the particles depends upon their size and density, qualities which are difficult to measure due to the fragile nature of aggregates in the water column, and the different densities of different types of particles. A further complication is that particle characteristics may vary over short and long time scales ranging from rapid response to changes in turbulence in the water column to seasonal variations in the source and type of primary particles (Eisma and van Leussen, 1997; Fettweis et al., 1998; Van Leussen, 1994). Important factors determining aggregation in estuaries include suspended sediment concentration, turbulent shear in the water, differential settling of the particles, and the amount of sticky organic compounds in the water (Eisma et al., 1991).The different effects of these processes have led to certain paradigms regarding aggregation in estuaries, including the general result that aggregates in the water column tend to settle around 1 mm/s (Hill and McCave, 2001). The applicability of these paradigms however, depends upon the physical and biologic regimes of the specific estuaries. A settling velocity of 1 mm/s may be an upper constraint for aggregates, but it is still important to understand aggregation dynamics because significant transport may occur before aggregation and because the efficiency of contaminant scavenging depends upon particle sizes and constituents (O'Connor, 1988).

This paper will explore aggregate size dynamics in three estuaries located relatively close to each other geographically, but with different physical and biological regimes. The first study area is the York River, VA, an energetic and physically dominated estuary. The second is the Cherrystone site in the lower Chesapeake Bay, which has a relatively energetic physical regime and a biologically dominated benthos. Lastly, the Elizabeth River, VA, a low energy, heavily polluted, urban estuary will be considered.

Particle Dynamics in Estuaries:

Factors that affect the formation and breakup of particle aggregates in estuaries include the degree of turbulent shear, differential settling of particles, Brownian motion, suspended sediment concentrations, prevalence of sticky polymer compounds from biota, and salinity. Previous work has found that in estuaries, physical processes in the water column are the most important of these, namely, turbulence, differential settling, and sediment concentration, although the organic constituent may also play an important role (Chen et al., 1994). Salinity has been postulated to affect the fragility of particle aggregates (Eisma et al., 1991a). However, the effects of varying salinity on flocculation are only important at concentrations of less than 1 to 3 (Gibbs et al., 1989), which is well below the levels in the estuaries under consideration in this paper. The relative importance of the physical factors listed above at different elevations in water column and in different environments will be used to identify separate depth dependent aggregation dynamic regimes and how they vary according to the environmental settings.

Suspended sediment concentration may be related to particle settling velocity via aggregate size through its effect on particle encounter frequency (e.g. van Leussen, 1994; Dyer, 1989). Variations in concentration might be expected to be important to particle size where there is a range of low concentrations, for example near the surface of the water column. This is suggested by the tidally varying size distribution and concentrations at the surface of the Elbe estuary found by Chen et al. (1994). A similar trend is seen in the more turbid environment of the Amazon R. estuary where Berhane et al. (1997) found a strong relationship between concentration and maximum aggregate diameter. Conversely, ten Brinke (1994) found in the Oosterschelde tidal basin that there was not a strict relationship between concentration and particle sizes, even at relatively low concentrations. Wolanski and Gibbs (1995) found in the very turbid Fly River Estuary that surface aggregate dynamics were dominated by tidal velocity rather than concentration. Gibbs et al. (1989) also found that maximum aggregates sizes did not

occur at the estuarine turbidity maximum in the Gironde Estuary where concentrations were highest. The effect of suspended sediment concentration on particle size is still unclear, and will be examined in this paper.

Turbulent shear in the water column also works to increase aggregate size through encounter frequency, but at the same time may limit the maximum attainable size. At low turbulence levels, particles may be in a growth stage where aggregate size increases with increasing turbulence. But as turbulent shear increases, it becomes limiting to the aggregate size when the length scale of the smallest turbulent eddies, characterized by the Kolmogorov microscale, reaches the same length scale as the aggregate diameters and the aggregate is torn apart (Berhane et al., 1997; Van Leussen, 1994) . The opposite effects of increased encounter frequency and increased shear on individual particles may work together to determine an equilibrium particle size for a given concentration and turbulence level (Chen et al., 1994). The mean particle size has been found to adjust rapidly to changes in turbulent shear (Chen et al., 1994, Gibbs et al. 1989). These paired processes of growth and destruction are likely to be important in the middle of the water column as well as near the bed.

Resuspension of particles from the bed is an important process affecting size distribution in the lower water column. Because particles on the bottom may be initially disaggregated by the turbulence which resuspends them, they may be reinput into the water column as smaller primary particles or aggregates. Conversely, primary particles or aggregates at the bottom may have had a chance to consolidate to form large robust aggregates (e.g. fecal pellets). In this case, higher stresses will be associated with resuspension of large aggregates and aggregate size is not directly related to the processes associated with turbulent shear described above.

Differential settling of particles may dominate the aggregation dynamics during times of reduced turbulent energy. The increase of encounter frequency without the destructive turbulent shear allows primary particles and aggregates sinking from the surface to form large aggregates in the middle water column. These falling particles may be concentrated in the pycnocline where their effective density approaches that of the higher density bottom water. Alternatively, if heavy enough, they may continue towards the bed where increased turbulent shear may disaggregate the particles or they may be

maintained at a constant size by the drag force of their sinking (Hill and McCave, 2001). Consequently, the effects of differential settling are most likely to be seen in the middle of the water column.

The amount of sticky organic material in the water column and particles mediates all of the above processes. Ten Brinke (1994) speculated that seasonal differences between aggregate sizes at comparable concentrations and elevations in the Oosterschelde tidal basin were caused by differences in the prevalence of sticky polymers from algae. Van Leussen (1999)found that the settling velocities varied for aggregates which had formed with the same mass concentrations along the Ems estuary. The difference was coined the 'flocculation ability' of the material, which is determined by the amount of dissolved organics in the water as well as the size of the primary particles which formed the flocs.

A last factor determining particle size distributions is the presence of a relatively constant background population of fine, 'truly suspended' particles. This background population may or may not be involved with the aggregation processes, but seems to persist in many estuaries at a concentration of around 15-30 mg/l (Fugate and Friedrichs, in press).

The above physical processes and factors are expected to have different degrees of importance at different depths depending upon the local depth varying hydrodynamics and proximity to different sources of particles. In addition, depth determined processes will be mediated by the overall hydrodynamic and biological conditions of the estuary. Particle size at the surface where suspended sediment concentration is low is expected to be dominated by the effect of concentration on encounter frequency. In the middle water column, at sufficiently high concentrations so that encounter frequency is not the limiting process, high turbulent shear is expected to limit aggregate growth. This was postulated by Chen et al. (1994) when they observed small particle dominance during periods of high velocity in the Elbe Estuary. At lower levels of turbulence, for example during slack tides, differential settling is expected to become the dominant process. Near bed size distributions are expected to mirror the type of size distribution of particles lying on the bed. Schubel (1971) found larger particles during periods of high velocity in the Chesapeake Bay and also attributed this to resuspension of bottom material. It is

postulated here that the near bed particle size distribution is dominated by resuspension, and that the response of the distribution to high bed stress is mediated by the benthic environment. High near bed stress in estuaries in which bottom sediment mixing is dominated by physical processes are likely to resuspend fine unconsolidated particles while high stress in estuaries whose benthos is biologically dominated is likely to resuspend consolidated aggregates and fecal pellets.

Measurement of Suspended Particle Properties:

Of particular difficulty in studying suspended sediment dynamics in estuaries is the high prevalence of sediment aggregates. Bulk water collection of these particles may result in disaggregation or further aggregation of the particles and can bias estimates of their size distribution, excess densities, and fall velocities. In situ instruments are therefore invaluable for studying aggregates, and simultaneous measurements from two or more of these instruments are desirable because they respond to different properties of the particles. Two in situ techniques used in this study that do not implicitly account for size are optical and acoustic backscatter. Optical Back Scatter (OBS) instruments respond to the cross sectional area of the particles, and are particularly sensitive to the size distribution of the suspended sediment. Changes in size distribution from that which is used to calibrate the OBS will cause biases in mass concentration estimates. Acoustic instruments with wave lengths much greater than constituent mineral grain size are less sensitive to aggregate size but are still sensitive to the particle density (Fugate and Friedrichs, in press), and similarly, changes in particle densities from that which are used to calibrate the instrument may cause biases.

A technique that explicitly accounts for particle size uses laser scattering. The Laser In Situ Scattering and Transmissometry (LISST) instrument is designed to measure size distribution in situ but is sensitive to the refractive index of the particles. Extensive descriptions of the instrument and its operation principles can be found in Agrawal and Pottsmith (1994; 2000)). The LISST works well in resolving unimodal silicate particle distributions (Battisto et al., 1999 Agrawal, 2000; Traykovski et al., 1999). However, the primary particle populations and loose aggregates found in biologically productive

estuaries are more complex than sand particles with respect to their refractive indices and size distributions, which may be multimodal with wide and narrow peaks or may be uniform (Kranck et al., 1996). Nevertheless, the LISST has been found to work reasonably well in qualitatively comparing size distributions in estuaries (Mikkelsen and Pejrup, 2000). The LISST used for this project measures particle distribution in the range of 5 to 500 microns, and the inversion routine is configured to determine the volume concentrations of 8 logarithmically spaced size classes within that range. Because of potential problems with measuring estuarine aggregates with the LISST, the median grain sizes reported here should not be taken as precise measurements but rather as an index with which to compare relative size distributions.

STUDY SITES

York River

About 50 km long with a central channel 10 meters deep, the York River empties into the Lower Chesapeake Bay just above the James R. (Fig. 2-1). It is partially mixed; average freshwater discharge is about 60 m^3/s (cms), and salinity at the mouth is around 20. (Friedrichs et al., 2000) Maximum vertical stratification during this study was 2.5 from top to bottom of the 10 meter depth. Near surface tidal currents can reach over 100 cm/s and dominate the physical energy regime, tidal range is 0.7 m at the mouth and 1 m at the head (Schaffner et al., 2001). The relatively deep channel and limited fetch generally prevent wind energy from making an important contribution to the hydrodynamic energy at the bottom. The study site is at 37° 22.2 ' N and 76° 38.2' W inside the main channel of the York. The width of the river there is 3.4 km., and there is a wide (2.4 km) shoal to the south of the main channel. Sediment enters the York from both the river and mouth (Nichols et al., 1991). Physical mixing in the soft muddy bed dominates bioturbation which may have mixing lengths up to a meter over a fortnightly time scale (Dellapenna et al., 1998). Maximum combined tidal, wave, and freshwater flow energies midway up the estuary length in the vicinity of the study site (Dellapenna et al., 1998).

Elizabeth River

In contrast to the York R., the Elizabeth River is a small, low energy, heavily industrialized and contaminated estuary. It is a partially mixed tributary of the James River located near the mouth of the James, which empties into the Southern Chesapeake Bay (Fig. 2-1). The distance from the mouth of the main stem of the Elizabeth R. to the head of its Southern Branch is 23 km., and the average depth of the main channel is about

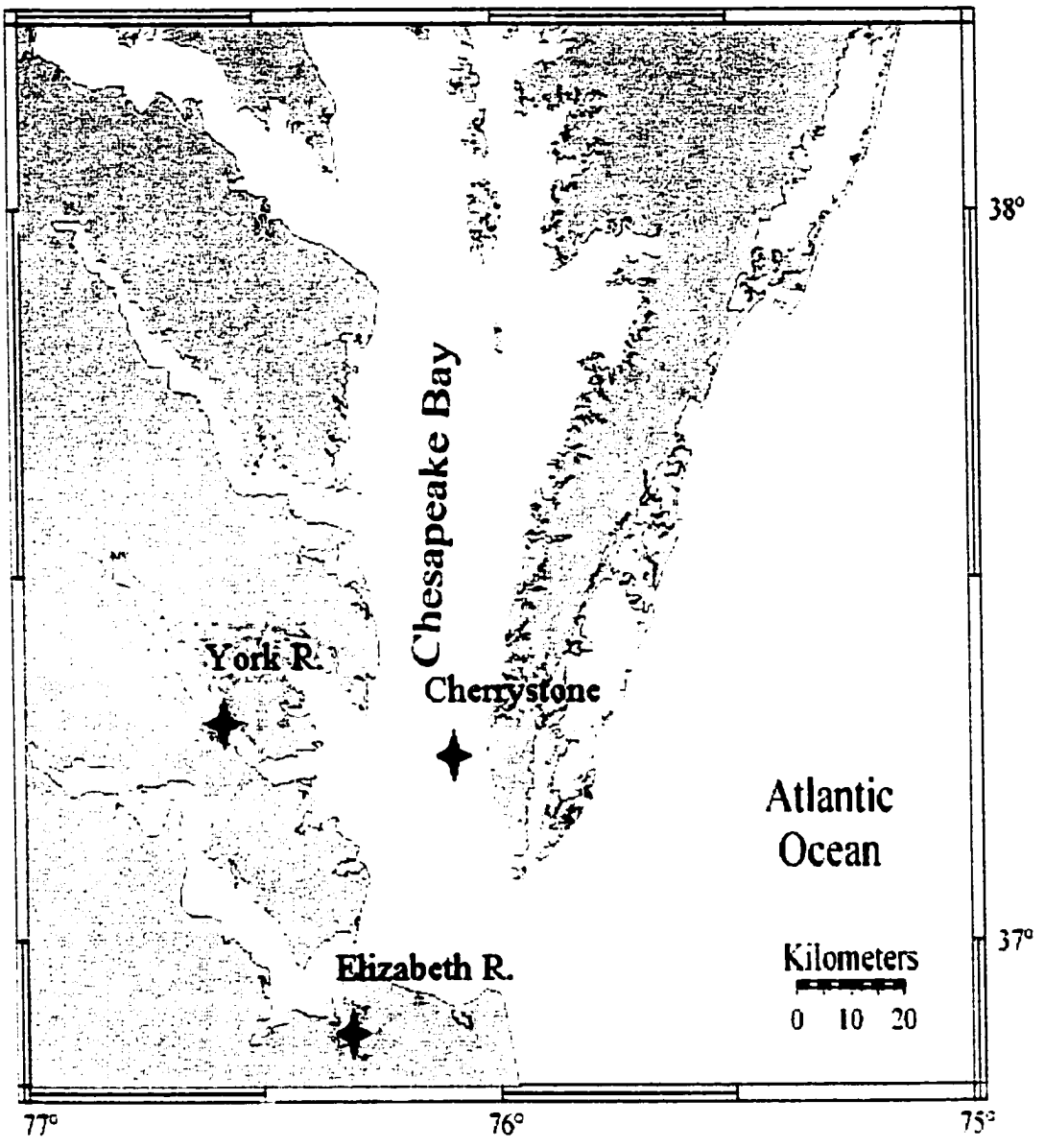

Fig. 2-1. Principle study site locations in Virginia, U.S.A.

12 meters. Freshwater input from the Dismal Swamp Canal at the head of the Southern Branch ranges from 11.9 m^3/s in February to 0.8 m^3/s in July. There is also a significant input of freshwater from point source effluents of sewage treatment plants which is of the same order of magnitude as the input from the Dismal Swamp Canal. Spring tide currents are around 50 cm/s and the tidal range is 80 cm. Wind energy probably does not significantly affect the bed due to the narrow and deep channel. Salinity during moderate freshwater flows in the Elizabeth R. and James R. ranges from around 17 at the mouth to 13 near the head. Vertical stratification in salinity under these conditions is about 5 between surface and bottom at the mouth and around 2 within the rest of the estuary (Neilson, 1975).

The main stem and two of the three major branches of the ER have undergone extensive industrial development since colonization of the area by Europeans in the 1600's (Nichols and Howard-Strobel, 1991). Dredging and infilling modified the geometry of the estuary from an irregular bottom profile with broad shoal and marsh areas to a regular, deeper, longitudinal stair step bottom profile with a narrower lateral extent. In addition, landing docks, extended piers and narrow dredged tributaries create significant lateral roughness in some extents of the river. The channel depth at our sampling site (36° 47.736' N and 76° 17.558 W) is maintained at 14 meters and the width is 40 meters.

Chesapeake Bay

The Chesapeake Bay is a large estuary of length 200 km and width of up to 30 km. The principal data set in the Chesapeake Bay is from the Cherrystone region. Data were collected in August 1996 at the Cherrystone site in the southern Chesapeake Bay (Fig. 2-1). This site and the nearby Wolftrap site have been extensively studied with regard to benthic biology, and bed characteristics (Lee, 1995; Schaffner, 1990; Thompson and Schaffner, 2001; Wright et al., 1992; Wright et al., 1997). The mean depth of the study site is 14 meters, mean tidal range is 0.6 meters, and salinities typically range from 17-23. The bed is soft and composed of fine sand and mud (Lee, 1995). Seasonally, benthic organisms such as *Chaetopteris pergamentaceus* and *Euclymene zonalis*

vigorously bioturbate the sediment (Wright et al., 1987). Data from the estuarine turbidity maximum (ETM) are used primarily to evaluate the analysis of turbulent energy production. The ETM is found in the upper bay where depths are generally around 4 m, but up to 12 m in the narrow shipping channel. The location of the ETM varies seasonally; our site was located at 39° 22.225' N and 76° 7.287 W at a depth of 12 m. Maximum tidal velocities were around 75 cm/s and tidal range is about 0.6 m.

DATA COLLECTION AND ANALYSIS

Hydrodynamic, physical, and geochemical data were collected similarly for each of the surveys. An instrument profiling lander, or 'profiler', containing a suite of physical and hydrodynamic instruments took vertical profiles of the water column about 8 times per tidal cycle. The sampling elevations in the Elizabeth R. were bottom, 1 meter above the bottom (mab), 3 mab, the middle of the water column (~6 mab, depending on the tide) and 1 meter below the surface. Sampling in the York was similar, but no data were collected at 3 mab. The Cherrystone site was sampled only at the bottom, and ADV's were mounted on a nearby tripod sampling 11 minute bursts every 15 minutes at 5 Hz. The ETM site was sampled irregularly because of equipment problems. All of the study sites except for the ETM site were sampled for 2 or more tidal cycles. Each elevation was sampled for a few minutes after which the profiler was left to continually sample at 1 mab until time for the next vertical profile.

The instruments on the profiler generally were a Sontek Acoustic Doppler Velocimeter (ADV) sampling at 10 Hz, a Downing Optical Back Scatter sensor (OBS) in conjunction with a Applied Microsystems 12+ CTD sampling at 1-2 Hz, a Sequoia Science Laser In Situ Scatterer and Transmissometer (LISST) sampling at 2 Hz, and a submersible pump intake at 30 cm above the bottom of the profiler. One liter bulk water samples were collected at each elevation and analyzed for Total suspended solids (TSS). Total suspended solids (TSS) were analyzed by passing a measured subsample through a preweighed 0.8 μm poresize glass fiber filter, followed by drying and weighing. Additional bulk water samples were taken for trace metal and nutrient analysis which are not considered in this paper. An upward looking Sontek Acoustic Doppler Profiler (ADP) was deployed nearby each profiling site sampling every 10 seconds with 0.25 meter depth bins. Indirect settling velocity estimations are made with the ADV backscatter using the method described in Fugate and Friedrichs (in press). The ADV

backscatter was calibrated to mass concentrations using the 1 mab to surface TSS values from the York R. (r^2=0.93).

RESULTS AND DISCUSSION

Hydrodynamics and Concentration

Time series of along channel velocities, salinities and acoustic backscatter (a proxy for sediment concentration) for the 3 estuaries are shown in panels a-c of Figs. 2-2 to 2-5. The York River and Chesapeake Bay velocities are much higher and more regular that those in the Elizabeth River. Along channel ebb velocities in the York R. reach 90 cm/s, in addition, there are significant cross channel velocities up to 15 cm/s. Upper water column velocity gradients were negative at the beginning of flood tides, but in general the vertical velocity profiles increase regularly upwards. Along channel velocities at the Cherrystone site are even higher than those of the York, reaching 100 cm/s during ebbs. Ebb velocities from the ETM in the upper Chesapeake Bay are over 80 cm/s. In contrast to these two estuaries, velocities in the Elizabeth R. are weak, maintaining currents up to 40 cm/s during spring tide, and rarely reaching that high during neap. The lower water column currents are quite irregular, reflecting the interaction of the mild currents with the narrow and unnaturally irregular geometry.

Time series of salinities for the three estuaries are shown in Figs. 2b-5b. The York R. data set shows typical stratification patterns of a partially mixed estuary, with ebb tides more highly stratified, about 17 to 14.5 from the bottom to the top of the 10 meter water column. Similarly, the Cherrystone site in the Chesapeake Bay is more stratified on ebb, around 23 to 17 over a 12 meter water column, but tending to become completely mixed after flood. The ETM site (not shown) is well mixed with low salinity at the beginning of flood, and only reaches a gradient of about 2.5 to 1.2 from the bottom to the top of the 12 meter water column near the end of flood. Two salinity figures are shown for the Elizabeth R., one over a neap tide and other over a spring (the profiler failed during part of the spring tide experiment). Stratification at the Elizabeth R. site

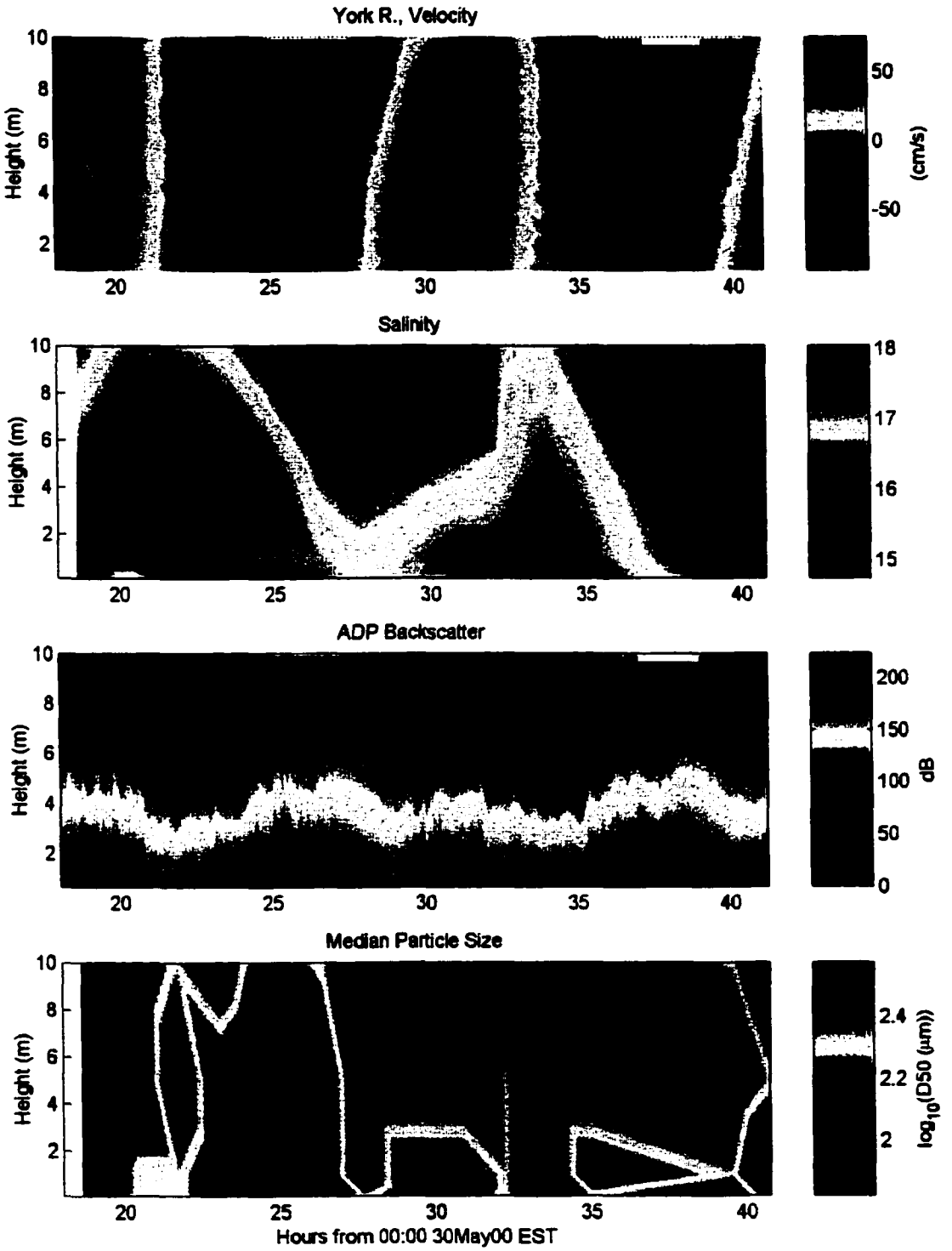

Fig. 2-2. Time series of York R. Physical Data. (a) Velocity (cm/s), flood positive, (b) Salinity, (c) ADP Backscatter (dB), (d) $\log_{10}$ (Median Particle Size (μm)).

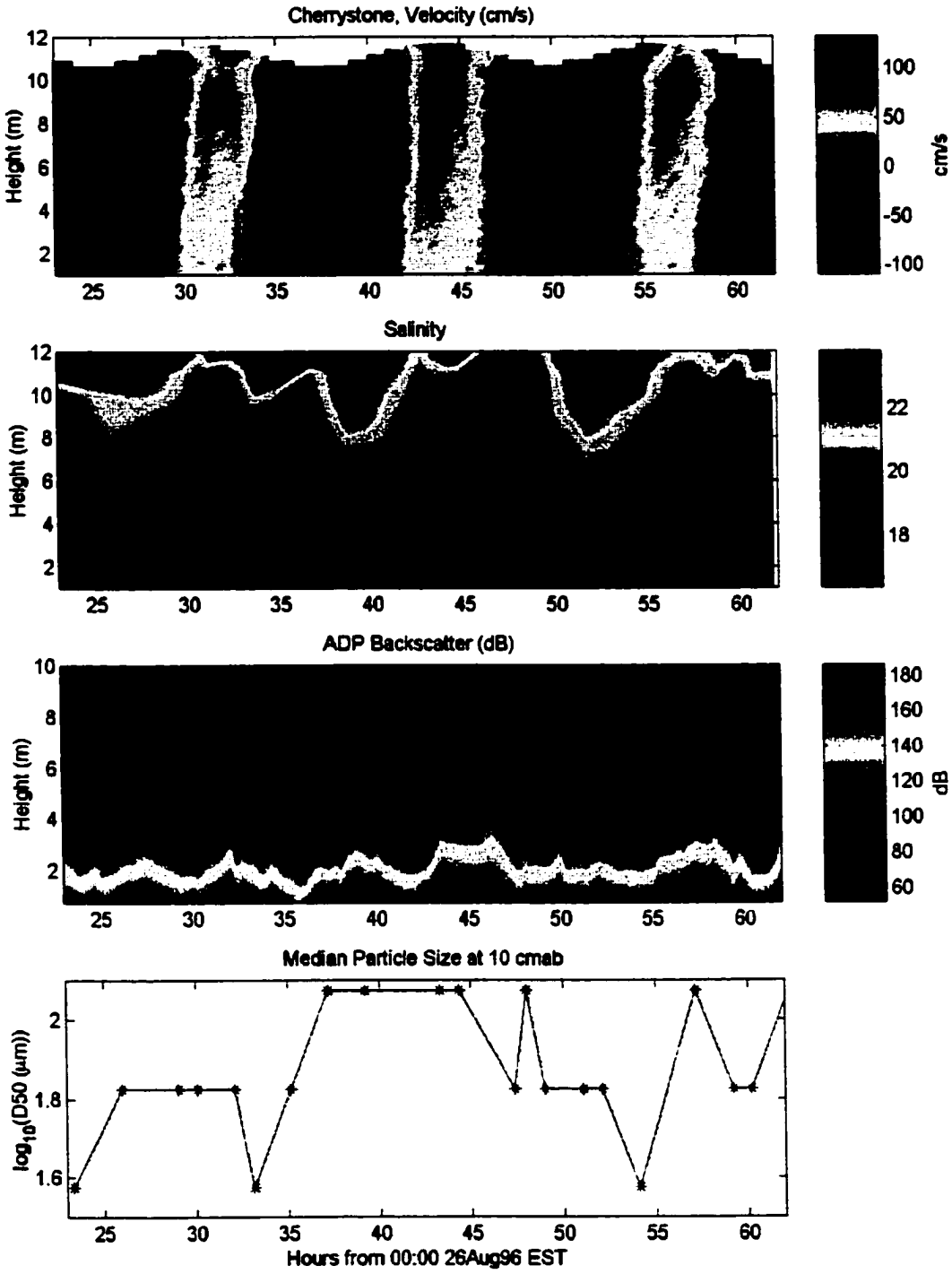

Fig. 2-3. Time series of the Cherrystone Site Physical Data. (a) Velocity (cm/s), flood positive, (b) Salinity, (c) ADP Backscatter (dB), (d) $\log_{10}$ (Median Particle Size (μm)) at 10 cmab.

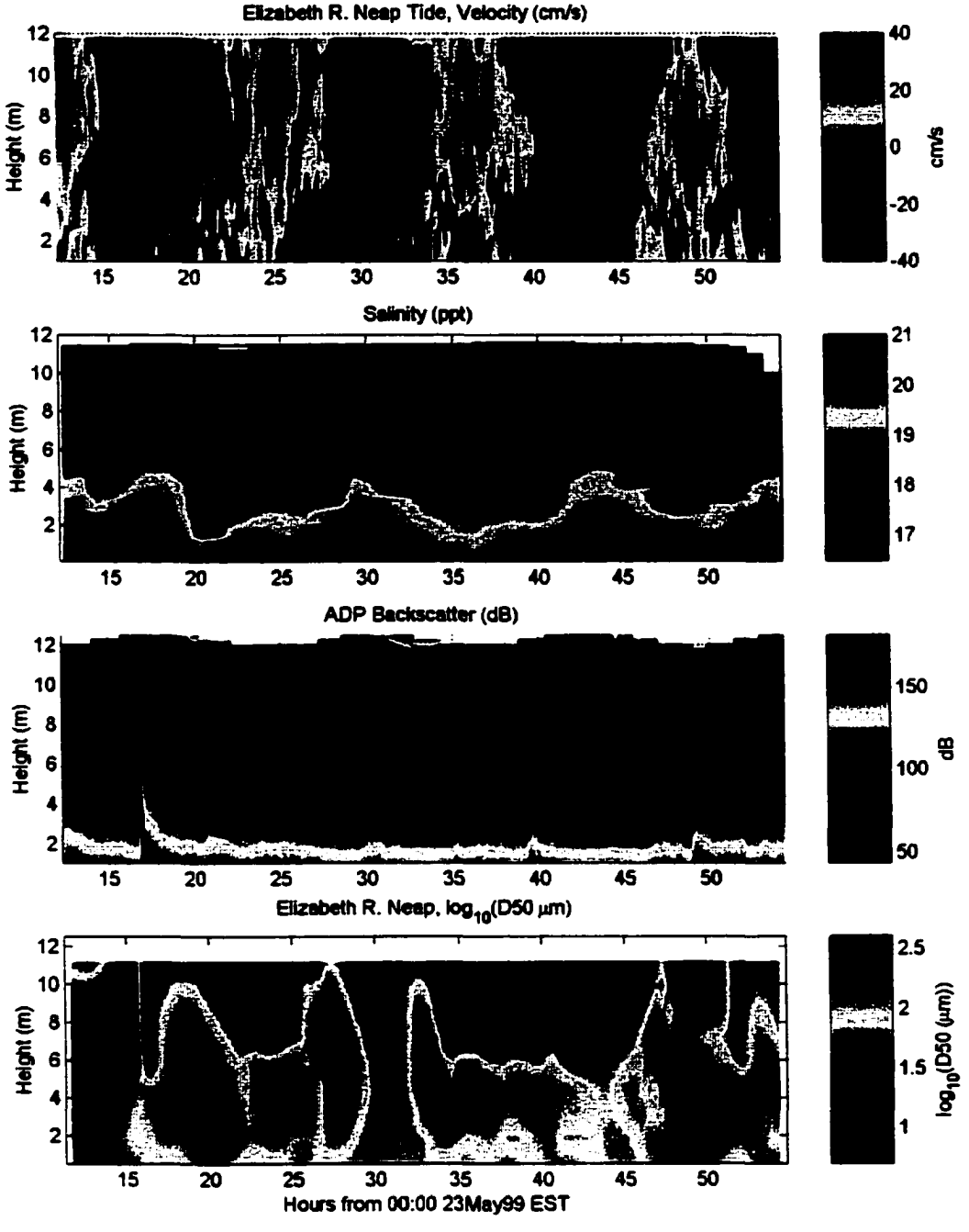

Fig. 2-4. Time series of Elizabeth R., Neap Tide Physical Data. (a) Velocity (cm/s), flood positive, (b) Salinity, (c) ADP Backscatter (dB), (d) $\log_{10}$ (Median Particle Size (μm)).

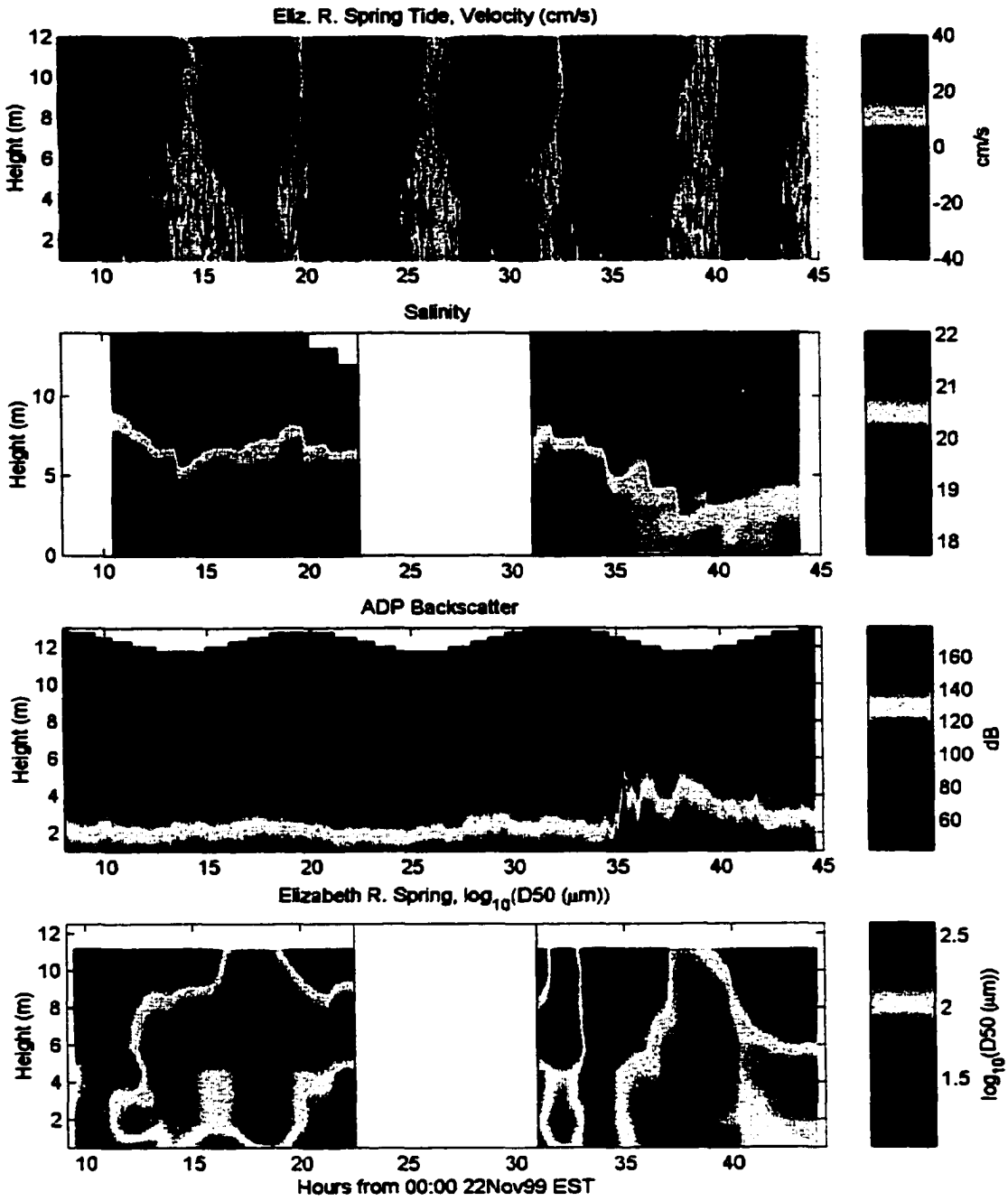

Fig. 2-5. Time series of Elizabeth R., Spring Tide Physical Data. (a) Velocity (cm/s), flood positive, (b) Salinity, (c) ADP Backscatter (dB), (d) $\log_{10}$ (Median Particle Size (μm)), Profiling instruments were inoperable during a portion of the experiment.

ranges are similar to the Lower Chesapeake Bay, around 23 to 17 over a 12 meter water column ranging to well mixed. Maximum density gradients during neap are centered around 4.5 mab during ebb and around 2 mab during flood.

Time series of suspended sediment concentration as represented by the ADP backscatter are shown in Fig.s 2-2c to 2-5c. Suspended sediment concentrations were highest in the York, with bottom concentrations ranging from 50 mg/l to over 300 mg/l. Resuspension during ebb is slightly higher than resuspension during flood, consistent with higher velocity on ebb. Surface concentrations peaked near 40 mg/l. Bottom concentrations in the Lower Chesapeake ranged from 15 mg/l to over 70 mg/l. The suspended sediment profile at the ETM in the Bay is much 'peakier', suggesting a higher fall velocity than the sediments found in the York and Elizabeth R. (consistent with resuspension of lots of dense aggregates.) Suspended sediment concentrations were generally high at the ETM site, ranging up to 170 mg/l. Concentrations in the Elizabeth R. are much lower than the other estuaries in both surveys shown, usually below 10 mg/l at the bottom, reaching near 20 mg/l at peaks. During neap tide the middepth water column shows occasional concentration peaks during slack phases (hours 24, 29, and 40) and the surface shows higher concentrations during ebb. These surface peaks are corroborated by the OBS signal, and are not artifices of surface anomalies on the ADP. Spring tide sediments are resuspended higher into the water column than neap. During spring tide there is a tidal signal of bottom peak concentrations during flood. Suspended sediment concentration is dominated by a resuspension event after the passage of a large cargo ship at hour 34.

Measurement of Turbulent Energy Production with Contaminated Data

Under ideal conditions, the high frequency sampling rate (10 Hz) of the ADV should allow measurement of the turbulent energy production in the water column through:

$$P = \tau \frac{dU}{dz}$$

(e.g. Nezu and Nakagawa, 1993) where P is energy production, τ is shear stress, and dU/dz is the vertical velocity gradient, and either:

$$\tau = \rho(-\overline{u'w'})$$

(e.g. Dyer, 1986) where ρ is density, and $-\overline{u'w'}$ is the Reynolds stress, or the empirical relationship:

$$\tau = C \times TKE$$

(Gordon and Dohne, 1973; Kim et al., 2000; Soulsby, 1983; Stapleton and Huntley, 1995), where C is a constant and TKE is turbulent kinetic energy measured by the ADV. With the profiler resting on the bottom, shear stress may be measured directly in the form of Reynolds stress as well as TKE. However, measurements further up in the water column are partially contaminated by boat motion and the dangling motion of the ADV on the deployment line. This motion can be seen as a low frequency (~0.4 Hz) peak in the spectra of the velocity components as shown in a typical record from the Elizabeth R. neap tide survey (Fig 2-6a).

In order to make estimates of the turbulent energy structure in the water column from the potentially contaminated ADV data, an alternate method is proposed and compared to estimates of energy dissipation made at the bottom using Reynolds stress. Because the bottom data were taken with the profiler resting on the bottom, they do not suffer from problems with boat or dangling motions. The alternate method is further compared with estimates made higher in the water column, and from different hydrodynamic environment, using the Kolmogorov –5/3 law.

Total kinetic energy (TKE) is first calculated in the standard method, $TKE = 0.5\left(\overline{u'^2} + \overline{v'^2} + \overline{w'^2}\right)$, from the 3 fluctuating velocity components, u', v', and w'. Velocity components for each burst are then high pass filtered with a cutoff at 1.5 Hz and a 3 point taper. The cutoff frequency was determined empirically from observation of the velocity spectra which contained no obvious peaks in spectral density at frequencies higher than 1.5 Hz. Most peaks occur at frequencies less that 1 Hz. The turbulent kinetic energy contained in only the high frequency fluctuations of the 3 components is then calculated from these filtered series. An additional modification is made by using the median of fluctuating velocities instead of the mean. ADV data from the principal datasets in this study often contain short episodes of electrical noise, whose bias can be minimized by using medians of the fluctuating velocity components. It is possible that this method produces an alternate negative bias in the estimate of true TKE if intermittent turbulent bursting is important. However, examination of the ETM data suggests that this bias is minimal or nonexistent. This quantity obtained from the sum of the median fluctuating high frequency velocity components will be called TKE_h. The velocity shear (dU/dz) is also needed to obtain a proxy estimate of the turbulent kinetic energy production via $TKE_h \times dU/dz$. Figure 2-7 shows that there is a good relationship between turbulent energy production estimated with a Reynolds stress at the bottom and the quantity $TKE_h \times dU/dz$ (r^2=0.61).

A further comparison is made of this alternate method with estimates of energy dissipation from higher in the water column where the ADV data actually suffered contamination from boat motion. Instead of comparing against production calculated from estimates of Reynolds stress which will also be contaminated by boat motion, the Kolmogorov -5/3 law and Taylor's frozen turbulence hypothesis is used to estimate TKE dissipation:

$$\varepsilon = \left[S(\omega)\omega^{5/3}U^{-2/3}\alpha^{-1}\right]^{3/2}$$

(Gross et al., 1994) where ε is energy dissipation, $S(\omega)$ is the spectral density of wave frequency ω, U is the mean current, and α is an empirical constant set to 0.48 (Kim et al.,

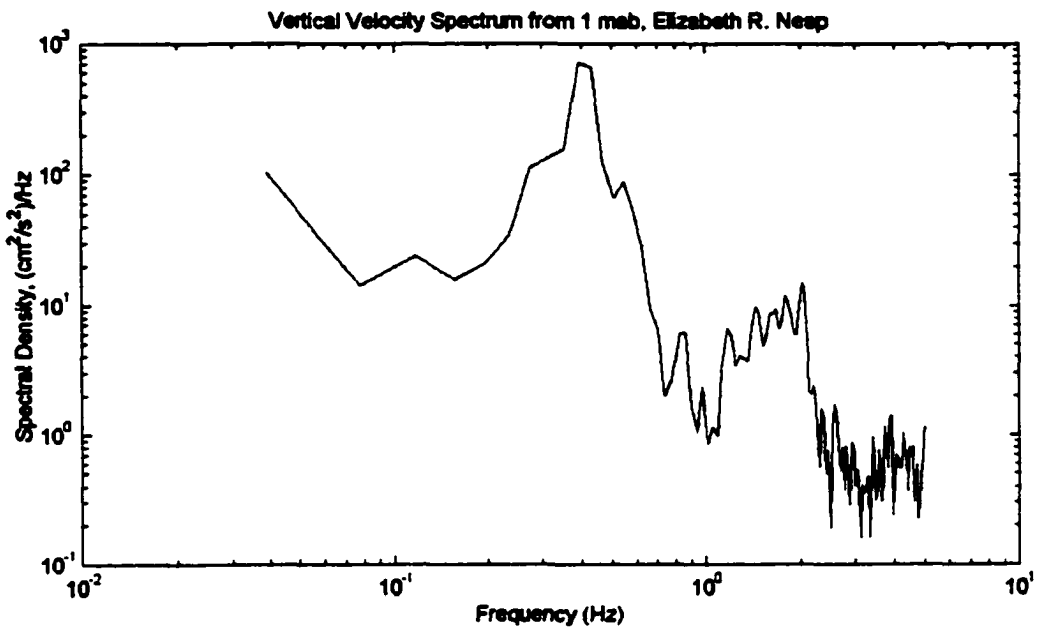

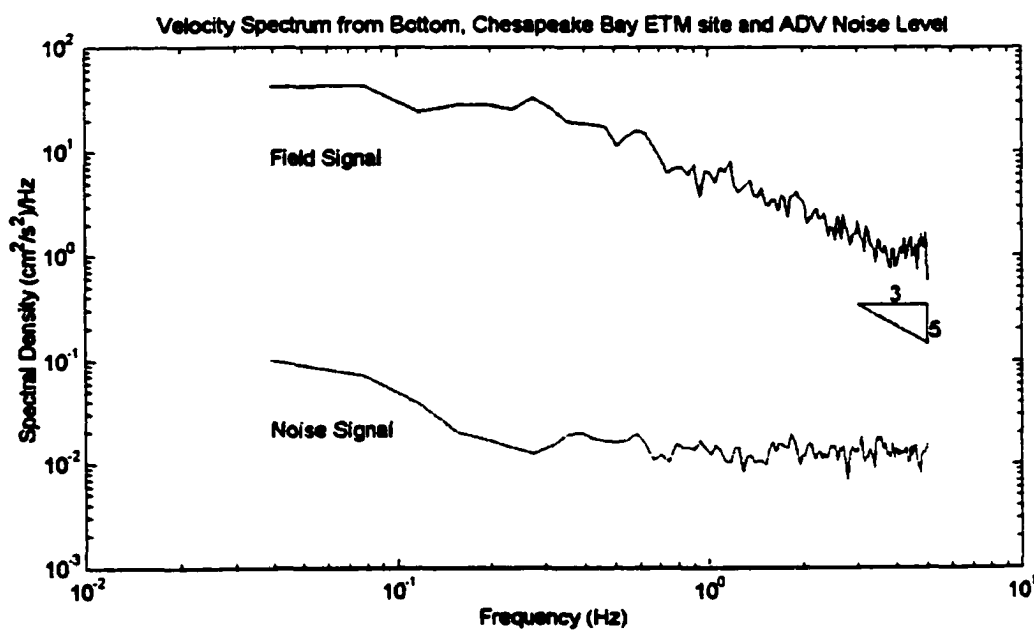

Fig. 2-6. Spectral Density from selected ADV bursts. (a) Elizabeth R. Neap Tide, 1 mab, (b) Top spectrum is from Chesapeake Bay, ETM site, bottom spectum is from ADV noise experiment.

2000) . When applicable, this method should produce a robust estimate of the energy dissipation since the presence of an inertial subregion implies that kinetic energy is neither input nor dissipated in this range. Thus, information from these frequencies is not liable to bias from the lower frequencies where the contamination typically occurs.

It would be desirable to use the Kolmogorov -5/3 law itself to estimate energy dissipation from the data. However, there are several problems with application of this method with the principle datasets. An inertial subregion is often missing from the spectra in the York and Elizabeth R. datasets, suggesting that the frequencies of energy input and dissipation are not sufficiently distant from each other. Also, in order to apply Taylor's frozen turbulence hypothesis, the time scale of rotation of the turbulent eddies must be much longer than the time required for the mean velocity to advect the eddy past the sensor (Gross et al., 1994). This condition is often not met in the low energy environment of the Elizabeth R. Finally, buoyancy production in the stratified York and Elizabeth R. is potentially a significant sink for turbulent energy such that dissipation alone may not balance turbulent energy production.

The upper portion of the Chesapeake Bay, VA is an environment more amenable to application of the Kolmogorov -5/3 law, and allows comparisons of energy production estimates made by $TKE_h \times dU/dz$ with energy dissipation further up in the water column. Velocity spectra from this site usually have distinct inertial subregions (e.g. Fig. 2-6b), and tidal velocities are relatively high. Insignificant density stratification at this site permits the assumption that turbulent kinetic energy production is balanced by dissipation over the relatively short time scales of interest, and that any energy consumed in buoyancy production is insignificant. Since the ADV on the profiler was hanging by a cable, dangling and wave motions constantly adjusted its orientation. For this reason, and the fact that the fin on the profiler maintained a rough orientation into the current, velocity components have not been rotated in these calculations. Minimum contamination from this motion is expected in the vertical component of velocity, especially as the profiler neared the bottom. For bursts in which an inertial subregion could be identified in the upper Bay data, energy dissipation was calculated from the vertical component of velocity spectra using Kolmogorov's 5/3 law and the median value of $S(\omega)\,\omega^{5/3}$ within the subregion.

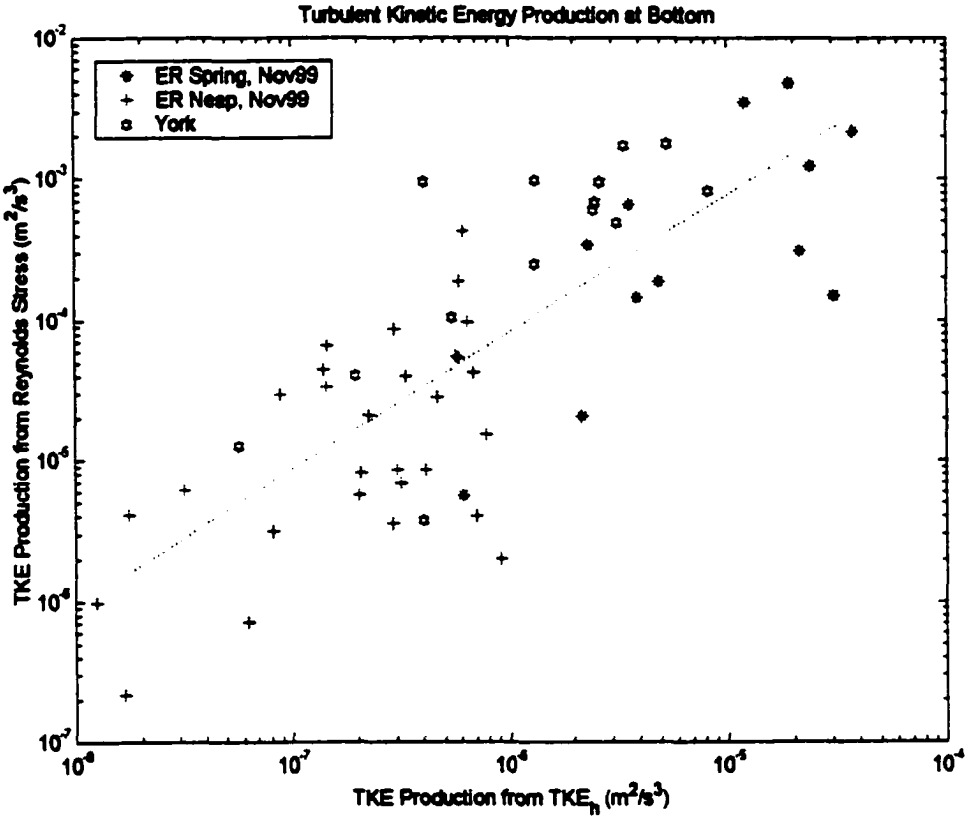

Fig. 2-7. TKE production as measured by Reynolds stress at the bottom from the Elizabeth R., Spring Tide (*), Elizabeth R. Neap Tide (+), and York R. (hexagon) compared with TKE production as measured by $TKE_h \times dU/dz$. This relation is used to calibrate the $TKE_h \times dU/dz$ values.

The quantity $TKE_h \times dU/dz$ for the upper Chesapeake Bay data is compared with the energy dissipation obtained by the -5/3 law in Fig. 2-8b. Excluding one observation, there is a good relationship between the $TKE_h \times dU/dz$ and dissipation (r^2=0.73), while the same quantity measured using the standard TKE was a poor predictor of the energy dissipation (Fig. 2-8a, r^2=0.14). Figure 2-9 shows the relationship between horizontal velocity, depth and both energy dissipation estimated by the –5/3 law and the proxy for turbulent energy production given by $TKE_h \times dU/dz$. There is a general trend of higher production and dissipation near the bottom than further up in the water column, and there are two distinct depth determined relationships with mean total horizontal velocity. At the bottom, higher velocities result in larger values of energy production and dissipation. Further up in the water column, increased velocities result in decreased production and dissipation. This relationship results from a decreased velocity shear at the surface where the velocities are higher. In Figs. 2-7 and 2-8, vertical velocity shear is determined from the ADP at 1, 4, and 7 meters above the surface (mab). For each sample in the bottom to the middle of the water column, the median dU/dz between 4 and 1 mab of the previous 15 minutes up to the sampling time was used to estimate vertical velocity shear. Similarly, samples in the upper water column were assigned the velocity shear between 4 and 7 mab.

While the relationship between the Kolmogorov dissipation estimates and $TKE_h \times dU/dz$ production estimates is strong, the magnitudes of the Kolmogorov estimates seem rather high compared to many estimates from flumes, shallow channels and shelf environments. For example, Nikora et al. (1994) found energy dissipation from 0-6 $\times 10^{-4}$ m^2/s^3 in a 1 meter deep canal with mean velocity 55-75 cm/s. Gross and Nowell (1985) found energy dissipation from 0-3$\times 10^{-4}$ m^2/s^3 in an irrigation canal of 4 meters depth with velocities from 60-90 cm/s. Gross et al. (1994) got estimates of energy dissipation from 10^{-7} to 10^{-5} m^2/s^3 from spectral analysis of the bottom boundary layer on the central shelf. However, in the Hurunai R., Nikora and Smart (1997) found energy dissipations from 6×10^{-3} to 1.2×10^{-1} m^2/s^3, closer to the estimates found here for the ETM of the Chesapeake Bay. Nevertheless, since the bottom Reynolds stress estimates

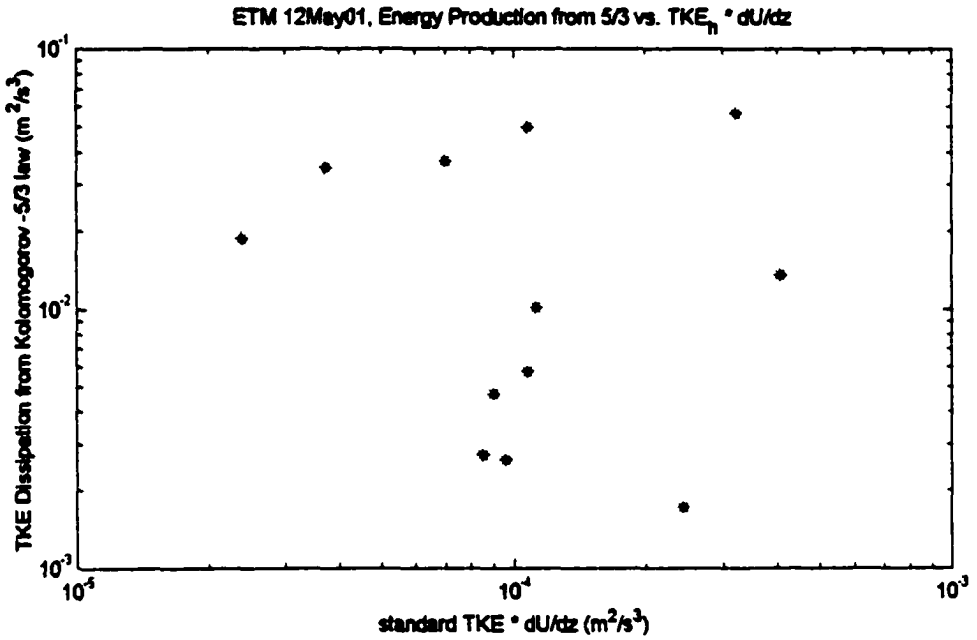

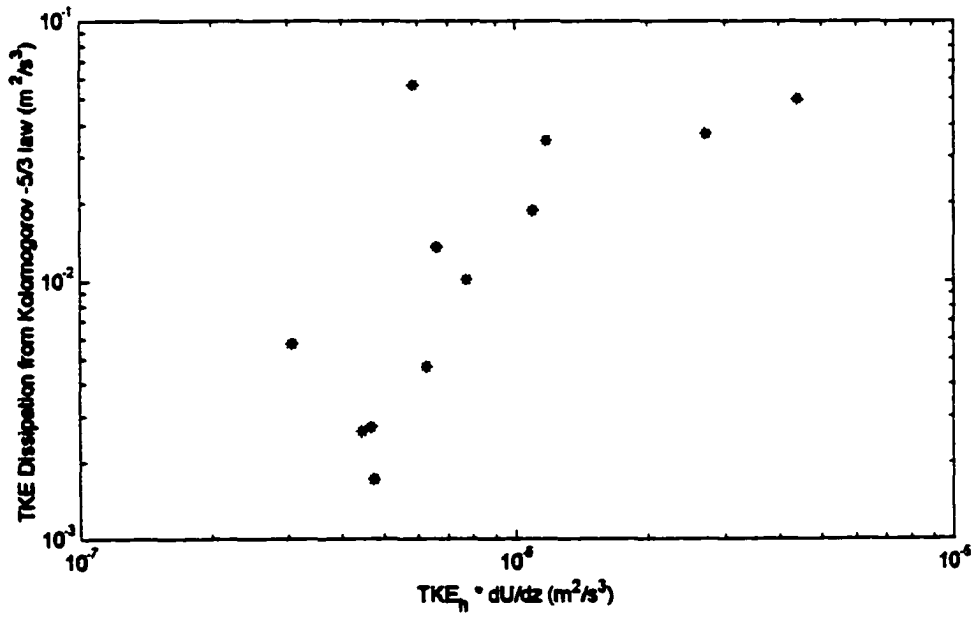

Fig. 2-8. (a) TKE production as measured using Kolmogorov –5/3 law from the ETM site, Chesapeake Bay compared with TKE production as measured by the standard TKE×dU/dz, (b) TKE production as measured using Kolmogorov –5/3 law from the ETM site, Chesapeake Bay compared with TKE production as measured by TKE $_h$×dU/dz.

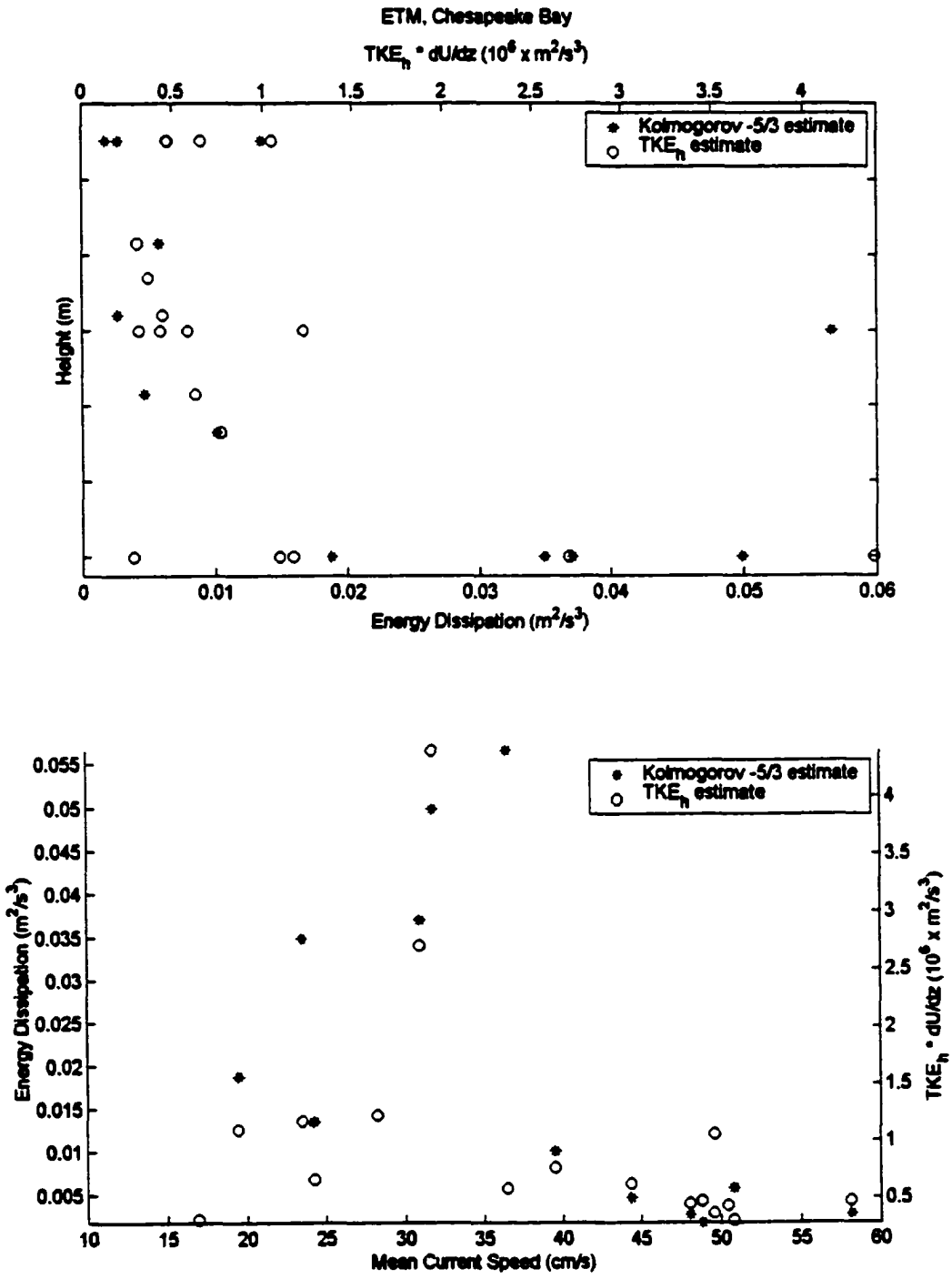

Fig. 2- 9. TKE production as measured using Kolmogorov –5/3 law from the ETM site, Chesapeake Bay (*) and TKE production as measured by $TKE_h \times dU/dz$ (circle) by (a) height above the surface (m), and, (b), mean current speed (cm/s).

seem to be more reasonable compared to most other studies, this is the curve which will be used to calibrate TKE_h * dU/dz values to turbulent energy production.

The high frequency region of the velocity spectrum where the inertial subrange usually occurs is also the region most prone to errors from noise in the ADV measurements. Some sources of error in the ADV record are: Particles moving in and out of the sampling volume during a measurement; particles moving at different speeds within the sampling volume; errors in calculating the Doppler phase shift from a host of factors which broaden the acoustic spectral peak of the transmitted pulse. In addition, smaller velocity ranges result in higher precision (Nikora and Goring, 1998; Voulgaris and Trowbridge, 1998). The type and concentration of particles also make a difference to the amount of noise generated. Nikora and Goring (1998) found that bubbles resulted in 4 to 5 times more noise than glass seeds, and silt particles 2 to 3 times.

In order to get a gross estimate of the noise generated by the ADV, an experiment was set up according to the procedure suggested by Nikora and Goring (1998). Measurements were made in a 5 gallon plastic bucket containing estuarine water and particles from the bottom, middepth and surface of the York R. The ADV was mounted so that the sensors were in the middle of the bucket and not affected by proximity to the solid surfaces. The setup was allowed to sit for 10-15 minutes so that there would be no water motion, and the top was protected from wind disturbance. Ten to fifteen minute bursts were recorded in each of the three bulk water samples. This method will still not measure the amount of noise generated by small scale turbulence (i.e. motion of particle relative to one another), however, it should give a gross estimate of the other sources of noise. Spectral plots of the noise generated were flat and very low, about 2 orders of magnitude lower that the spectral density levels where the inertial subregions were found in the above calibration (see Fig. 2-6b). Consequently, ADV noise turns out to be insignificant to the measures of TKE dissipation. This result is consistent with Nikora and Goring's findings which found an average ratio of corrected to uncorrected mean velocity fluctuations of 0.98.

TKE Production Results

Time series of turbulent kinetic energy production in the York R. is shown by depth in Fig. 2-10a and as tidal phase diagrams in Fig 10b-10e. TKE production ranged from 4.4×10^{-6} to 6.4×10^{-4} m^2/s^3. Local minima occur at middepth during slack tides, and maximum values occur with peak ebb currents. Despite the peaks at ebb, there is a general symmetry of TKE production about zero velocity. The phase diagram of the surface values shows the effects of tidal acceleration. High currents are initially accompanied by high values of TKE production. As the vertical velocity shear drops, TKE production also drops even though the current velocity is still high. Time series and phase diagrams of near bed (23 cmab) TKE production at the Cherrystone site are shown in Figs. 2-11a and 2-11b. TKE production ranges from 3.0×10^{-8} to 1.1×10^{-4}. The phase figure suggests that there are two distinct relationships between velocity and TKE production during ebb, both of which are steeper than that during flood (observation at ~0 cm/s and TKE production = 3.0×10^{-8} omitted from phase figure).

Figure 2-12a shows time series of turbulent kinetic energy production in the Elizabeth R. during spring tide by depth and Fig.s 2-12b to 2-12e show the values as tidal phase diagrams. TKE production ranged from 3.4×10^{-6} to 2.8×10^{-3} m^2/s^3. Local minima tend to occur at slack or slightly ebbing currents. The largest change in production appears right around hour 38 when TKE production drops significantly throughout the water column. This is concomitant with a slack after flood and is soon after the passage of a large cargo vessel at hour 35, both of which may have contributed to mixing of the water column (see Figs. 2-5b,c). In contrast to the York R., middepth maxima tend to occur during flood tides. Considered in the context of strain induced partial stratification, these results suggest that production of TKE in the York and at Cherrystone is dominated by the effects of the velocity shear component of TKE production, which is stronger during ebb. In contrast, production of TKE during a spring tide in the Elizabeth R. is stronger during flood, when mixing by the TKE component dominates production. Time series of turbulent kinetic energy production in the Elizabeth R. during neap tide are shown by depth in Fig. 2-13a and as tidal phase diagrams in Figs. 2-13b to 2-13e. TKE production ranged from 3.4×10^{-6} to 2.8×10^{-3} m^2/s^3. While local minima and maxima are

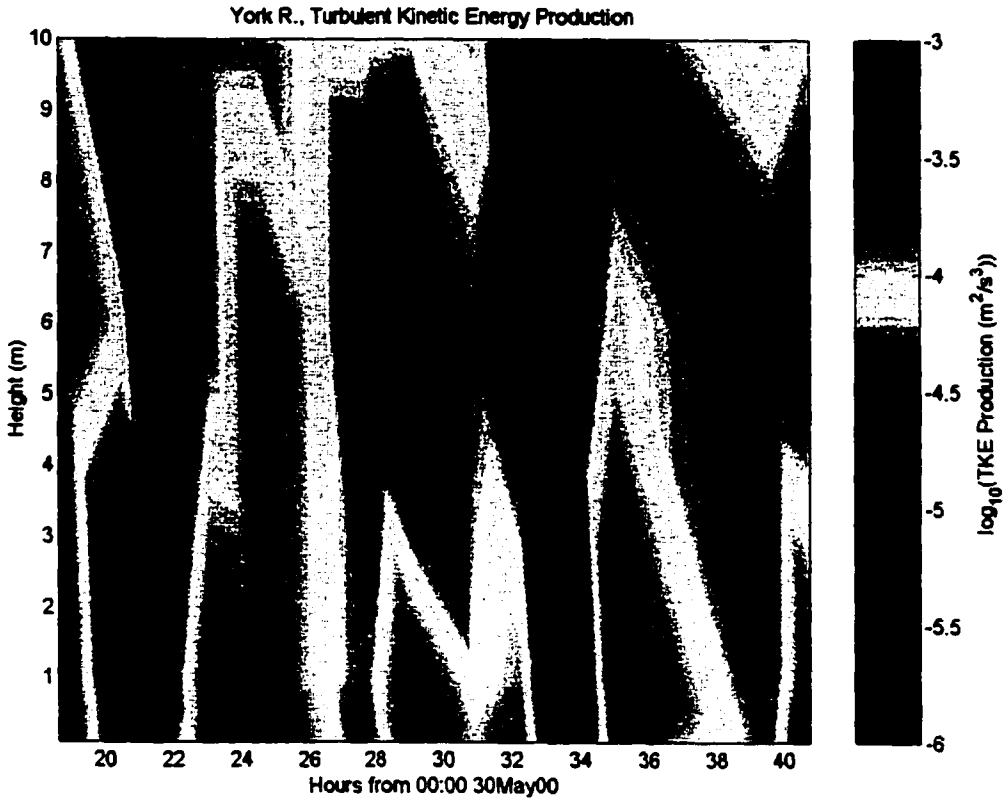

Fig. 2-10 (a) Time series of turbulent kinetic energy production (m^2/s^3) for the York R.

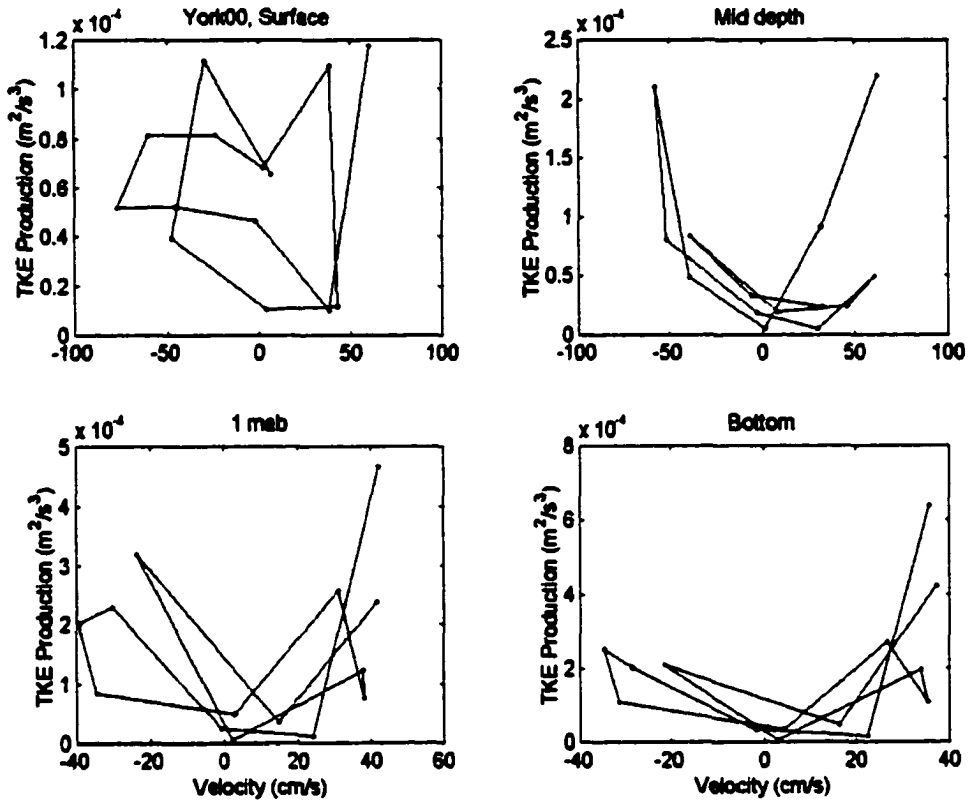

Fig. 2-10 cont. Tidal phase diagrams of TKE production (m^2/s^3) for the York R. Flood velocities are positive. (b) Surface, (c) Middepth, (d) 1 mab, (e) Bottom.

generally associated with slack and peak currents respectively, there is a lot of scatter in the data due to the weak and irregular currents during neap.

Maximum TKE production in the two energetic estuaries appears to be of the same order of magnitude as that in the low energy Elizabeth R. This is an artifact of the calibration curve (Fig. 2-7). Notice that TKE production values as estimated via Reynold's stress for the York River are generally higher than those for the Elizabeth River, so that the predictions associated with the York tend to underestimate TKE production. Separate calibration curves might be more appropriate if the emphasis were on comparisons between estuaries. Nevertheless, the more general calibration curve is suitable for comparing relative TKE production with particle size within each estuary, which will be undertaken in the next section.

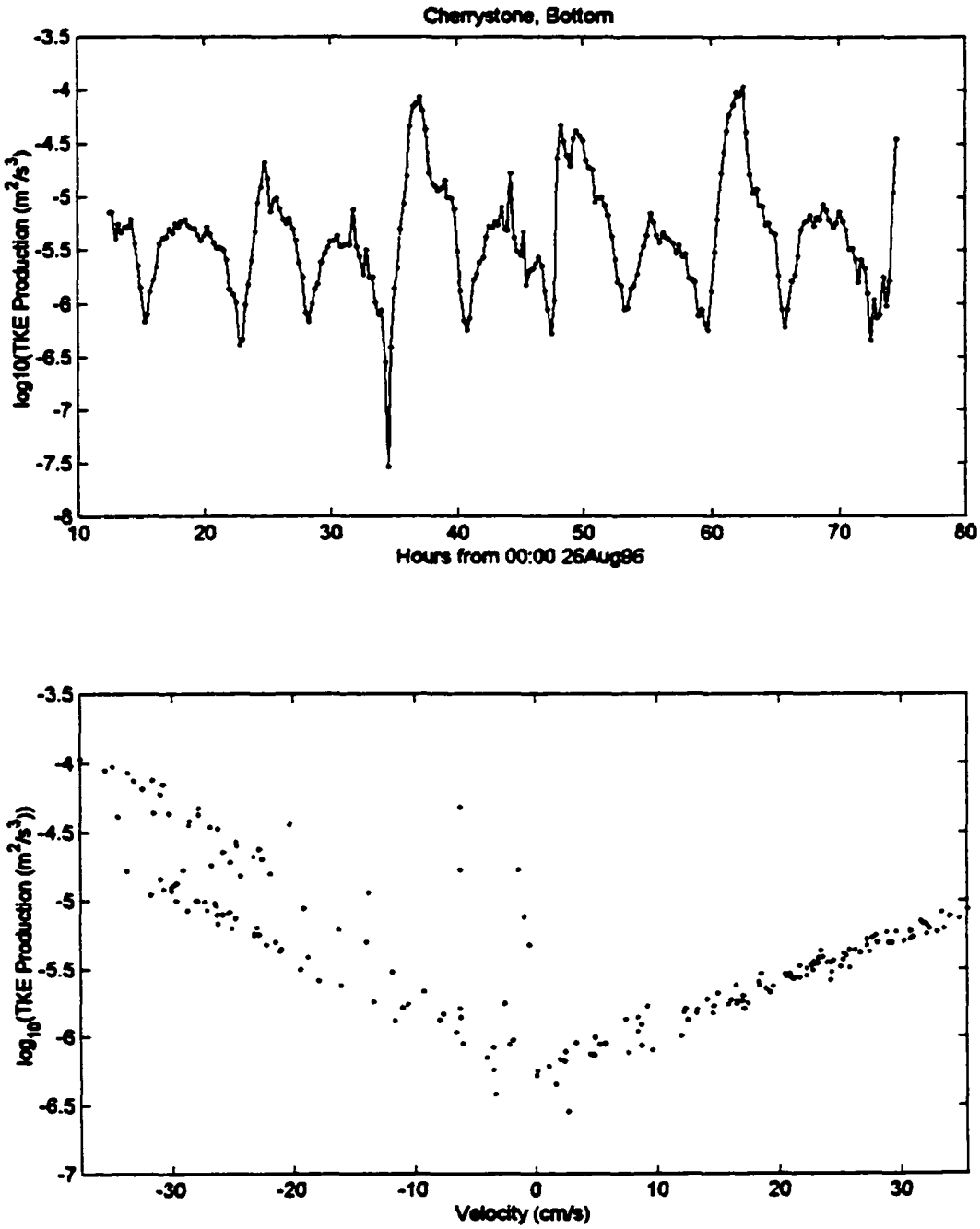

Fig. 2-11. Near bed (23 cmab) turbulent kinetic energy production at the Cherrystone Site. (a) Time series, (b) by velocity, flood values are positive.

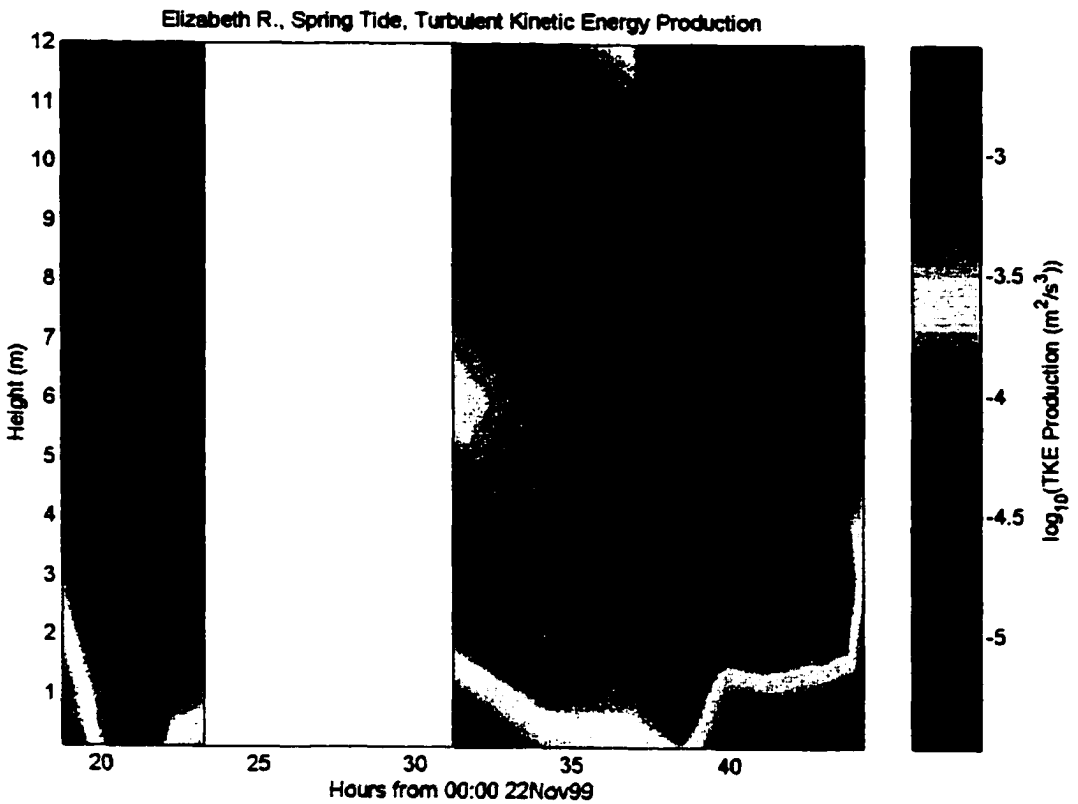

Fig. 2-12. (a) Time series of turbulent kinetic energy production (m^2/s^3) for the Elizabeth R., spring tide.

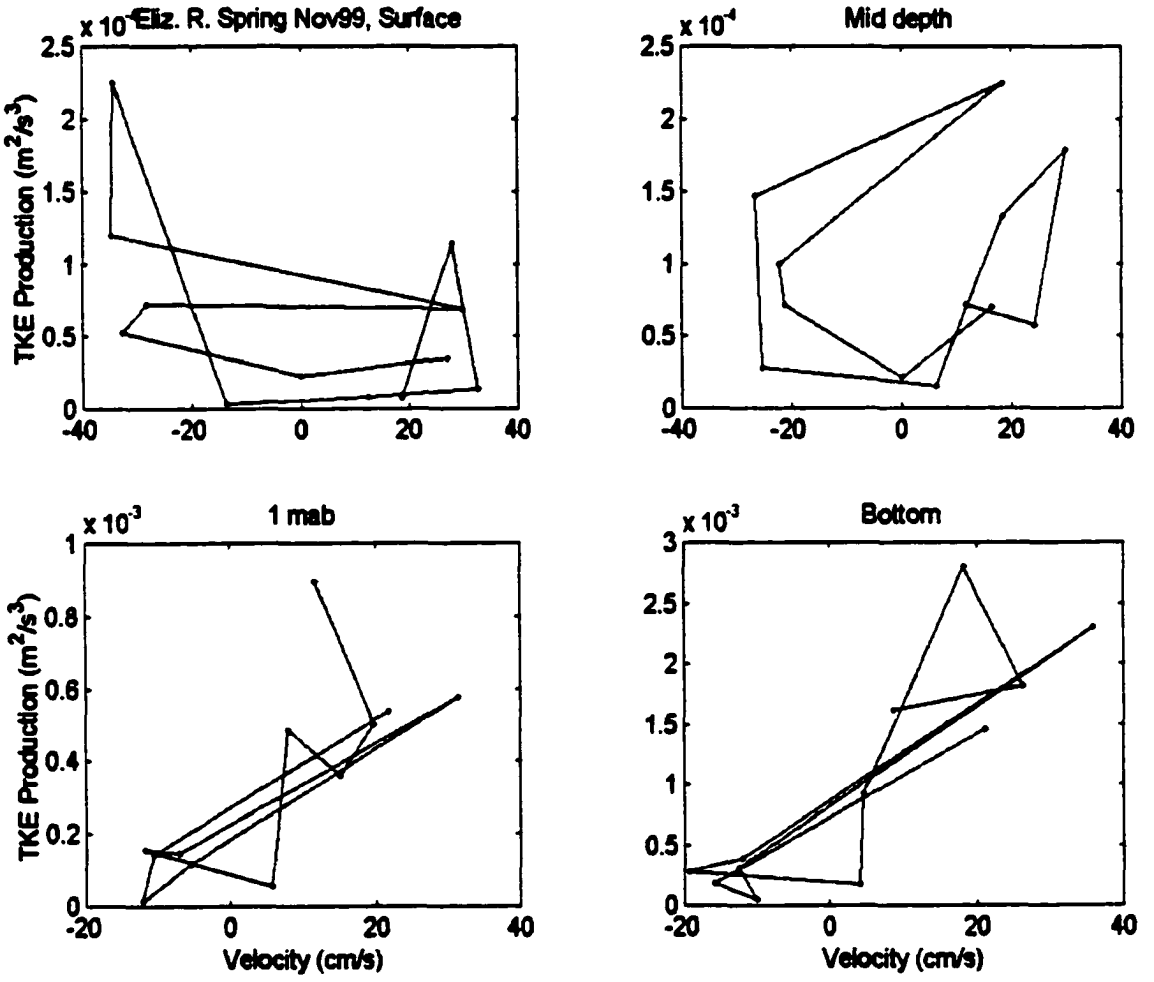

Fig. 2-12 cont. Tidal phase diagrams of TKE production (m^2/s^3) for the Elizabeth R., spring tide. Flood velocities are positive. (b) Surface, (c) Middepth, (d) 1 mab, (e) Bottom.

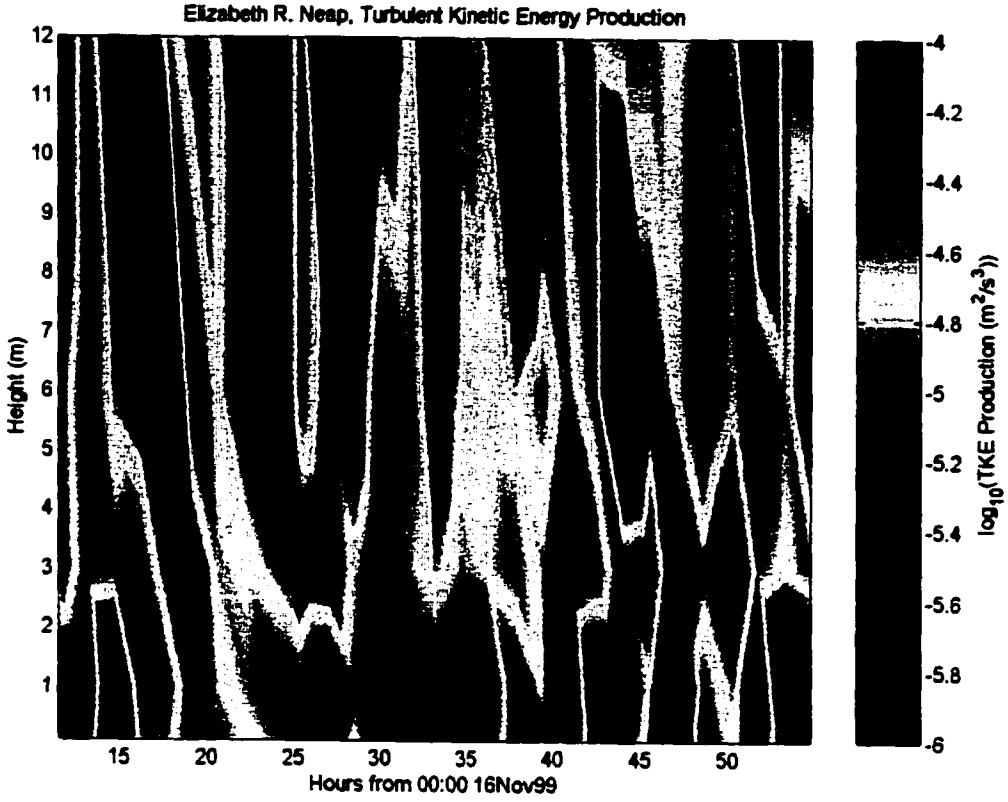

Fig. 2-13. (a) Time series of turbulent kinetic energy production (m^2/s^3) for the Elizabeth R., neap tide.

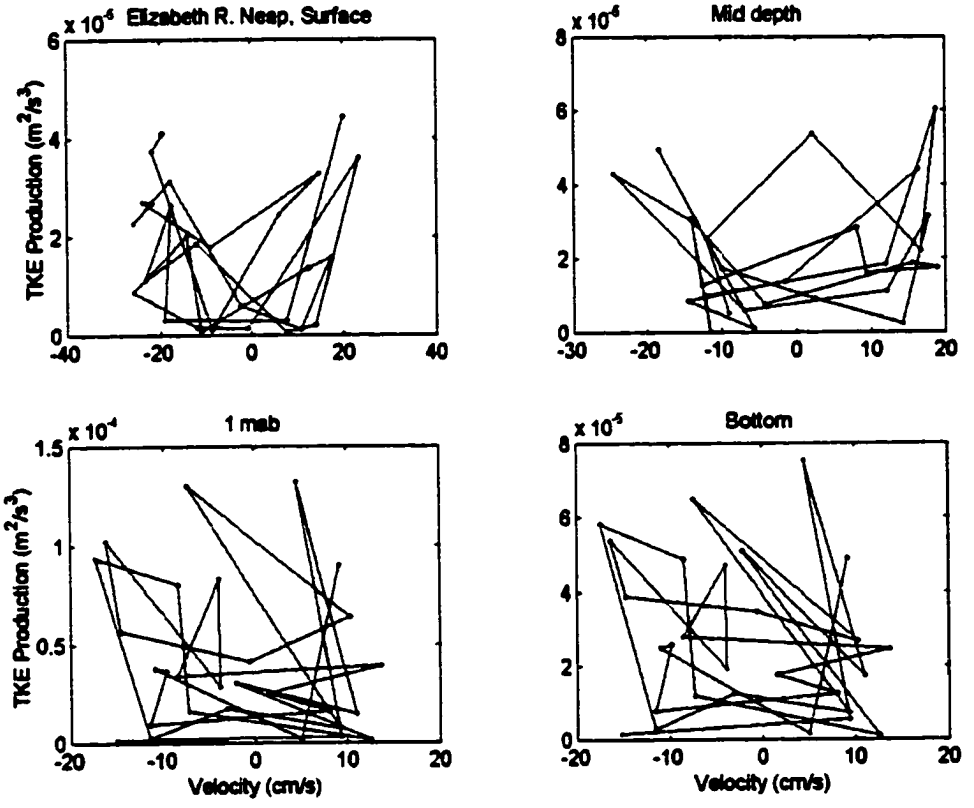

Fig. 2-13 cont. Tidal phase diagrams of TKE production (m^2/s^3) for the Elizabeth R., neap tide. Flood velocities are positive. (b) Surface, (c) Middepth, (d) 1 mab, (e) Bottom.

Particle Size Distribution

Time series of median particle diameters (D50) by depth as measured by the LISST and tidal phase diagrams are shown in Figs. 2d and 14a-d for the York R. In Figs. 2-14a to 2-14d, TKE production values are labeled positive during flood and negative during ebb. At this point it is worth reemphasizing that the median particle diameter as reported by the LISST should be thought of as a relative index of the median particle size rather than as a precise measure. Relative particle sizes may be compared with sediment concentration as measured by the ADV backscatter (Fig. 2-15). Peak surface and middepth concentrations in the York R. lag peak velocities (see Fig. 2-2). We might expect these conditions to lead to a pattern of small particles at the onset of high currents, followed by larger particles as concentration increases and turbulent shear decreases with decreasing velocity shear. However, this relation, if it exists, is overwhelmed by the unvarying presence of large particles appearing with the second flood cycle (Figs. 2-2d, 2-14a-b). These particles may have been advected into surface region either from the head of the estuary, or from the shoals with cross channel currents.

Excluding the surface, particle size distributions in the rest of the water column are consistent with the combined processes of high turbulent shear reducing maximum aggregate size and differential settling increasing aggregate size (Fig. 2-14). The former is likely to be dominant during high TKE production and the latter during low TKE production. The bias of large particles during the second tidal cycle is evident at these levels, though the variation in size distribution continues to respond to the physical forcing. This supports the idea that large robust particles were introduced at the surface and sunk to the lower elevations where their effect on particle size distribution was

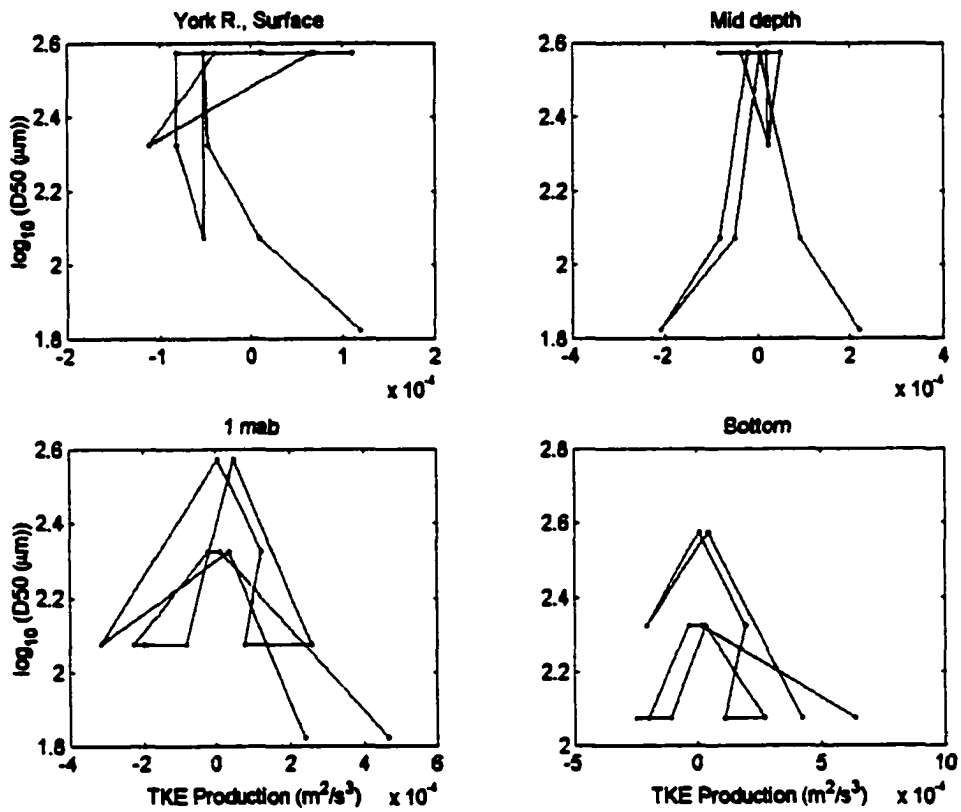

Fig. 2-14. Tidal phase diagrams of $\log_{10}$(median particle size (μm)) as measured by the LISST by TKE production (m^2/s^3) in the York R.. TKE production values during flood are labeled positive, ebb values are labeled negative. (a) Surface, (b) Mid depth, (c) 1 mab, (d) Bottom.

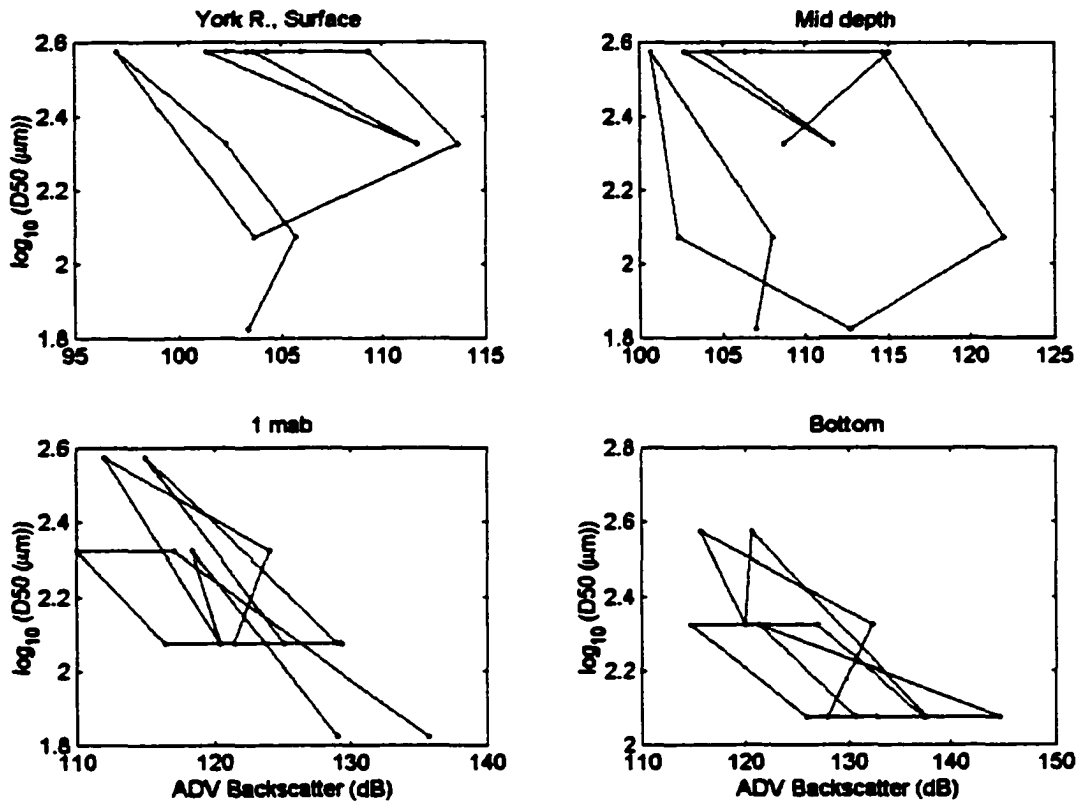

Fig. 2-15. Log_{10}(median particle size (μm)) as measured by the LISST by ADV backscatter (dB) in the York R., (a) Surface, (b) Mid depth, (c) 1 mab, (d) Bottom.

diluted by the higher local population of suspended sediment. The inverse relation between size and concentration near the bed (Fig. 2-15 c-d) is also indicative of aggregate break-up at high shear. Loosley bound aggregates at the bottom are resuspended and immediately disaggregated by the high stress.

Median particle sizes from near bed at the Cherrystone site are shown in Fig. 2-16a. In contrast to the relationship in the York R., high TKE production tends to be associated with larger particles. Like the York, this is a relatively energetic hydrodynamic regime, but the dominant benthic processes are different. Resuspension in the York inputs fragile aggregates into the water column which are immediately broken up by high stress, whereas strong resuspension at Cherrystone inputs larger biologically aggregated and pelletized particles into the water column. Figure 2-16b displays the positive relation seen at the Cherrystone site between particle size and concentration, which is also consistent with higher stress suspending increasingly larger aggregates.

Figures 2-4d and 2-5d show the time series of median particle size by depth for the spring and neap tides from the Elizabeth R. In general, the largest particles tend to be found in the middle of the water column, the smaller particles tend to be near the surface, and the near bed exhibits intermediate size particles. Local areas of large particles may be seen to migrate vertically about 2 meters in concert with the tidally moving pycnocline. Data from the Elizabeth R. are erratic and the relationships between particle size, concentration, and TKE production are best viewed collectively from all elevations and tidal phases. During spring tide, the strongest relationship is between concentration and minimum median particle size (Fig. 2-17a). That is, as concentrations increase, median particle size is at least some value which is also increasing, but may be larger. The relationship appears to be strongest near the bed. Since TKE production is also positively related to concentration (Fig. 2-17b), this suggests that much of the relationship between minimum median particle size and concentration is related to resuspension of larger particles from the bed. Median particle size is only weakly positively related to TKE production (Fig. 2-17c).

During neap tide in the Elizabeth R. there is a similar relationship between concentration and median particle size (not shown) excluding surface values. As concentration rises, the minimum median particle size also rises. However, neither

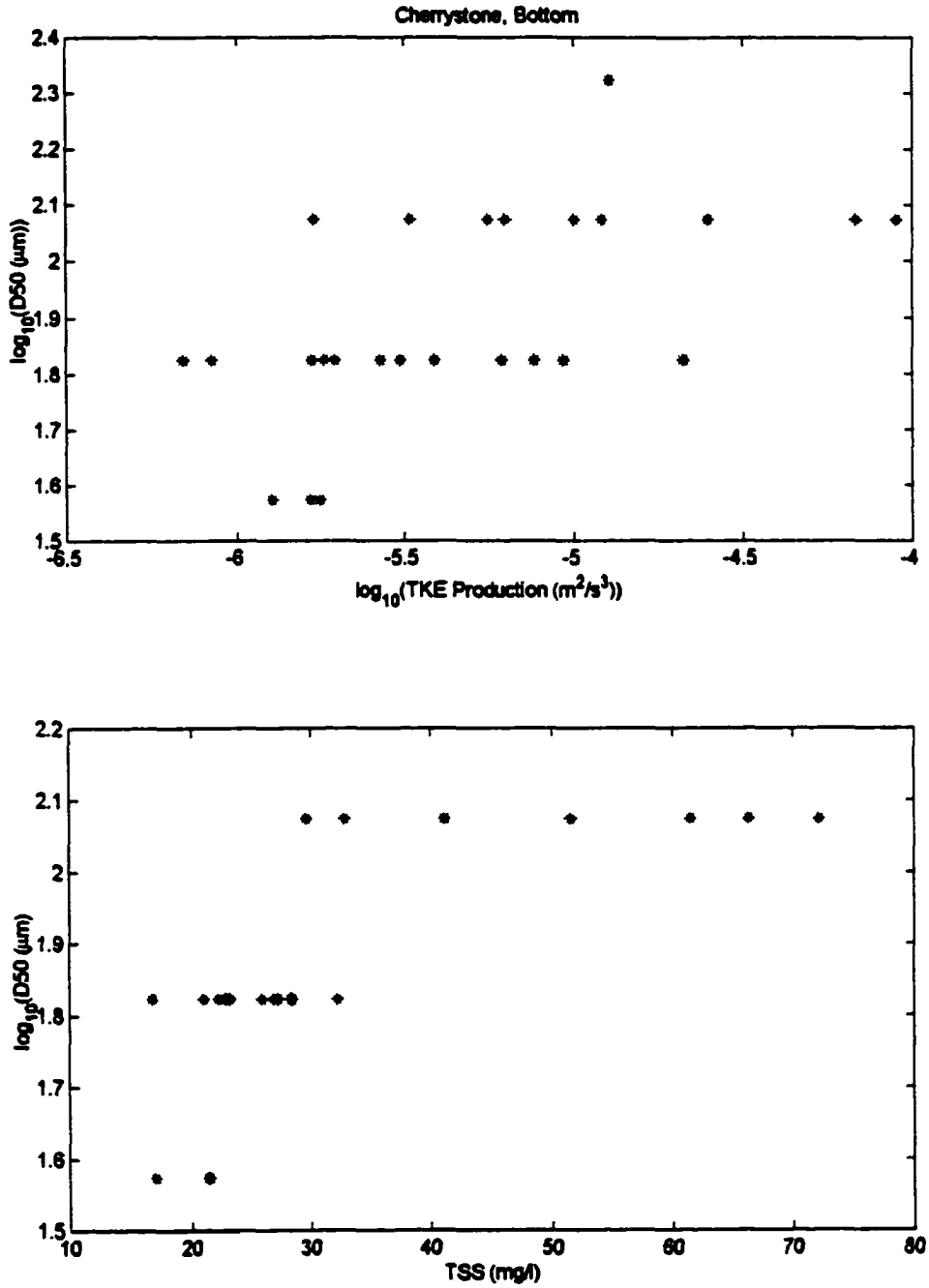

Fig. 2-16 (a). Log_{10}(median particle size (µm)) as measured by the LISST by TKE production (m^2/s^3) at the Cherrystone site. (b) Log_{10}(median particle size (µm)) as measured by the LISST by Total Suspended Solids (mg/l) at the Cherrystone site.

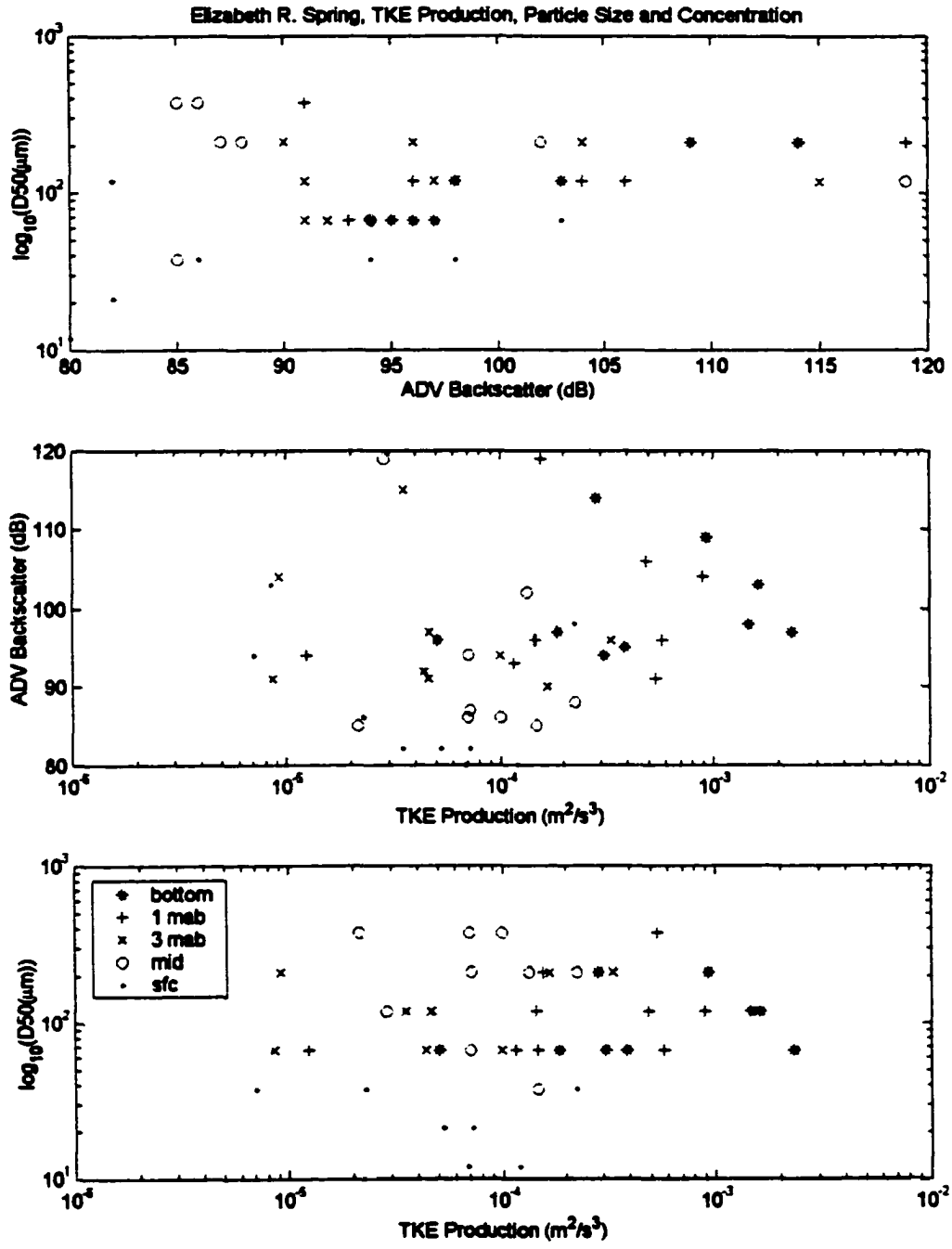

Fig. 2-17. Relations between TKE production (m^2/s^3), $\log_{10}$(median particle size (μm)) as measured by the LISST, and ADV backscatter (dB) from Elizabeth R. Spring tide. (a) particle size by ADV backscatter, (b) ADV backscatter by TKE production, (c) particle size by TKE production.

concentration nor median particle size seem to be related to TKE production during neap tide.

Near Bed Settling Velocity

Knowledge of the settling velocity of near bed suspended particles is useful to understanding particle type and aggregation dynamics. Since we also have an idea of the relative particle size distributions from the LISST, we can gain insight into the relative densities of near bed suspended material. The settling velocity may be indirectly estimated by making the common assumption of a lowest-order sediment concentration balance between gravitational settling and upward turbulent diffusion (Fugate and Friedrichs, in press; Glenn and Grant, 1987; Sherwood et al., 1994; Sleath, 1984).

$$- w_{sn} C_n = K \, dC_n/dz$$

where w_{sn} is settling velocity of particle type n, C_n is the concentration of particle type n, and K is the eddy diffusivity. Turbulent diffusion can be estimated by the Reynolds diffusive flux:

$$K \, dC_n/dz = - \langle w'C_n' \rangle$$

where w' is the vertical fluctuating component of velocity and C' is the deviation from mean concentration as estimated by the ADV backscatter. One can then solve for settling velocity simply by dividing both sides by C (Fugate and Friedrichs, in press). Figure 2-18 displays plots of $\langle w'C' \rangle$ vs. C for each of the surveys with w_s determined from the slope of the best-fit regression. In each case, the x-axis intercept of the best fit regression at $\langle w'C_l' \rangle = 0$ is interpreted as the background non-settling component of concentration. The settling velocity results are presented in Table 2-1.

The settling velocity of near bed particles in the York R. (0.6 +- 0.1 mm/s) is larger than that in the Elizabeth R. (0.4 +- 0.1 mm/s), and smaller than the settling velocity at Cherrystone (1.3 +- 0.05 mm/s). Since resuspended bottom particles in the

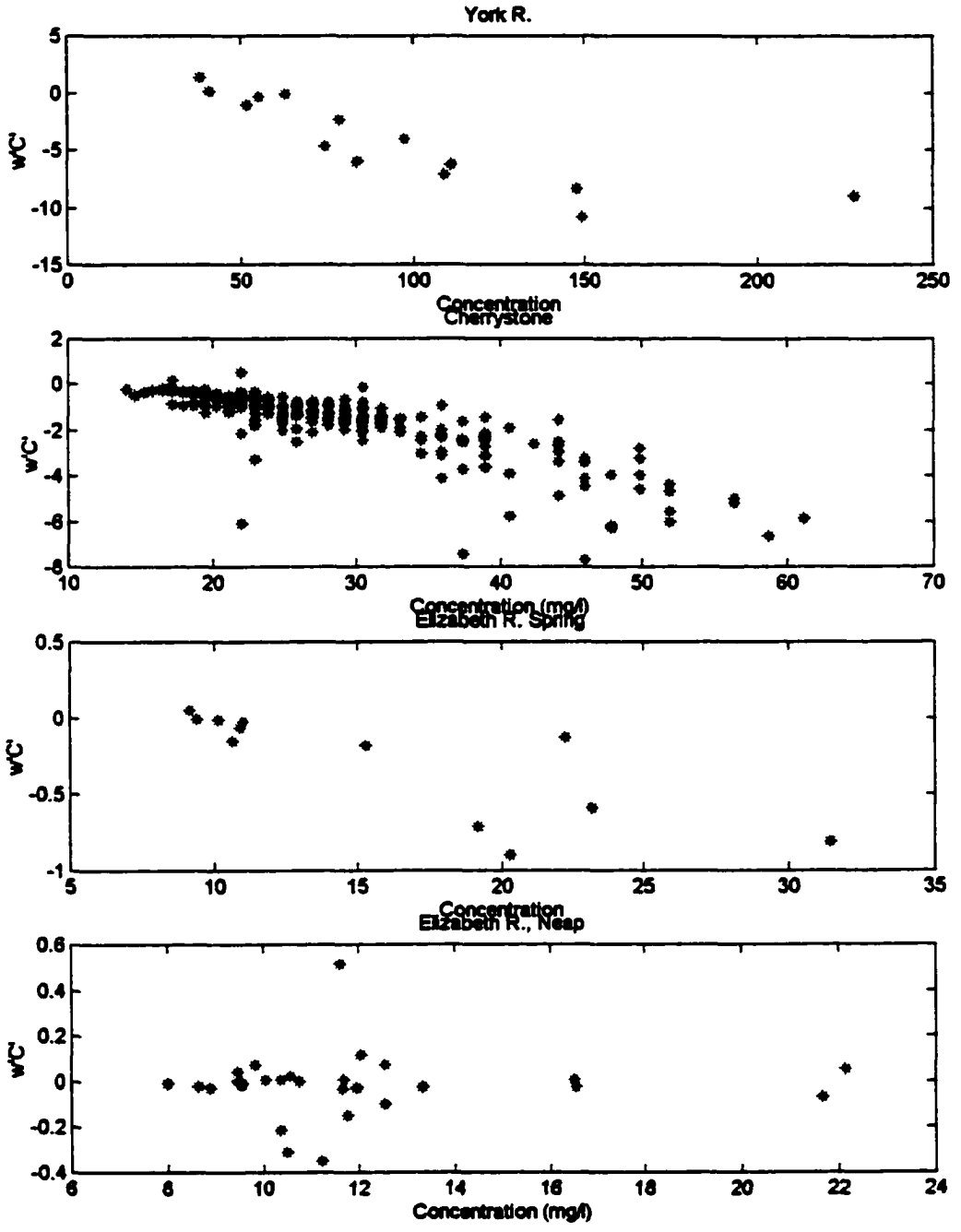

Fig. 2-18. Reynolds flux (w'C') by Concentration (mg/l) for bottom elevations of (a) York R., (b) Cherrystone site, (c) Elizabeth R. Spring tide, (d) Elizabeth R. Neap tide.

TABLE 2-1

Estuary	Settling Velocity +/- 1 s.e. (mm/s)	Background Concentration +/- 1 s.e. (mg/l)	r^2	n
York R.	0.6 +/- 0.1	29 +/- 12	0.89	14
Cherrystone	1.3 +/- 0.05	16 +/- 2	0.69	250
Elizabeth R. Spring	0.4 +/- 0.1	9 +/-1	0.79	11 (1 observation excluded)
Elizabeth R. Neap	N.A.	N.A.	No Relation	29

Elizabeth R. tend to be larger than those resuspended from the York R., but settle more slowly, it is reasonable to conclude that near bed particles in the Elizabeth R. are less dense than those from the York R. Since the particles resuspended from the York R. are smaller than those resuspended at Cherrystone it cannot be determined whether the higher settling velocity at the Cherrystone site is due to higher density particles or to their larger size or both. The background concentration estimates reemphasize the low concentrations found in the Elizabeth R. compared to the other two estuaries. The higher settling velocity and larger particles at Cherrystone keep the background concentrations lower than in the York, even though both are physically energetic. It is also worth noting the opposite curvature in the trend of the w'C' vs. concentration scatter plots for the York and Cherrystone sites. Best-fit of a quadratic curve to the York data in Fig. 2-18a would be concave upward, consistent with decreasing fall velocity at higher concentrations and higher shear, and smaller particle size due to aggregate breakup. A best-fit of a quadratic curve to the Cherrystone data (Fig. 2-18b), in contrast, would be concave downward, consistent with increasing fall velocity and larger particle site at higher concentrations and higher shear due to resuspension of resilient aggregates.

Conceptual Model of Factors Determining Size Distributions in Partially Mixed Estuaries

The different hydrodynamic regimes and particle sources at different levels in the water column suggest examination of the particle aggregation processes by depth. Surface conditions are characterized by a range of TKE production values, which may be low even though velocities are high, since velocity shear may be reduced. Suspended sediment concentration is low at the surface. The higher velocities at the surface and remoteness from the bed make the immediate source of particles most likely to be from horizontal advection. Near bed conditions are characterized by lower velocities and high TKE production from velocity shear. Suspended sediment concentrations are high and resuspension from the bed provides the major source of sediments. Mid depth regions experience a range of TKE production values and particle sources may be either from

resuspension from the bed, or sinking from the surface. The relevant processes which determine aggregate size in each of these depth categories will be discussed with regard to their respective hydrodynamic regime and sediment concentrations and sources and are summarized in Table 2-2.

Surface regime

Low values of turbulent shear at the surface are not accompanied by large particle formation because the surface is generally bereft of particles. Low TKE production values occur not only at slack, but also during peak currents when velocity shear is low and relative concentration is high. The primary processes affecting size distribution and concentration at the surface in both the York R. and Elizabeth R. appear to occur on a subtidal time scale. In the York R., large particles appear to have been advected into the surface region, possibly from transverse currents during a slack after ebb at hour 27. Elizabeth R. concentrations are erratic and dominated by boat wakes and horizontal advection.

Middepth regime

Middepth particle aggregation dynamics in the York R. are consistent with conventional models. Differential settling allows large particles to aggregate during reduced levels of TKE production. High levels of TKE production are accompanied by smaller disaggregated particles. The median size may be biased by the input of sinking particles, but the variations of the distributions respond to the hydrodynamic conditions. In contrast to the York R., aggregation dynamics in the Elizabeth R. cannot be attributed to these models. The low energy levels and low concentration levels permit stochastic processes such as boat wake, advection, and possibly industrial discharge to dominate the particle size regime. Nevertheless, there is still a consistent vertical pattern of particle sizes in that whenever larger particles do appear, they tend to be trapped at the pycnocline. This conclusion is supported by the vertical migration of larger particles with the tidally moving pycnocline.

Table 2-2.

Dominant Factors and Time Scales
Determining Particle Size Distribution in Partially Mixed Estuaries

	High Energy High Concentration	Low Energy Low Concentration
Surface	Advection Sub-tidal frequency	Advection Sub-tidal frequency
Middepth	Turbulent Shear Differential Settling Tidal frequency	Differential Settling Sub-tidal frequency
Near bed	Turbulent Shear Resuspension Benthic Environment Tidal frequency	Resuspension Benthic Environment Sub-tidal frequency

Bottom regimes

Bottom regimes in each of the three estuaries are different, reflecting their different particle types and hydrodynamic regimes. During the relatively mild currents of spring tide in the Elizabeth R., large porous particles were resuspended as evidenced by the increasing particle size with increasing turbulent energy and concentration. The slow settling velocity in combination with their large size reveals that these particles are low density aggregates which are not broken up by the low extant velocities. In contrast to the Elizabeth R., high currents and associated shear in the York disaggregated particles as they were suspended, as evidenced by the decreasing particle size with increasing turbulent energy and concentration. The higher settling velocity of the small particles in the York compared to the lower settling velocity of the large particles in the Elizabeth R. reveals that the constituent components of the York R. disaggregated by the high stress near the bed are small and dense. Near the bed, there is some evidence that fall velocity decreases with increases in TKE production because of the disaggregation into smaller particles. In contrast to both of these estuaries are the particles at the Cherrystone site in the Chesapeake Bay. Like the York R., this is also a high energy region, but particle size increases with increased stress here. These particles have the highest settling velocity and are likely large dense aggregates formed by biologic aggregation and pelletization. In addition, their relationship to TKE production is opposite of that in the York; higher turbulent energy resuspends larger particles and leads to higher fall velocities.

CONCLUSIONS

An alternate method of estimating TKE production with ADV data potentially contaminated by spurious motion proved to be a good estimator when compared with measurements made with Reynolds stress and Kolmogorov's –5/3 law. This method may be useful to measuring TKE production with an ADV in the presence of long period waves. Along with other conventional methods, this method was used to reach the below conclusions regarding turbulent kinetic energy production and particle aggregation dynamics in partially mixed estuaries.

Turbulent kinetic energy production in the estuaries studied is generally larger near the bottom. In the middepth regions, local maxima occur during peak ebb currents in the energetic York R. and during flood currents in the low energy Elizabeth R. The effects of tidal acceleration can be seen in the York R. where initially high currents are accompanied by high values of TKE production. As high currents persist, velocity shear decreases and TKE production drops. During the spring tide in the Elizabeth R. the largest factor in TKE production was the passage of a large cargo. During the neap tide in the Elizabeth R., currents were weak and irregular and tidal patterns are difficult to discern. TKE production in the York and Cherrystone sites appear to be governed by velocity shear, while TKE production in the Elizabeth R. appears to be governed by mixing in the TKE component of TKE production.

The processes that determine particle aggregation dynamics in estuaries are a function of the elevation in the water column, as well as the overall hydrodynamic and biological environment. For low energy low concentration estuaries such as the Elizabeth R., stochastic events such as advection, boat wake or other forcings dominate the physical processes conventionally held to be important, although concentration does seem to exert some influence on minimum particle size. Despite the dominance of random events on particle dynamics, vertical profiles tended to be consistent, with the

largest particles found in the middle of the water column, the smallest at the surface, and intermediate sizes near the bed. One result important to characterizing particle dynamics in estuaries is that important advective events occur at time scales longer than the tidal period, and surveys intended to measure mean particle parameters such as size or concentration should endure as long as possible. Even in more typical estuaries such as the York R., particle sizes in low concentration surface regions that were expected to respond to changes in concentration were instead dominated by stochastic events. Aggregation dynamics in the middepth region of the York R., a relatively high energy and high concentration estuary, were determined by the combined processes of turbulent shear and differential settling. Particle size distributions near the bed were different in each of the three principle study sites, reflecting their hydrodynamic and benthic environments. Near bed particles in the low energy Elizabeth R. were large porous aggregates, those in the energetic physically dominated York R. were smaller and more dense, while those at the energetic, biologically influenced Cherrystone site were large and denser than the large particles in the Elizabeth R. Depending on the relative energy and biological activity, relations between tidally varying TKE production and tidally varying particle size, concentration and fall velocity also differed systematically among the three sites.

REFERENCES FOR CHAPTER 2

Agrawal, Y.C. and Pottsmith, H.C., 1994. Laser diffraction particle sizing in STRESS. Cont. Shelf Res., 14(10-11): 1101-1121.

Agrawal, Y.C. and Pottsmith, H.C., 2000. Instruments for particle size and settling velocity observations in sediment transport. Marine Geology, 168: 89-114.

Battisto, G.M., Friedrichs, C.T., Miller, H.C. and Resio, D.T., 1999. Response of OBS to mixed grain-size suspensions during Sandyduck '97, Coastal Sediments '99: Proceedings of the 4th International Symposium on Coastal Engineering and Science of Coastal Sediment Processes Reston, ASCE, pp. 297-312.

Berhane, I., Sternberg, R.W., Kineke, G.C., Milligan, T.C. and Kranck, K., 1997. The variability of suspended aggregates on the Amazon Continenetal Shelf. Cont. Shelf Res. 17(3): 267-285.

Chen, S., Eisma, D. and Kalf, J., 1994. In situ size distribution of suspended matter during the tidal cycle in the Elbe Estuary. Netherlands Journal of Sea Research, 32(1): 37-48.

Dellapenna, T.M., Kuehl, S.A. and Schaffner, L.C., 1998. Sea-bed mixing and particle residence times in biologically and physically dominated estuarine systems: a Comparison of Lower Chesapeake Bay and the York River Subestuary. Estuarine and Coastal Marine Science, 46: 777-795.

Dyer, K.R., 1986. Coastal and Estuarine Sediment Dynamics. John Wiley & Sons, 341 pp.

Eisma, D. et al., 1991. Suspended-matter particle size in some west-European estuaries; Part 2: A review on floc formation and break-up. Neth. J. Sea Res. 1991, 28(3): 215-220.

Eisma, D. and van Leussen, W., 1997. The in situ determination of the settling velocities of suspended fine-grained sediment - a review. In: N. Burt, R. Parker and J. Watts (Editors), Cohesive sediments: 4th Nearshore and Estuarine Cohesive Sediment Transport Conference, INTERCOH '94, 11-15 July 1994 Wallingford, England, UK. John Wiley, Chichester, pp. 458.

Fettweis, M., Sas, M. and Monbaliu, J., 1998. Seasonal, neap-sppring and tidal variation of cohesive sediment concentration in the Scheldt Estuary, Belgium. Estuar. Coast. Shelf Sci., 47: 21-36.

Friedrichs, C.T., Wright, L.D., Hepworth, D.A. and Kim, S.C., 2000. Bottom-boundary-layer processes associated with fine sediment accumulation in coastal seas and bays. Continental Shelf Research 20(7): 807-841.

Fugate, D.C. and Friedrichs, C., in press. Determining Concentration and Fall Velocity of Estuarine Particle Populations, Using ADV, OBS and LISST. Cont. Shelf Res.

Gibbs, R.J., Tshudy, D.M., Konwar, L. and Martin, J.M., 1989. Coagulation and transport of sediments in the Gironde Estuary. Sedimentology, 36: 987-999.

Glenn, S.M. and Grant, W.D., 1987. A suspended sediment stratification correction for combined wave and current flows. J. Geophys. Res. (C Oceans). 92(C8): 8244-8264.

Gordon, C.M. and Dohne, C.F., 1973. Some observations of turbulent flow in a tidal estuary. Journal of Geophysical Research, 78(12): 1971-1978.

Gross, T.F. and Nowell, R.M., 1985. Spectral scaling in a tidal boundary layer. Journal of Physical Oceanography, 15(5): 496-508.

Gross, T.F., Williams, A.J. and Terray, E.A., 1994. Bottom boundary layer spectral dissipation estimates in the presence of wave motions. Cont. Shelf Res. 14(10-11): 1239-1256.

Hill, P.S. and McCave, I.N., 2001. Suspended particle transport in benthic boundary layers. In: B.P. Boudreau and B.B. Jorgensen (Editors), The Benthic Boundary Layer: Transport Processes and Biogeochemistry. Oxford University Press, Oxford.

Kim, S.-C., Friedrichs, C.T., Maa, J.P.Y. and Wright, L.D., 2000. Estimating bottom stress in tidal boundary layer from Acoustic Doppler Velocimeter data. Journal of Hydraulic Engineering, 126: 399-406.

Kranck, K., Smith, P.C. and Milligan, T.G., 1996. Grain-size characteristics of fine-grained unflocculated sediments II: 'multi-round' distributions. Sedimentology, 43(3): 597- 606.

Lee, C.H., 1995. Resuspension behavior of natural estuarine sediments. Ph.D. Thesis, School of Marine Science, College of William and Mary.

Mikkelsen, O.A. and Pejrup, M., 2000. In situ particle and density of particle aggragates in a dredging plume. Marine Geology 170: 443-459.

Neilson, B.J., 1975. A water quality study of the Elizabeth River: The effects of the army base and Lambert Point STP effluents, Virginia Institute of Marine Science, Gloucester Pt., VA, USA.

Nezu, I. and Nakagawa, H., 1993. Turbulence in Open-Channel Flows. A.A.Balkema, Rotterdam, 281 pp.

Nichols, M.M. and Howard-Strobel, M.M., 1991. Evolution of an urban estuarine harbor: Norfolk, Virginia. Journal of Coastal Research, 7(3): 745-757.

Nichols, M.M., Kim, S.C. and Brouwer, C.M., 1991. Sediment characterization of the Chesapeake Bay and its tributaries, National Estuarine Inventory: Supplement, NOAA Strategic Assessment Branch, Virginia Province, pp. 88 pp.

Nikora, V.I. and Goring, D.G., 1998. ADV measurements of turbulence: Can we improve their interpretation. Journal of Hydraulic Engineering, 124(6): 630-634.

Nikora, V.I., Rowinski, P., Suchodolov, A. and Krasuski, D., 1994. Structure of river turbulence behind warm-water discharge. J. Hydraul. Eng. 120(2): 191- 208.

Nikora, V.I. and Smart, G.M., 1997. Turbulence characteristics of New Zealand gravel-bed rivers. J. Hydraul. Eng. 123(9): 764-773.

O'Connor, D.J., 1988. Models of sorptive toxic substances in freshwater systems, I: Basic Equations. Journal of Environmental Engineering, 114(3): 507-551.

Schaffner, L.C., 1990. Small-scale organism distributions and patterns of species diversity: evidence for positive interactions in an estuarine benthic community. Marine, Ecology Progress Series 61:107-117 # 8 of 14 from Set 88 - ASFA.

Schaffner, L.C. et al., 2001. Physical energy regimes, seabed dynamics, and organism-sediment interactions along an estuarine gradient. In: J.Y. Aller, Woodin, S.A., Aller, R.C. (Editor), Organism-Sediment Interactions. University of South Carolina Press, Columbia, S.C., pp. 159-179.

Schubel, J.R., 1971. Tidal variation of the size distribution of suspended sediment at a station in the Chesapeake Bay Turbidity Maximum. Netherlands Journal of Sea Research, 5(2): 252-266.

Sherwood, C.R. et al., 1994. Sediment-transport events on the northern California continental shelf during the 1990-1991 STRESS experiment. Cont. Shelf Res., 14(10-11): 1063-1069.

Sleath, J.F.A., 1984. Sea bed mechanics. Ocean Engineering. John Wiley, New York, 335 pp.

Soulsby, R.L., 1983. The bottom boundary layer of shelf seas. Elsevier Oceanography Series, 35. Elsevier, Amsterdam.

Stapleton, K.R. and Huntley, D.A., 1995. Seabed stress determinations using the inertial dissipation method and the turbulent kinetic energy method. Earth Surf. Process. Landforms, 20: 807-815.

ten Brinke, W.B.M., 1994. In situ aggregate size and settling velocity in the Oosterschelde Tidal Basin (The Netherlands). Netherlands Journal of Sea Research, 32(1): 23-35.

Thompson, M.L. and Schaffner, L.C., 2001. Population biology and secondary production of the suspension. Limnologyand Oceanography, 46(2): 1899-1907.

Traykovski, P., Latter, R.J. and Irish, J.D., 1999. A laboratory evaluation of the laser in situ scattering and transmissometery instrument using natural sediments. Marine Geology [Mar. Geol.] 0025-3227 19990701, 159(1-4): 355-367.

Van Leussen, W., 1994. Estuarine Macroflocs: their role in Fine-Grained sediment Transport. CIP-Gegevens Koninklijke Bibliotheek, Den Haag, Utrecht.

Van Leussen, W., 1999. The variability of settling velocities of suspended fine- grained sediment in the Ems estuary. Journal of Sea Research, 41(1-2): 109-118.

Voulgaris, G. and Trowbridge, J.H., 1998. Evaluation of the Acoustic Doppler Velocimeter (ADV) for turbulence measurements. Journal of Atmospheric and Oceanic Technology, 15(1): 272-289.

Wolanski, E. and Gibbs, R.J., 1995. Flocculation of Suspended Sediment in the Fly River Estuary, Papua New Guinea. Journal of Coastal Research, 11(3): 754-762.

Wright, L.D., Boon, J.D., Xu, J.P. and Kim, S.C., 1992. The bottom boundary layer of the bay stem plains environment of lower Chesapeake Bay. Estuarine,Coastal and Shelf Science, 35: 17-36.

Wright, L.D., Schaffner, L.C. and Maa, J.P.Y., 1997. Biological mediation of bottom boundary layer processes and sediment suspension in the lower Chesapeake Bay. Marine Geology, 141(3): 27-50.

Chapter 3. Relationships between Physical and Biochemical Properties of Suspended Particles in an Industialized Urban Estuary, the Elizabeth R. VA, USA

To be submitted with authors D.C. Fugate, C.T. Friedrichs, and C. Chisholm- Brause

ABSTRACT

The extent to which the fate and transport of particle adherent contaminants such as heavy metals follow the fate and transport of the particles themselves depends in part upon the level of affinity that the contaminants have for the particles. Hydrophobic organic contaminants and trace metal contaminants have a strong affinity for suspended particulates, especially aggregates containing organic material. The particle constituents as well as particle properties such as the degree of porosity, amount of surface area, and particle size are important to the adsorption process. Numerous studies have shown a strong relation between particle size and contaminant concentrations. Particle sizes in these studies are typically determined from disaggregated sediment samples. However, loosely bound in-situ aggregates of fine particles may have the high concentrations of the constituent small particles, but settle to the bed like larger particles. Thus the associated high concentration of contaminants may experience a different fate and transport than that of small particles that never aggregate or deposit, but remain suspended in the water column over subtidal timescales. The interrelationships between metal concentrations, particle size, percent fixed solids (PFS), chlorophyll a, and molar Carbon to Nitrogen (C/N) ratios of suspended sediment are investigated in a heavily industrialized and polluted estuary, the Elizabeth R., VA, USA. The relationship between PFS , C/N and aggregate size are also investigated in a relatively energetic, high concentration, and undisturbed estuary, the York. R., VA, USA. Standard paradigms of contaminant concentration relationships with particle size and particle constituents were not supported in the low energy, low concentration suspended sediments of the Elizabeth R. No significant seasonal relationships were found in the PFS values, nor were there any relationships found between PFS and median grain size or metal concentrations. Chlorophyll a values did vary seasonally, but also were not related to grain size or metal concentrations. Chlorophyll a values tended to be higher at the surface and upstream from the study site. C/N was vertically homogenous and varied significantly over timescales longer than the tidal period. C/N was not related to grain size or metal concentrations, or PFS or chlorophyll a values. There is a tendency for lower C/N downstream of the study site, suggesting that the source of the higher organic constituent material downstream is not marine phytoplankton. Metal concentrations were not related to median grain sizes nor to tidally varying hydrodynamics, but showed a strong tendency to be high at surface and middepth during stratified conditions. It is speculated that most net transport of trace metals in the Elizabeth R. occurs in the dissolved or colloidal phase and ultimately depends on the hydrodynamics of the system, including stratification, vertical mixing patterns and overall processes of tidal dispersion. In contrast to the Elizabeth R., measures of organic content from PFS levels and C/N in the York R. were related to aggregate size, consistent with standard paradigms. Lower PFS levels and C/N were associated with larger size aggregates.

INTRODUCTION

The extent to which the fate and transport of particle adherent contaminants such as heavy metals follow the fate and transport of the particles themselves depends upon the level of affinity that the contaminants have for the particles. Hydrophobic organic contaminants and trace metal contaminants have a strong affinity for suspended particulates, especially aggregates containing organic material (Ko and Baker, 1995; Mitra et al., 1998). The particle constituents as well as particle properties such as the degree of porosity, amount of surface area, and particle size are important to the adsorption process (Titley et al., 1987). Numerous studies have shown a strong inverse relation between particle size and contaminant concentrations (Benoit and Rozan, 1999; Hahn and Xanthopoulos, 1990; Kango et al., 1987; Warren and Zimmermann, 1994). Particle sizes in these studies are typically determined from disaggregated sediment samples. However, loosely bound in-situ aggregates of fine particles may have the high concentrations of the constituent small particles, but settle to the bed like larger particles. Thus the associated high concentration of contaminants may experience a different fate and transport than that of small particles that never aggregate or deposit over short time scales, but remain suspended in the water column. Once deposited, dredging operations or other physical disturbance of contaminant laden sediment may resuspend and introduce remobilized contaminants back into the water column (Hayes et al., 2000; Latimer et al., 1999; Mitra et al., 1999) making them available for further transport. This paper will focus on the relationship between hydrodynamics, suspended particle properties and the particle constituents in the Southern Branch of the Elizabeth River, a heavily industrialized and polluted urban estuary. Suspended sediment concentrations of the contaminant trace metals cadmium, copper, and zinc, as well as the sediment associated metals iron, manganese, chromium, and aluminum will be examined and compared to in-situ particle size and organic content of the particles. Some comparisons will also be made with a more energetic and less disturbed estuary, the York River.

BACKGROUND

Contaminants associated with suspended sediments may adsorb or be incorporated into algae and subsequently enter the trophic system of the estuary. Zooplankton (Marshall et al., 1981) , mysids (Schofield, 1988) , zebra mussels (Gossiaux et al., 1998), darter gobies (Gregg et al., 1997) , bluegills (Cope et al., 1996) and flamingos (Nelson et al., 1998) are just some of the biota which have been documented to accumulate metals in their systems. Metals and hydrophobic organic contaminants may be carcinogenic or result in other toxic effects to these biota. Understanding the fate and transport of these contaminants is necessary to effectively ameliorate and manage their discharge into urban estuaries.

Small particles are more efficient at scavenging particle adherent contaminants because of their increased surface to volume ratio. In addition to the well established relationship between contaminant concentrations and disaggregated particle size, the contaminant scavenging ability of the particles is also related to specific concentrations of sediment associated metals such as Fe, Al, and Mn. These metals may all be used to normalize trace metal contaminant concentrations because the contaminants have different affinities for the particles depending upon the amount of these metals in the oxidized state (Balls et al., 1994; Feng et al., 1999; Kango et al., 1987). This is especially useful when investigating sources in an estuary by examining spatial variation in contaminant concentrations when particle types also vary spatially. For example, Feng (1999) used Fe and Al concentrations to normalize for grain size differences in concentrations of the metal contaminants Cu, Zn and Cd. They found the spatial distribution of these contaminants in the Hudson River estuary to be scattered and inconsistent and attributed this to multiple sources.

The affinity of contaminants for particles depends not only upon the size and metal hydroxide content, but upon the quality and quantity of organic matter in the particles. Numerous studies have suggested that particle constituents determine particle aggregation in estuaries along with the hydrodynamics. (Alber, 2000; Blanton et al., 1999; Eisma et al., 1991a, 1991b; Engel, 2000; Riggs, 1996). The organic compounds in the water that become integrated into the aggregates provide a glue which allows the particles to attach to each other upon encounter. The availability of these compounds may help determine the maximum size that the aggregates may attain. Eisma et al. (1991b) performed an extensive investigation of dissolved and particulate carbohydrate levels, algal cell concentration, and particle size in several West-European estuaries. Their results suggest that carbohydrates in the form of polysaccharides or long chain organic compounds such as humic and fulvic acids become mobilized at lower salinities. Consequently, the sticky compounds that hold flocs together in the more saline regions become dissolved and disaggregation ensues in fresh water. These dissolved carbohydrates may then be utilized by standing stock of plankton in the water or remain dissolved in the water column, depending on seasonal effects. So the organic content of the particles may affect scavenging efficiency indirectly through its relation to particle size, but also has direct affect on the scavenging of organic and metal contaminants through preferential binding of the contaminants to the organics (Lu and Allen, 2001). Seasonal variations of contaminant concentrations (Neal et al., 2000; Ongley et al., 1981) may be related to the seasonal variations in organic matter caused by phytoplankton blooms.

Studies have shown that particles which have slow settling velocities and remain permanently suspended in the water column have higher organic content that larger particles which are regularly deposited and resuspended (Alber, 2000). These two populations of particles have different transportation modes and so will their respective associated contaminants. Padmalal and Seralathan (1993) found Fe, Mn and Zn higher in bed sediments, while Cu, Ni, and Zn were higher in suspended particulates.

Once deposited, diagenetic processes may alter the affinity of contaminants to the particles. Changes in pH, dissolved oxygen, dissolved organic carbon, and salinity are all factors which affect the partition coefficients of the contaminants. (Balls et al., 1994;

Comber et al., 1995; Lu and Allen, 2001; Ng et al., 1996; Stroemberg and Banwart, 1999) . Metals associated with rapidly settling particles were remobilized during resuspension and input into water column in a study by Williamson et al. (1996), and Latimer (1999) found remobilization of PAH's from resuspended dredge material. In contrast, Brassard et al. (1997) found that the concentration of metals in the water column was not elevated by resuspension of surficial sediments..

Various techniques are available to characterize the degree of organic matter in the particles. A simple method is to determine the percent fixed solids (PFS) of the suspended sediment, which is the percentage weight left after ashing. Another indicator of the organic content is the molar ratio of particulate organic carbon to particulate nitrogen (C/N). Material that has a low C/N is likely to contain labile nutrients that are more sticky than older refractory material with a high C/N. Terrestrial plant material has a C/N greater than 15 (Matson and Brinson, 1990), live phytoplankton have a C/N near 7, in accordance with the Redfield ratio, and marine bacteria C/N may be as low as 4 (Church, pers. comm.). The last indicator of organic content which will be considered is the chlorophyll *a* concentration of the suspended particles. Wiltshire et al. (1996) found that Cd, Cu, and Pb concentrations were correlated with chlorophyll *a* and POC. Zn, Fe and Mn did not have clear relationships with chlorophyll *a*.

SITE AND METHODS

The Elizabeth River is a large tributary of the James River, located near its mouth, which empties into the Southern Chesapeake Bay (Fig. 3-1). The main stem and two of the three major branches of the Elizabeth R. have undergone extensive industrial development since colonization of the area by Europeans in the 1600's. Within the relatively small drainage basin (around 300 square miles), urban development has reduced the groundwater input and consequently increased the peak flows into the river from runoff. Freshwater input from the Dismal Swamp Canal at the head of the SBER ranges from 11.9 m^3/s (7000 Mg/month) in February to 0.8 m^3/s (500 Mg/month) in July (Neilson, 1975). There is also a significant input of freshwater from point source effluents of sewage treatment plants that is of the same order of magnitude as the input from the Dismal Swamp Canal. Spring tide currents range around 50 cm/s. Salinity during moderate freshwater flows in the ER and James range from around 17 ppt at Craney Island to 13 ppt at the Interstate Highway Bridge. Vertical stratification under these conditions is about 5 ppt difference between surface and bottom at the mouth and around 2 ppt difference within the rest of the estuary (Nielson, 1975).

Nichols and Howard-Strobel (1991) provide a comprehensive history of the anthropogenic changes to the geometry of the Elizabeth R. estuary. By the mid - 1800's, increased commercial activity in Hampton Roads and increased ship size and draft brought about intensive waterway development in the Elizabeth R. Channels were dredged, small tributaries were filled, and bulkheads were constructed and backfilled along the banks. Intensive development continued into the 1950's and dredge material was disposed in shoals, and in the open waters of the Chesapeake Bay. In modern times the disposal areas have been centralized, most notable is the site at Craney Island. These changes modified the geometry of the estuary from an irregular bottom profile with broad shoal and marsh areas to a regular, deeper, longitudinal stair step bottom profile with a

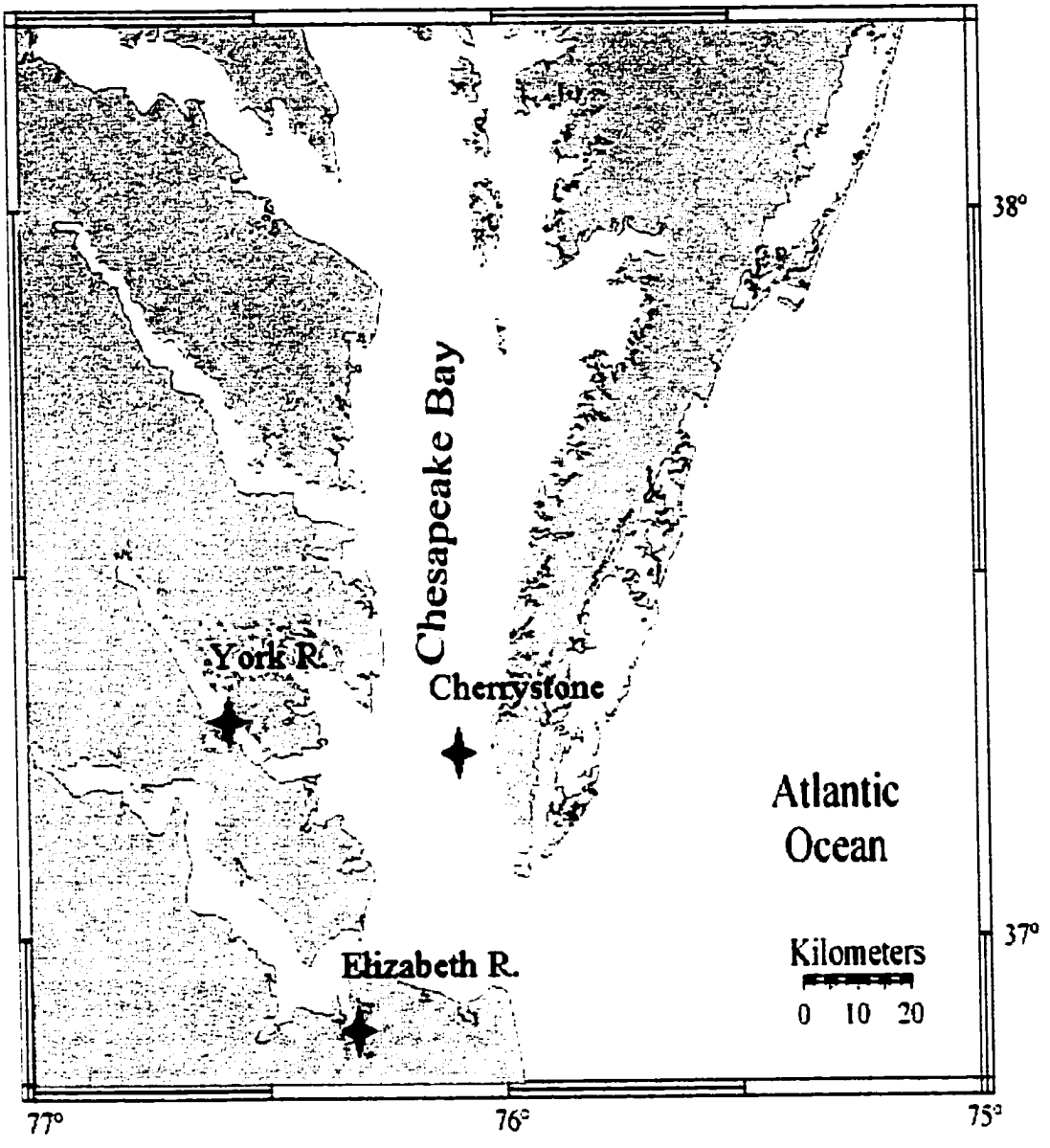

Fig. 3-1. Principle study site locations in Virginia, U.S.A.

narrower lateral extent, and a consequent reduction of the tidal prism in the estuary. Regular maintenance dredging rates in 1982 decreased landward, from 1.8 $*10^6$ m^3/y in the Norfolk Reach, to 0.4 * 10^6 m^3/y in the ER reach, to 0.1 * 10^6 m^3/y in the southern branch of the Elizabeth R. This trend is caused by the location of the major source of the sediment supply, which is from landward flowing salty bottom water.

Hundreds of years of industrial development and anthropogenic alterations of the morphology of the Elizabeth R. have created one of the country's most contaminated estuarine environments. Trace metal contaminant concentrations in sediment deposits increased from the late 1800's to the 1970's, followed by a significant decline up to the present (Conrad et al., 2000). Dauer and Lansau (2001) have determined that the condition of the benthic community in the Southern Branch of the Elizabeth R. near the sampling site has been degraded by as much as 76 %.

Effective amelioration of historic deposits and regulation of contemporary release of contaminants in estuarine systems requires an understanding of the hydrodynamic regime of the estuary, particle transport and accumulation rates, and the associations between specific toxins and specific particle types.

York River

The York River is a relatively energetic and undisturbed subestuary of the Chesapeake Bay. About 50 km long with a central channel 10 meters deep, the York River empties into the Lower Chesapeake Bay just above the James R. (Fig. 3-1). It is partially mixed; average freshwater discharge is about 60 m^3/s (cms), and salinity at the mouth is around 20. (Friedrichs et al., 2000) Maximum vertical stratification during this study was 2.5 from top to bottom of the 10 meter depth. Near surface tidal currents can reach over 100 cm/s and dominate the physical energy regime, tidal range is 0.7 m at the mouth and 1 m at the head (Schaffner et al., 2001). The relatively deep channel and limited fetch generally prevent wind energy from making an important contribution to the hydrodynamic energy at the bottom. The study site is at 37° 22.2 ' N and 76° 38.2' W inside the main channel of the York. The width of the river there is 3.4 km., and there is

a wide (2.4 km) shoal to the south of the main channel. Sediment enters the York from both the river and mouth (Nichols et al., 1991). Physical mixing in the soft muddy bed dominates bioturbation which may have mixing lengths up to a meter over a fortnightly time scale (Dellapenna et al., 1998). Maximum combined tidal, wave, and freshwater flow energies midway up the estuary length in the vicinity of the study site (Dellapenna et al., 1998).

DATA COLLECTION AND ANALYSIS

Three surveys of the Elizabeth R. were conducted on May 23, 1999, June 12, 1999, and November 22, 1999 near the Jordan Bridge at 36° 47.736' N and 76° 17.558 W. The survey of the York R. was conducted on May 30, 2000 at 37° 22.2 ' N and 76° 38.2' W. Hydrodynamic, physical, and geochemical data were collected similarly for each of the surveys. An instrument profiling lander, or 'profiler', containing a suite of physical and hydrodynamic instruments took vertical profiles of the water column 8 times per tidal cycle. The sampling elevations in the Elizabeth R. were bottom, 1 meter above the bottom (mab), 3 mab, the middle of the water column (~6 mab, depending on the tide) and 1 meter below the surface. Sampling in the York was similar, but not sampled at 3 mab. The surveys in the Elizabeth R. were carried on for about four tidal cycles and the survey in the York R. lasted 2 tidal cycles. Each elevation was sampled for a few minutes after which the profiler was left to continually sample at 1 mab until time for the next vertical profile. The instruments on the profiler were a Sontek Acoustic Doppler Velocimeter (ADV) sampling at 10 Hz, a Downing Optical Back Scatter sensor (OBS) operating in conjunction with an Applied Microsystems 12+ CTD sampling at 1-2 Hz, a Sequoia Science Laser In Situ Scatterer and Transmissometer (LISST) sampling at 2 Hz, and a submersible pump intake at 30 cm. above the bottom of the profiler . An upward looking Sontek Acoustic Doppler Profiler (ADP) was deployed nearby each profiling site sampling every 10 seconds with 0.25 meter depth bins.

One liter bulk water samples were collected at each elevation and analyzed for Total suspended solids (TSS). Total suspended solids (TSS) were analyzed by passing a measured subsample through a 0.8 poresize glass fiber filter, followed by drying and weighing. Percent Fixed Solids (PFS) were determined by the percentage of dry weight after ashing at 550° C. Metals were extracted from the filtrate by acid leaching for 22 to 24 hours, diluting with DI water, and centrifuged for 30 minutes. Metal concentrations

(Fe Al, Mn, Zn, Cu, and Cr) were analyzed with a Thermo Jarrell Ash TraceScan inductively coupled plasma atomic emission spectrophotometer (ICP_AES) with an axial torch. Cadmium was analyzed by atomic absorption using a Perkin-Elmer 800 with graphite furnace accessories. Chlorophyll *a* was determined using a Milton Roy Spectronic 1201 UV/VIS scanning spectrophotometer.

Ancillary data is presented that was collected by the Chesapeake Bay Foundation Water Quality Monitoring Program. This program is a cooperative effort between federal agencies and the states of Virginia and Maryland to routinely monitor various fixed stations within the Chesapeake Bay watershed.

RESULTS AND DISCUSSION

Hydrodynamics and Particle Sizes

Figures 3-2 to 3-5 show time and depth series of the salinity and median particle size for the Elizabeth R. May neap, June spring, and November spring tides and the York R. survey. Salinities range from 17 to 23 ppt in the Elizabeth R. and 14.5 to 18 ppt in the York R. In the Elizabeth R., salinity varied significantly on tidal as well as on longer time scales. Periodic mixing and stratification occur as a result of boat wakes or other events. Peak tidal currents are weak, ranging up to 40 cm/s during spring tides but often less. Suspended sediment concentrations are low, ranging up to 20 mg/l during spring tides and only up to 10 mg/l during neaps. Size distributions in the Elizabeth R. are determined by irregular resuspension and advection events rather than from consistent tidally varying aggregation dynamics (see Chapter 2). Larger particles introduced to the upper and middle water column tend to become concentrated at the pycnocline and are eventually disaggregated by increased shear as they near the bottom. While these larger particles may be aggregates formed by differential settling, they do not appear consistently during slack currents. Near bed particles tend to be larger during peak currents when larger porous aggregates are resuspended from the bed. Despite their apparent low density, the currents are too weak to break them up.

Figures 3-6a to 3-6d show the current speeds for the four surveys which are considered in this paper (flood currents are positive). Elizabeth R. currents tend to be weak and irregular, whereas those of the York energetic. Mean current speeds as registered at each sampling height by the ADV are shown for the June spring tide, since the ADP was unintentionally deployed upside down. See Chapter 2 for a more detailed description of the hydrodynamics.

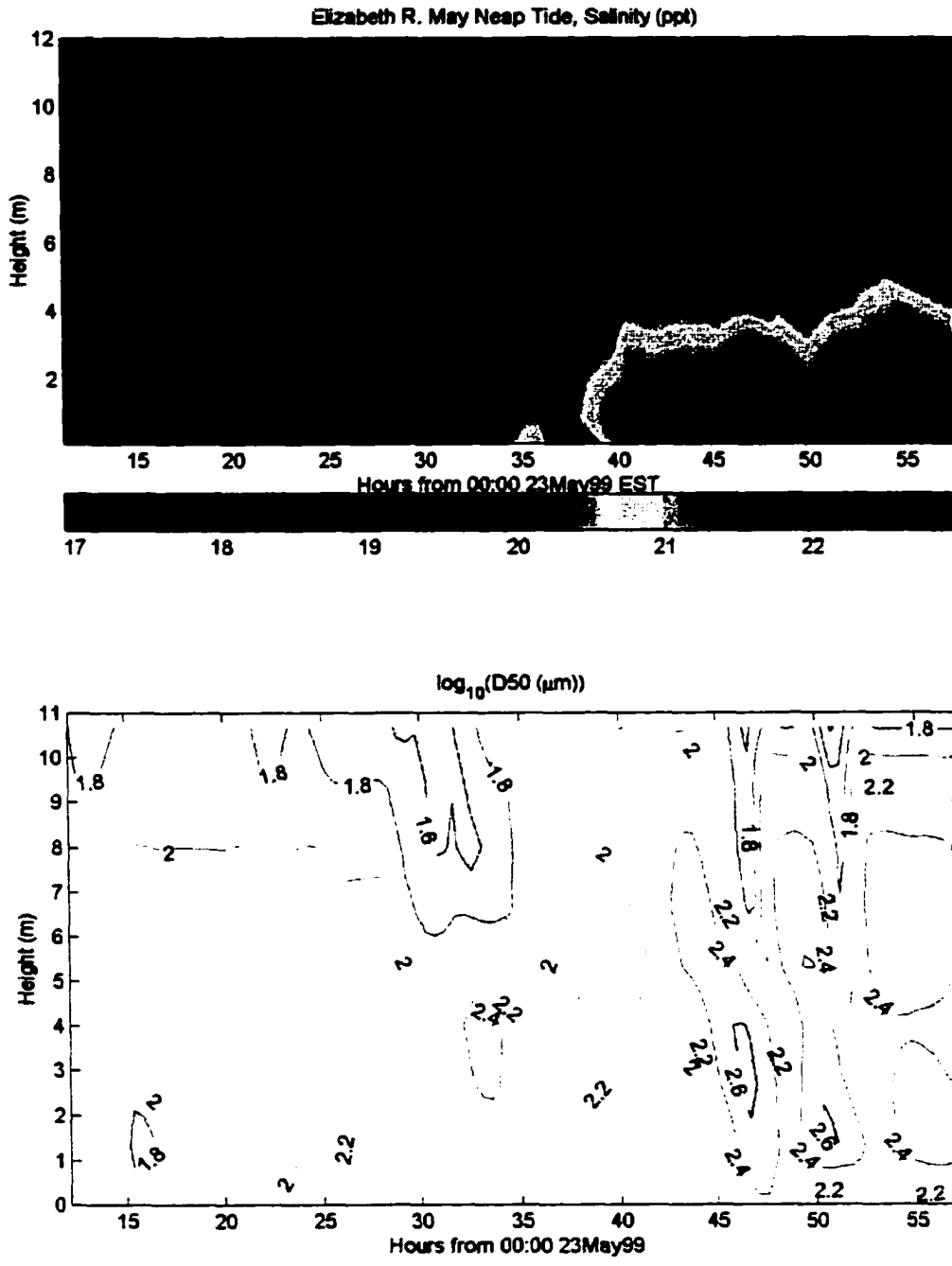

Fig. 3-2. Time series of Elizabeth R. May neap tide (a) Salinity (ppt), (b) $\log_{10}$ (Median Particle Size (μm)).

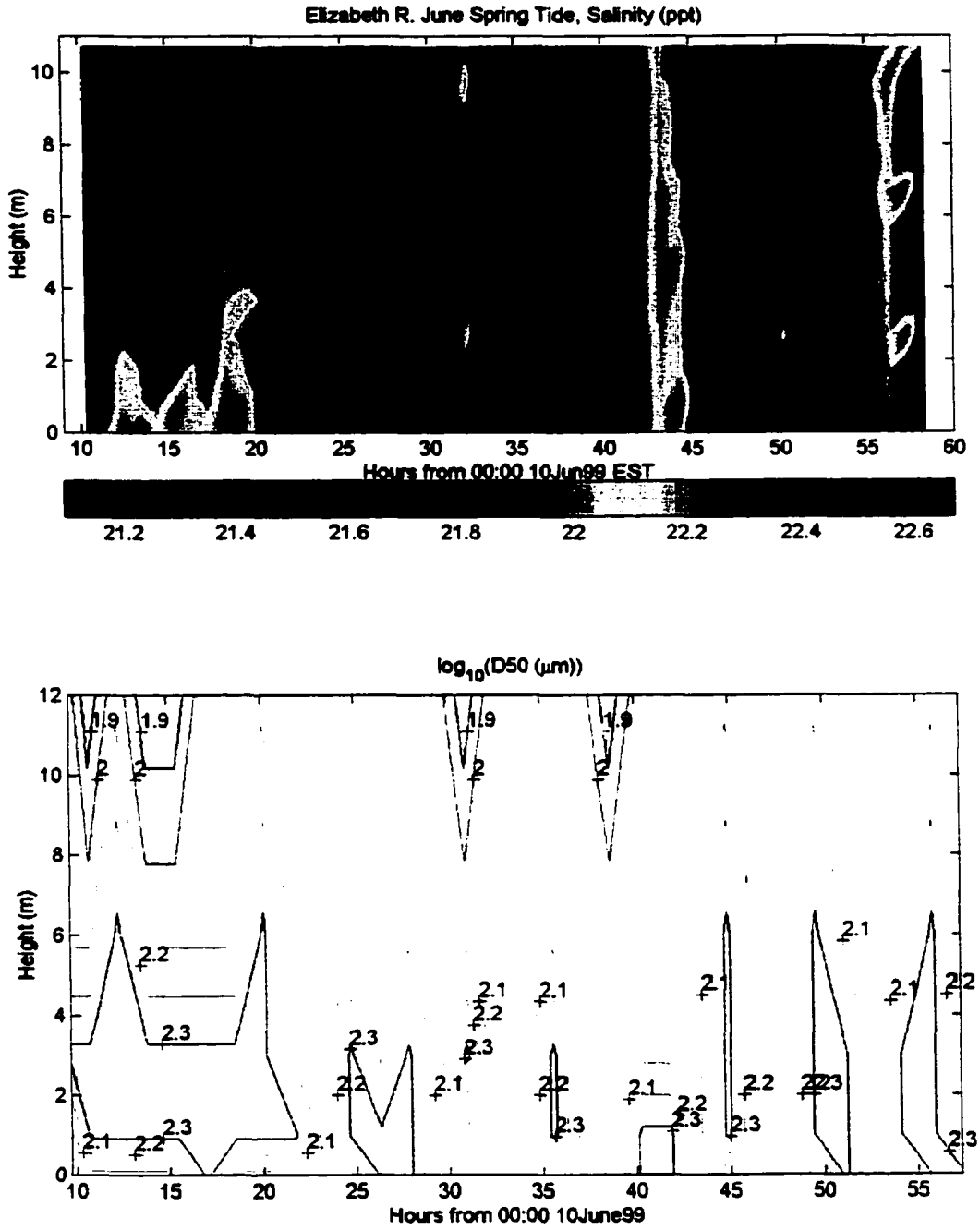

Fig. 3-3. Time series of Elizabeth R. June spring tide (a) Salinity (ppt), (b) $\log_{10}$ (Median Particle Size (μm)).

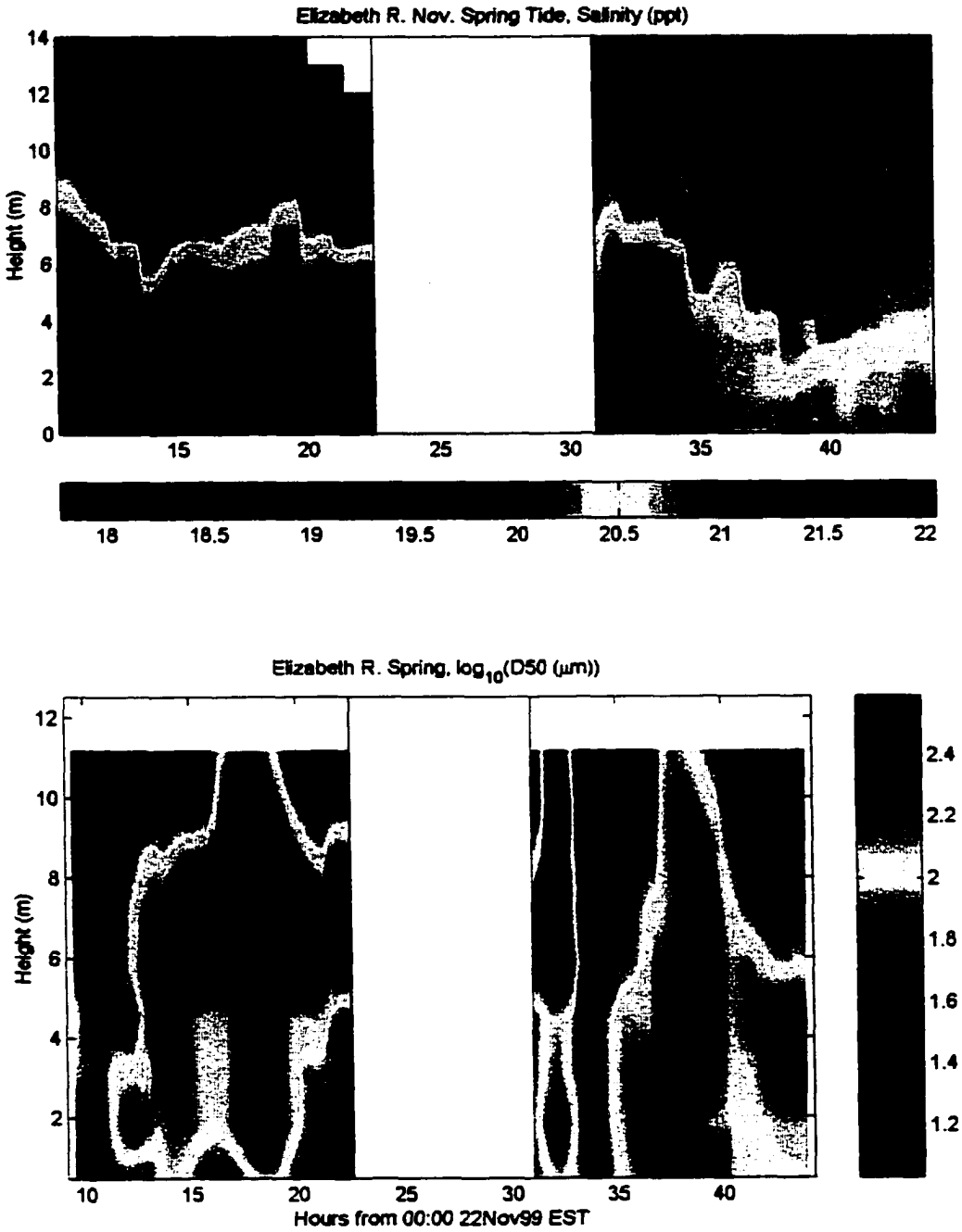

Fig. 3-4. Time series of Elizabeth R. November spring tide (a) Salinity (ppt), (b) $\log_{10}$ (Median Particle Size (μm)).

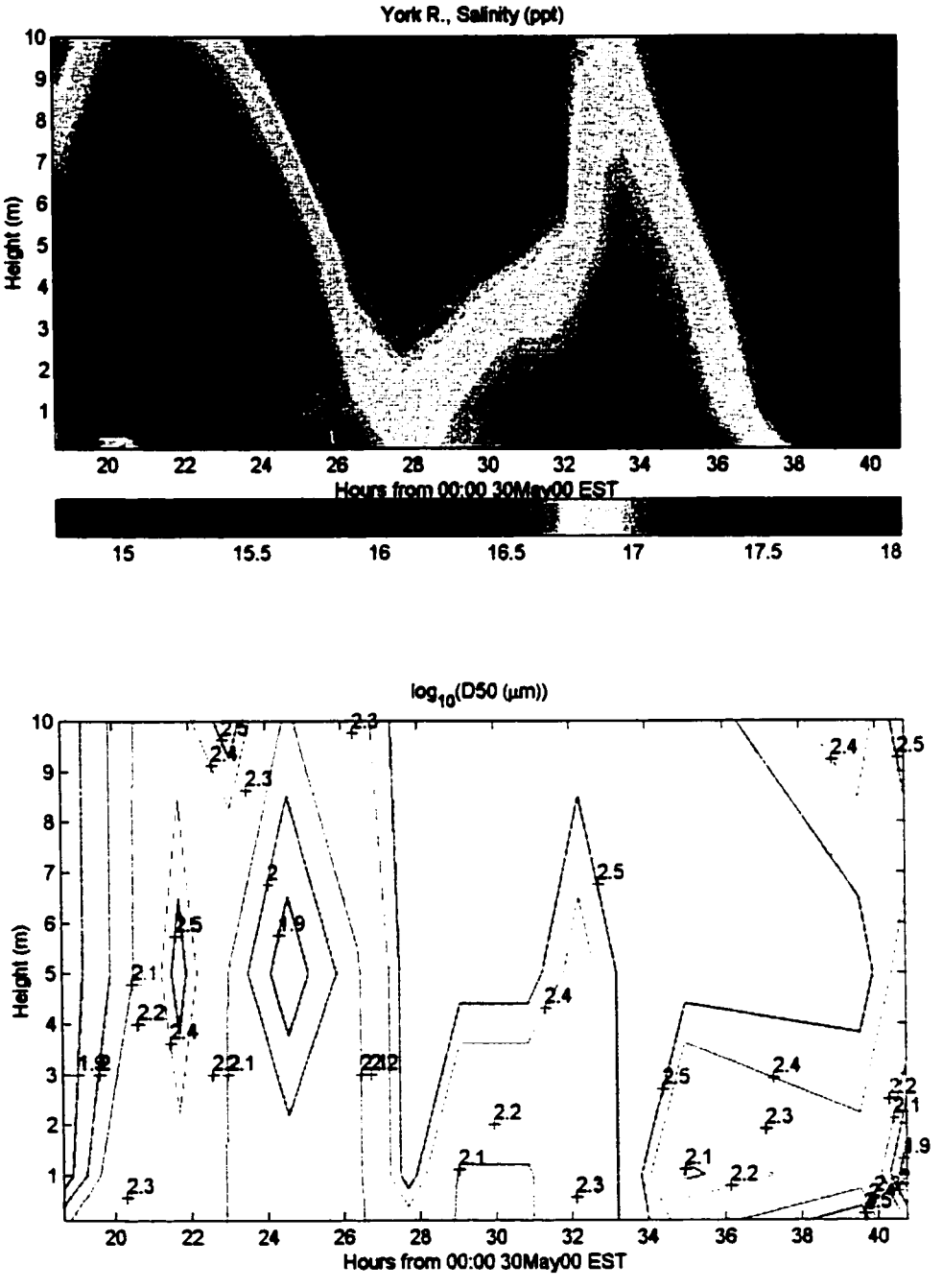

Fig. 3-5. Time series of York R. May spring tide (a) Salinity (ppt), (b) $\log_{10}$ (Median Particle Size (μm)).

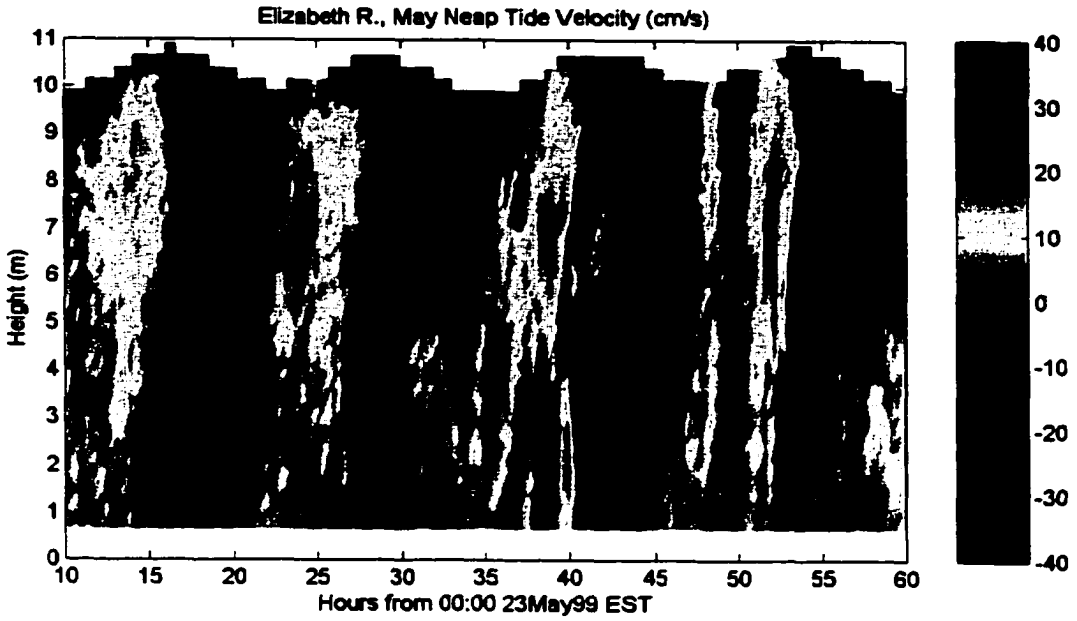

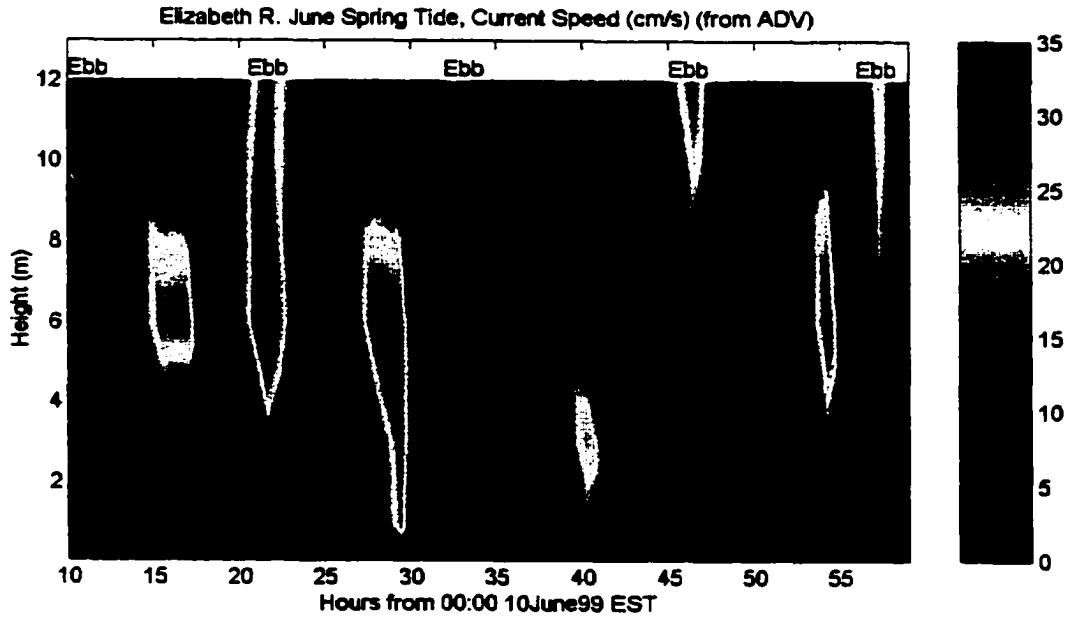

Fig. 3-6. Time series of velocity (cm/s) of (a) Elizabeth R. May neap tide, (b) Elizabeth R. June spring tide.

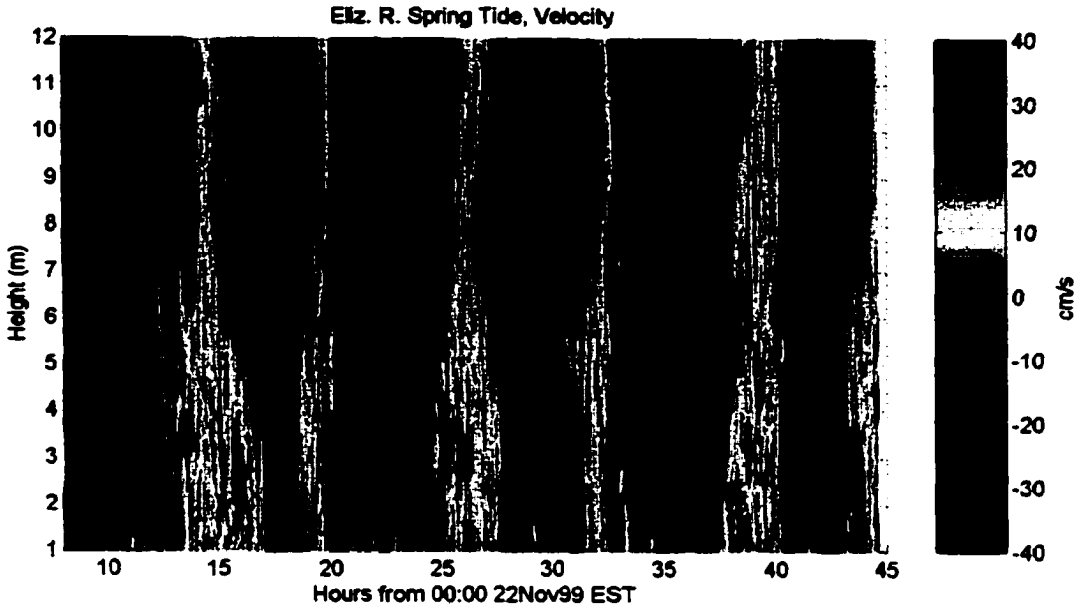

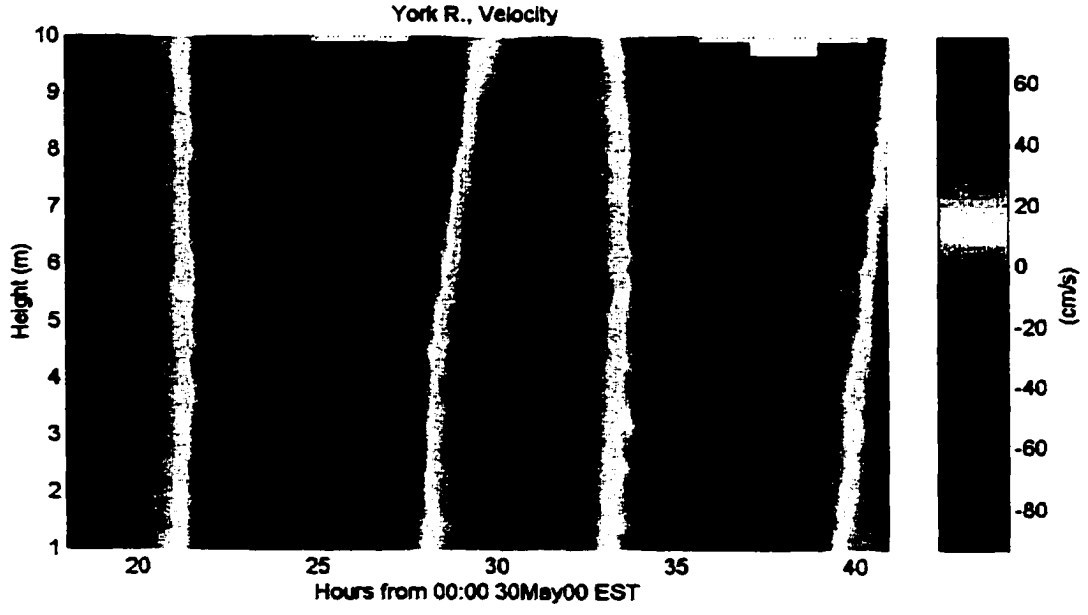

Fig. 3-6 cont. Time series of velocity (cm/s) of (c) Elizabeth R. November spring tide, (d) York R. May spring tide..

Percent Fixed Solids

Levels of percent fixed solids (PFS) are strongly related to the total suspended solids (TSS) (Fig. 3-7). There is a general trend of increasing PFS from the surface to the bottom elevations, with maximum values around 85%. Median values of the upper water column (1 mab to surface) PFS are not much different between surveys, 71%, 64%, 68 % for the May neap, June spring, and November spring surveys, respectively and 77% for the York R. survey. There appears to be little seasonal signal in the PFS. Figure 3-8 shows the relationship of PFS by median grain size (D50) for the summer neap and spring tides in the Elizabeth R. and for the May spring tide in the York R. There is no relationship between these values in the Elizabeth R. Although there is some spread to the data, there is a clear negative relationship between PFS and D50 in the York, supporting the idea that in this estuary, higher organic content allows larger aggregates to form. In the low energy and low concentration environment of the Elizabeth R., the dominant process affecting grain size is resuspension rather than aggregation, and so the organic content is not related to the grain size.

Chlorophyll a

Time series values of chlorophyll *a* normalized to TSS for surface and bottom regions during the May neap tide are shown in Fig. 3-9a. Absolute values of chlorophyll *a* ranged from around 1 to 9 μg/l at both elevations; normalized values ranged from 0 to 0.9 ppt at the surface, and generally between 0 and 0.3 at the bottom, excluding one high outlier of 0.55 ppt. Surface values of normalized chlorophyll a have definite peaks at the end of ebb currents. The two peaks before stratification set in are around 0.85 ppt; the two peaks after stratification are about 0.6 ppt. This suggests that particles from the marine end member are lower in chlorophyll a and that mixing after stratification diluted the surface concentrations. Similarly, the bottom values tend to be a little larger after

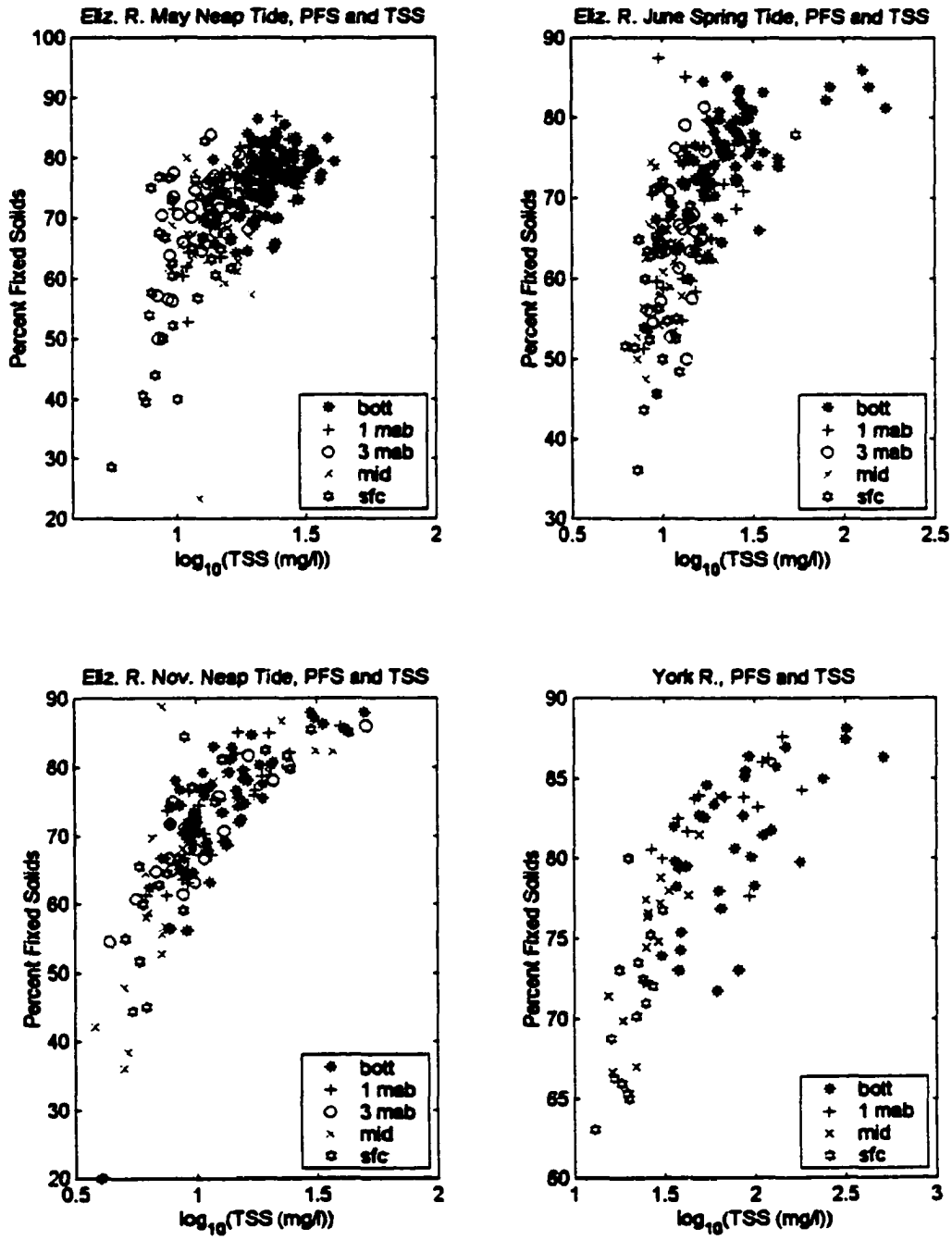

Fig.3-7. Percent fixed solids by $\log_{10}$(TSS (mg/l)) (a) Elizabeth R. May neap tide, (b) Elizabeth R. June spring tide, (c) Elizabeth R. November neap tide, (d) York R. May spring tide.

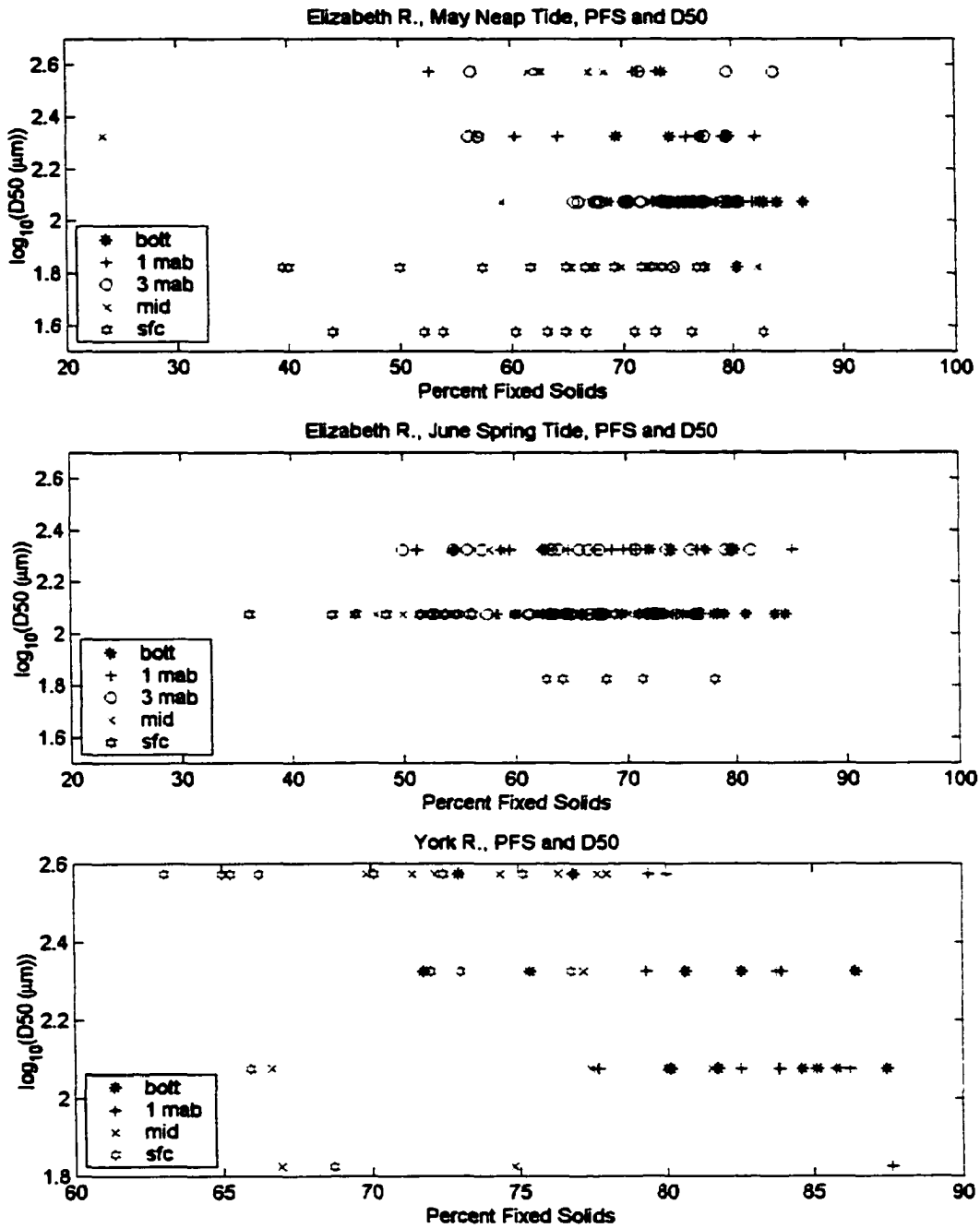

Fig. 3-8. Log_{10}(D50 (µm)) by percent fixed solids (a)) Elizabeth R. May neap tide, (b) Elizabeth R. June spring tide, (c) York R. May spring tide.

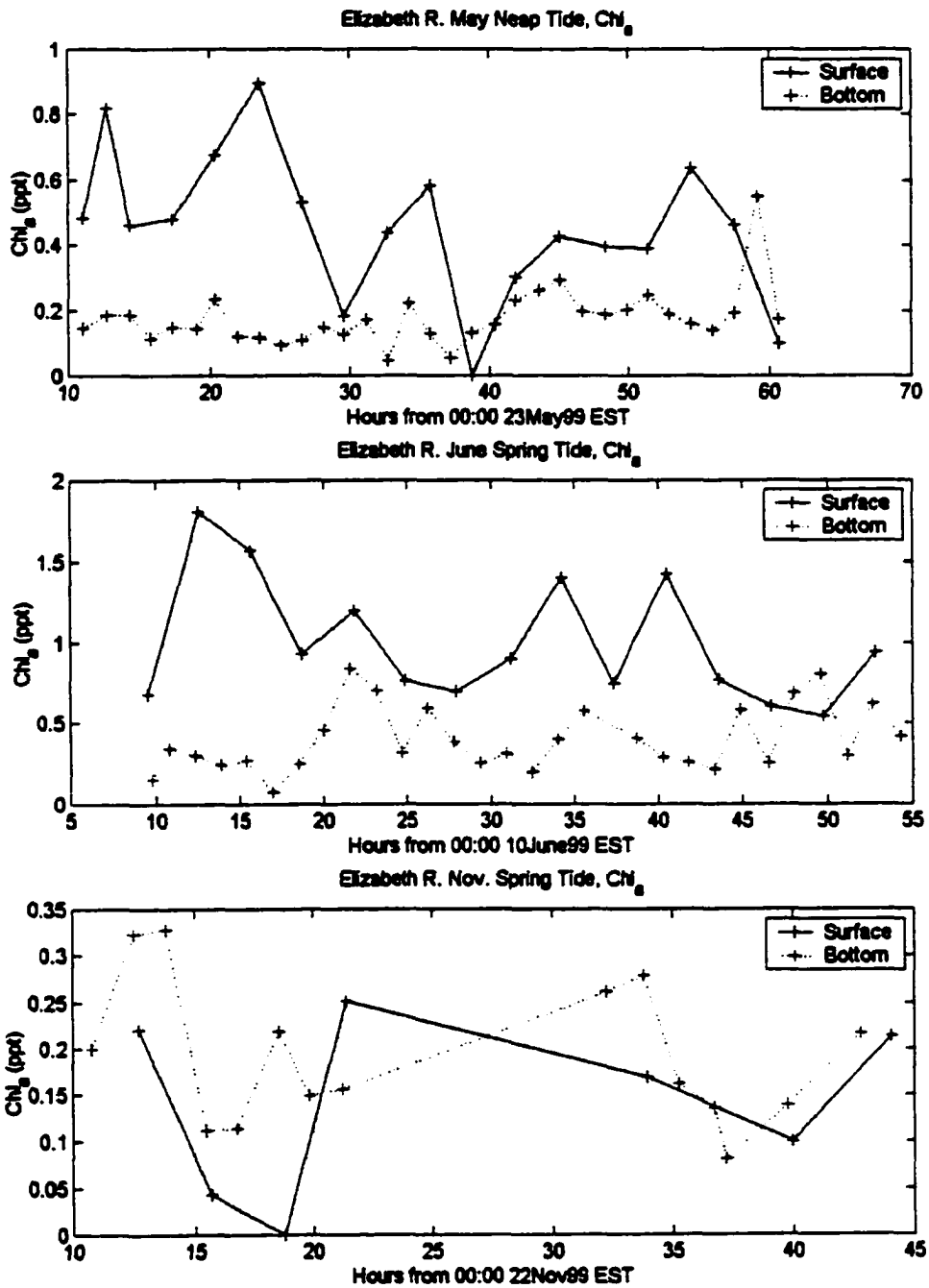

Fig. 3-9. Time series of chlorophyll *a* (ppt) at surface and bottom for (a) Elizabeth R. May neap tide, (b) Elizabeth R. June spring tide, (c) Elizabeth R. November neap tide.

stratification. There is little overall relation between median grain size and specific chlorophyll *a* concentrations (r^2=0.02 and r^2=0.29 between log of median grain size and chlorophyll *a* at the surface and bottom, respectively).

Time series values of chlorophyll *a* normalized to TSS for surface and bottom regions during the June spring tide are shown in Fig. 3-9b. Absolute values of chlorophyll a ranged from 6 to 26 μg/l near the surface, but generally below 14 μg/l. Normalized values ranged from 0.5 to 1.75 ppt. Bottom absolute values were generally between 5 and 10 μg/l and normalized values ranged between 0.05 and 0.8 ppt. There is no apparent tidal signal in the variation of normalized chlorophyll *a*. However, there is a precipitous drop at the surface and a steep rise at bottom when the water column becomes destratified around hour 18. This is consistent with the mixing processes observed during the May neap tide. There is no relation between median grain size and specific chlorophyll *a* concentrations (r^2=0.06 and r^2=-0.21 between log of median grain size and chlorophyll *a* at the surface and bottom, respectively).

Time series values of chlorophyll *a* normalized to TSS for surface and bottom regions during the November spring tide are shown in Fig. 3-9c. Absolute values of chlorophyll a ranged from 0 to 3 μg/l for both surface and bottom elevations. Normalized values were also low for both elevations, between 0 and 0.35 ppt. There is a clear decrease in surface and bottom values after the resuspension event around hour 35 followed by a steady rise. There are also mutually low values during the flood tide between hours 15 and 20. There is also no relation between median grain size and specific chlorophyll *a* concentrations (r^2=-0.43 and r^2=-0.25 between log of median grain size and chlorophyll *a* at the surface and bottom, respectively).

The occasionally higher values of chlorophyll after ebb tides, and low values during floods suggest that chlorophyll is generally higher upstream. Consequently, surface values tend to be high during stratified conditions but mixed down with destratification. There is no relationship between chlorophyll and median grain size.

Carbon and Nitrogen

Carbon and Nitrogen data are available for the May neap and June spring tides in the Elizabeth R., and for the York R. survey.

Time and depth series of C/N for the May neap tide in the Elizabeth R. are shown in Fig. 3-10a. C/N during the early part of the May neap tide survey are high, around 10-16, before hour 40 when the water column became stratified. Although there are a few middepth peaks early in the survey, the values are mostly vertically homogenous. The intermittent high values of C/N before hour 40 are not correlated with tidal currents. After hour 40, C/N decreases to a range of below 5 to about 9, and higher values during this period are associated with ebb tides.

Time and depth series of C/N for the June spring tide in the Elizabeth R. are shown in Fig. 3-10b. Similar to the May neap survey, C/N tends to be vertically homogenous with a few exceptions. During the hours 12-17, 30-33, and 47-48, there appears to be resuspension of high CN material. The highest C/N however came at middepth with the ebb tide of hour 22. In general though, C/N is intermittent without a consistent relationship to the tides.

Time and depth series of C/N for the York R. are shown in Fig. 3-10c. There are clear vertical variations in CN levels, with maxima and minima occurring at middepth. The middepth peak at hour 22 is associated with large particles aggregating at slack after flood. Conversely, the middepth peak at hour 25 is concomitant with small particles associated with the subsequent ebb. After hour 30, there is a clear relationship between C/N, particle size, and salinity. Large particles associated with the fresher water appear with very low C/N. This is suggestive of an advective event (see Chapter 2) of highly organic material. A high abundance of the stinging sea nettle, *Chrysaora quinquecirrha* was observed at this time and these are likely to have been feeding on a phytoplankton bloom associated with the warm fresh water. It is difficult to ascertain the extent to which the particles measured by the LISST were aggregates or phytoplankton.

Descriptive statistics for particulate organic carbon (POC), particulate organic nitrogen (PON), and molar C/N for the May neap and June spring tides from the Elizabeth R. and the York R. are shown in Table 3-1. In the Elizabeth R., median C/N ranges between 9.2 and 10.2. In contrast to the chlorophyll a and PFS measures, there are no significant differences with height above the bed. In the York R., median C/N ranges

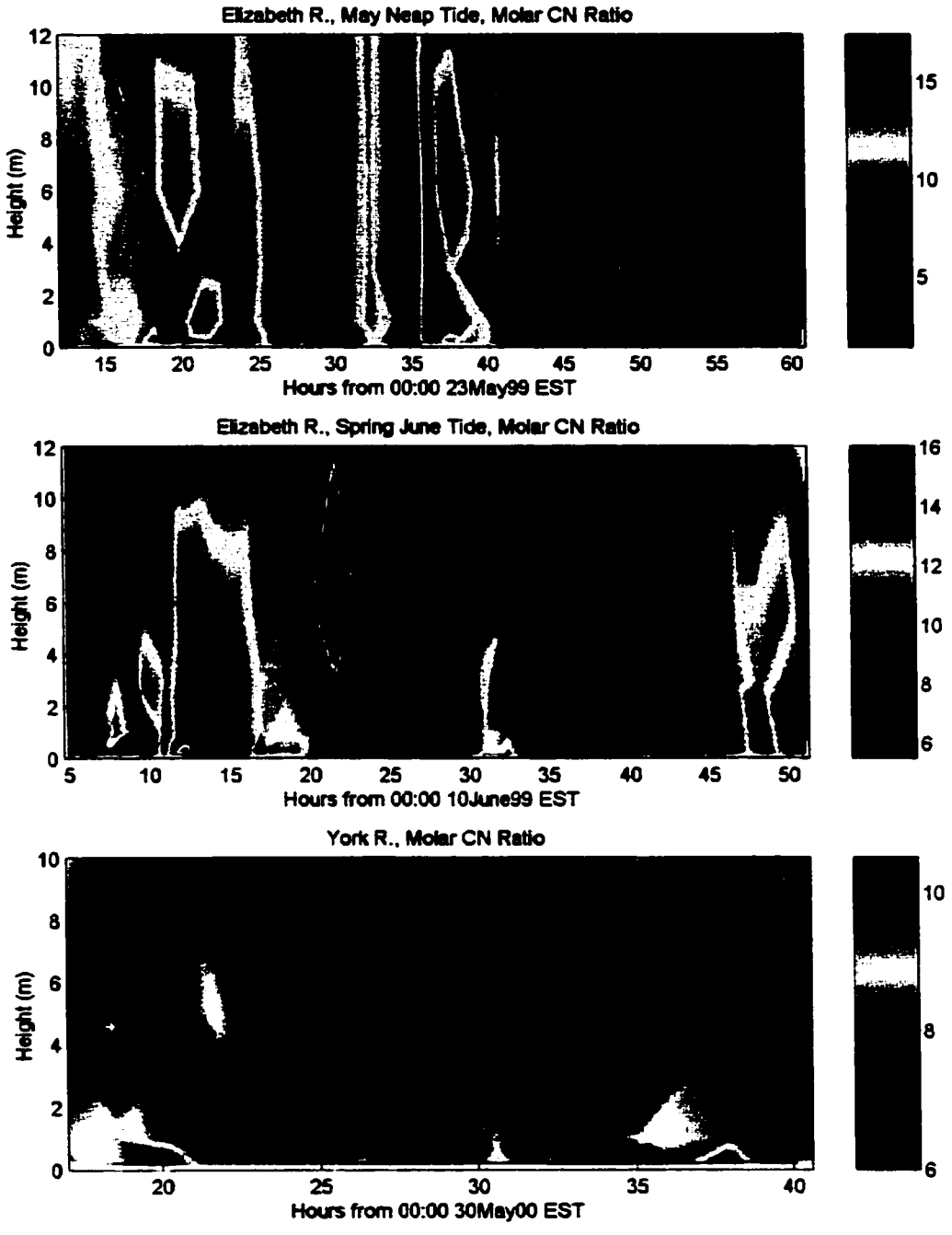

Fig. 3-10. Time series of molar carbon to nitrogen ratio (a) Elizabeth R. May neap tide, (b) Elizabeth R. June spring tide, (c) York R. May spring tide.

TABLE 3-1

Elizabeth R. May Neap Tide, CN Statistics

POC (mg/l)

	mean	median	min	max	std	n
Sfc	0.42	0.35	0.05	1.00	0.368	32
Mid	0.42	0.56	0.05	1.38	0.377	33
3mab	0.45	0.55	0.04	1.85	0.438	33
1mab	0.47	0.63	0.05	1.03	0.400	33
Bot	0.53	0.40	0.06	1.99	0.476	96

PN (mg/l)

	mean	median	min	max	std	n
Sfc	0.41	0.32	0.07	0.94	0.312	32
Mid	0.43	0.55	0.05	1.37	0.354	33
3mab	0.39	0.32	0.06	0.83	0.293	33
1mab	0.45	0.17	0.09	1.29	0.373	33
Bot	0.55	0.54	0.08	1.44	0.436	96

molar CN ratio

	mean	median	min	max	std	n
Sfc	0.1	10.1	5.7	15.9	2.640	32
Mid	10.5	10.1	1.1	18.0	3.420	33
3mab	10.4	9.7	4.6	17.0	3.223	33
1mab	10.4	9.6	6.4	16.5	2.661	33
Bot	10.6	10.2	5.1	17.2	2.785	96

TABLE 3-1 cont.

Elizabeth River June Spring Tide, CN Statistics

POC (mg/l)

	mean	median	min	max	std	n
Sfc	0.44	0.50	0.07	1.31	0.360	33
Mid	0.46	0.54	0.05	1.61	0.403	33
3mab	0.46	0.37	0.06	1.00	0.386	32
1mab	0.57	0.61	0.07	3.06	0.607	33
Bot	0.73	0.45	0.06	4.64	0.845	94

PN (mg/l)

	mean	median	min	max	std	n
Sfc	0.45	0.22	0.05	1.27	0.391	33
Mid	0.46	0.30	0.06	2.53	0.481	33
3mab	0.47	0.43	0.05	1.25	0.385	32
1mab	0.51	0.66	0.06	1.67	0.423	33
Bot	0.66	0.59	0.00	3.18	0.594	94

molar CN ratio

	mean	median	min	max	std	n
Sfc	8.9	9.2	5.9	12.8	1.784	33
Mid	10.1	9.4	6.0	27.8	4.024	33
3mab	10.1	9.6	6.1	15.0	2.451	32
1mab	10.1	9.6	5.5	16.3	2.755	33
Bot	12.4	10.2	5.6	201.8	19.893	94

TABLE 3-1 cont.

York River CN Statistics

POC (mg/l)

	mean	median	min	max	std	n
Sfc	1.48	1.46	1.08	1.91	0.246	16
Mid	1.56	1.46	1.03	2.55	0.409	16
1mab	2.68	1.96	1.36	6.01	1.339	16
Bot	4.14	3.30	.65	16.15	2.936	32

PN (mg/l)

	mean	median	min	max	std	n
Sfc	0.25	0.23	0.16	0.52	0.085	16
Mid	0.30	0.24	0.16	1.16	0.239	16
1mab	0.38	0.31	0.20	0.82	0.178	16
Bot	0.58	0.46	0.24	1.84	0.349	32

molar CN ratio

	mean	median	min	max	std	n
Sfc	7.4	7.7	3.2	8.8	1.361	16
Mid	7.2	7.6	1.2	9.0	1.761	16
1mab	8.1	8.1	6.8	9.1	0.689	16
Bot	8.2	8.3	2.9	10.5	1.370	32

from 7.6 to 8.3. Bottom and 1mab elevations are higher, but not significantly, than those further up in the water column.

Data archived by the Chesapeake Bay Foundation Water Quality Monitoring Program (Fig. 3-11) confirm that there is little vertical variation in C/N in the Southern Branch of the Elizabeth R. They also show that the upper reaches tend to have higher values than the lower reaches. Since chlorophyll a concentrations appear to be higher up estuary, these data suggest that the source of the high organic material coming from the marine end member is not from phytoplankton.

Since C/N is vertically homogenous and median grain size values are vertically heterogeneous, there is no apparent relationship between C/N and median grain size.

Metals

Metal data are available for the May neap, June and November spring tides in the Elizabeth R.

Time and depth series concentrations of metals for the May neap tide are shown in Fig. 3-12. Note from Fig 3-2a and 3-2b that around hour 35 the water column is stratified and larger particles appear. Up to the time of this stratification, Fe and Mn have peak concentrations at the surface and middepth at hours 15, 25, and 35. Afterwards, during stratification, the concentrations are generally elevated. Aluminum is correlated with Fe and Mn before stratification, then has two more surface and middepth peaks at hour 41 and 51. The peaks in these 'sediment associated' metals appear at 10 hour intervals. Cu peaks in the middepth after stratification at hours 35, 47, and 55 during slack current. Cr is correlated with Cu, but also has an additional middepth peak before stratification at hour 24. Peak metal concentrations for all metals appear to occur at approximately 10 hour intervals in the middepth and surface regions. In addition, Fe and Mn, and to some extent Cu and Cr, appeared to have higher concentrations throughout the water column with the onset of the stratification event.

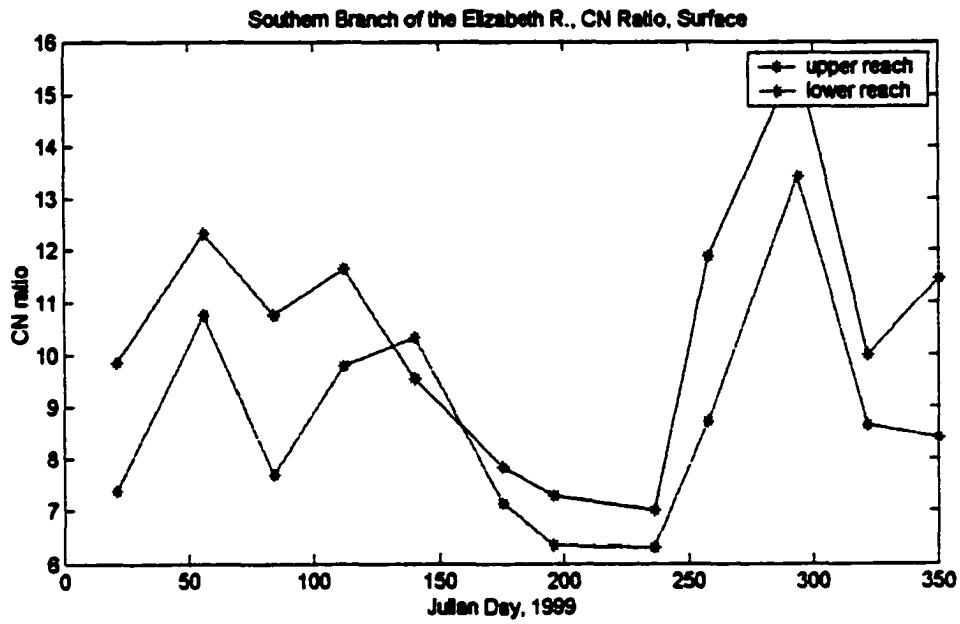

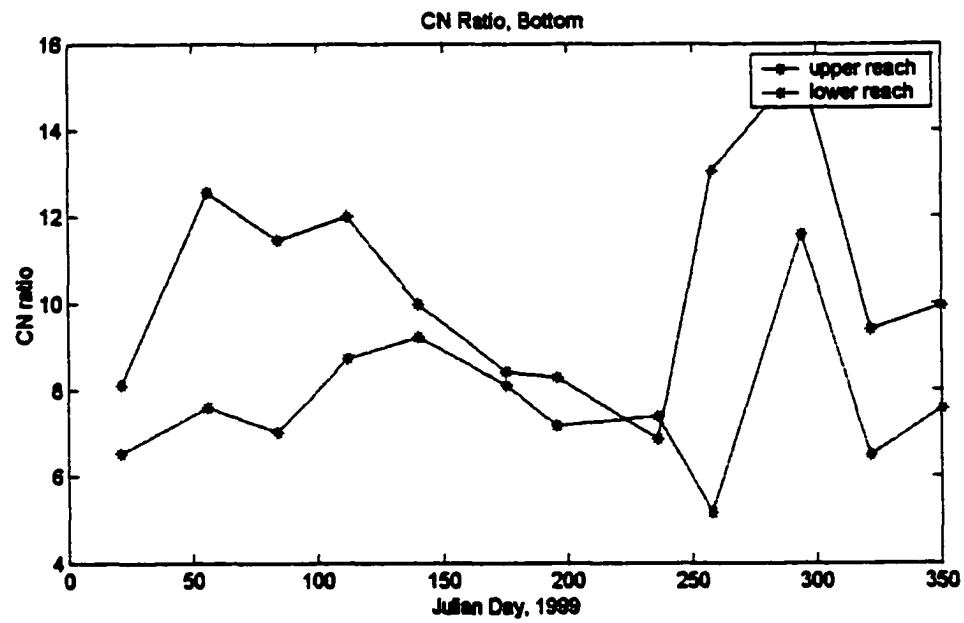

Fig. 3-11. Time series of Southern Branch of the Elizabeth R. molar carbon to nitrogen ratio for 1999 from Chesapeake Bay Foundation Water Quality Monitoring Program (a) Surface, (b) Bottom.

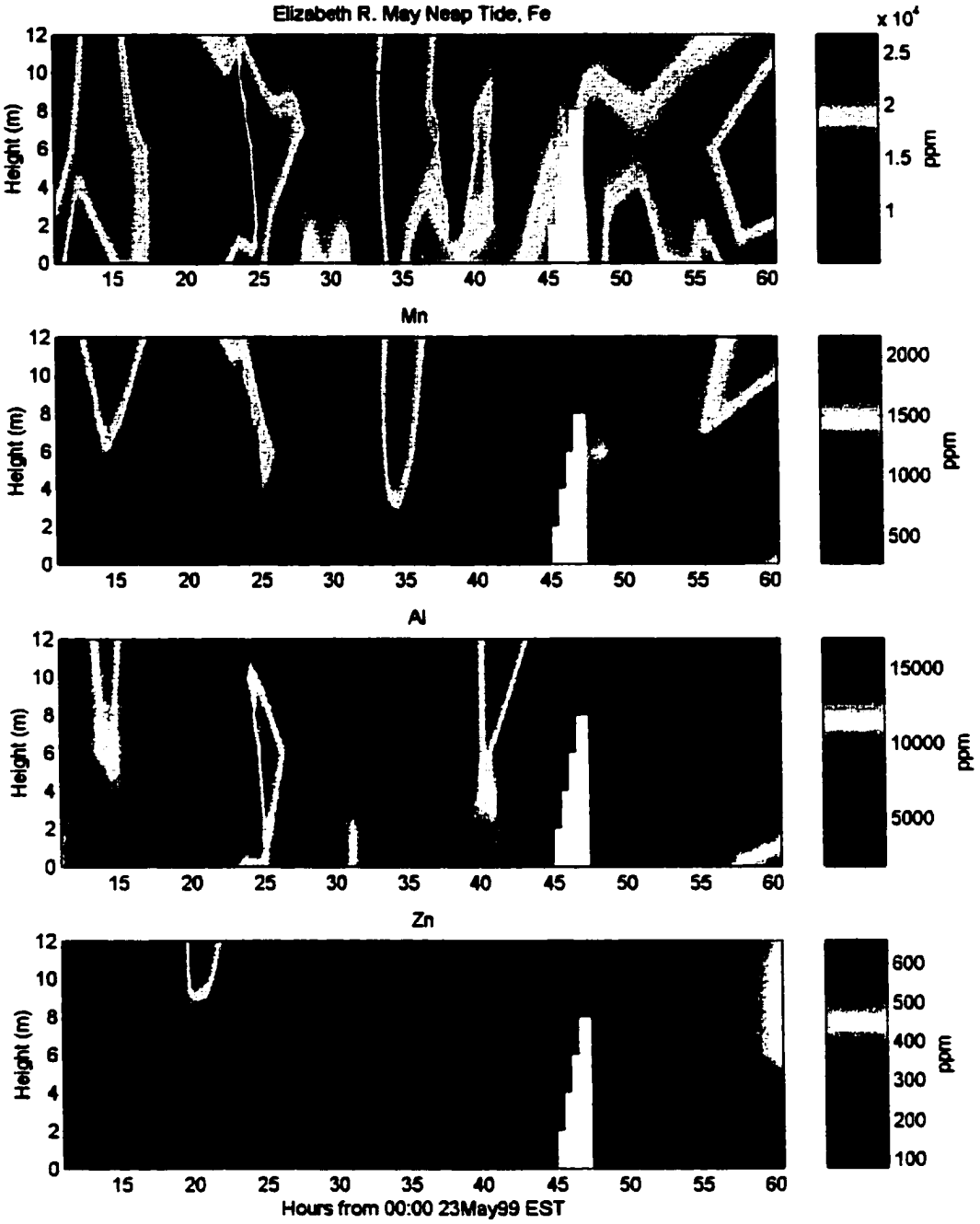

Fig. 3-12. Time series of specific metal concentrations for Elizabeth R. May neap tide, (a) Iron, (b) Manganese, (c) Aluminum, (d) Zn.

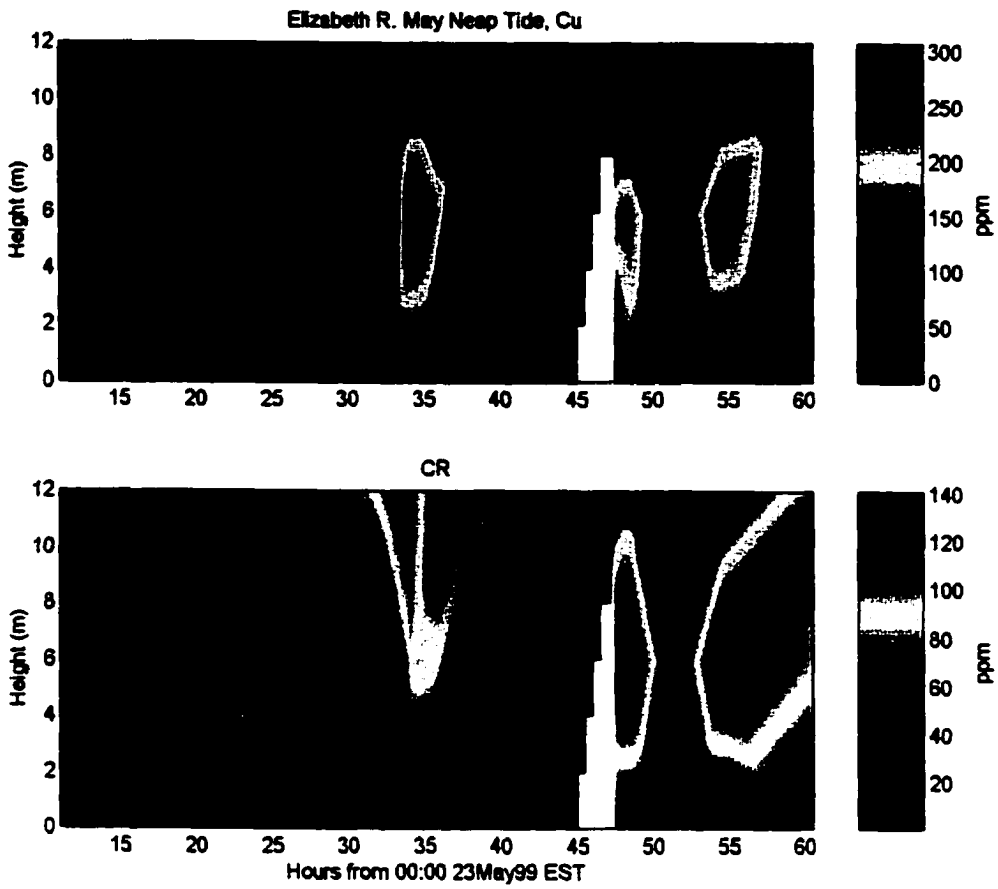

Fig. 3-12 cont. Time series of specific metal concentrations for Elizabeth R. May neap tide, (e) Copper, (f) Chromium.

Time and depth series concentrations of metals for the June spring tide are shown in Fig 3-13. Note from Fig. 3-3a and 3-3b that the water column was well mixed during this survey, and that maximum particle sizes were generally found at middepth. In contrast to the May neap tide values, June spring tide Fe and Al concentrations have regular peaks at the bottom during slack periods. Cu and Cr peak in the middle water column during floods at hour 17 and 40, but not at the flood during hour 29. Cd is lower around hours 15, 30, and 45.

Time and depth series concentrations of metals for the November spring tide are shown in Fig 3-14. Figure 3-4a and 3-4b show that the water column was generally well stratified until a large boat wake mixed the water column and resuspended lots of large particles. Fe and Al peak at middepth at hours 15 and 40 during slack tide. But during the slack around hour 33 there are small peaks at the bottom for both of these metals. Zn peaks at middepth at hour 34 and 40. Cu appears to be resuspended from the bottom at hours 18, 32, and especially around hour 37 during the large resuspension event from boat wake. Cr and Cd have isolated peaks in the middle of the water column around hour 40.

Summary of Metal Concentrations

Descriptive statistics for the metal concentrations are shown in Table 3-2 and correlation coefficients between the metals are shown in Table 3-3. Depth partitioned mean Fe specific concentration values ranged from 2225 ppm to 62107 ppm, Mn ranged from below detection level to 2667 ppm, and Al ranged from 1222 ppm to 17717 ppm. The contaminant trace metal mean specific concentrations ranged from 31 to 1638 ppm for Zn. Cu ranged from below detection to 550 ppm, and Cd was generally below detection. Chromium values were generally below detection but are often correlated with Cu concentrations, so are included as perhaps a qualitative indicator of variation. Iron, Mn, and Al are generally well correlated with each other.

The most notable results amongst the natural, or sediment associated, metal analyses are that the highest mean and maximum concentrations of Fe, Mn, and Al, occur

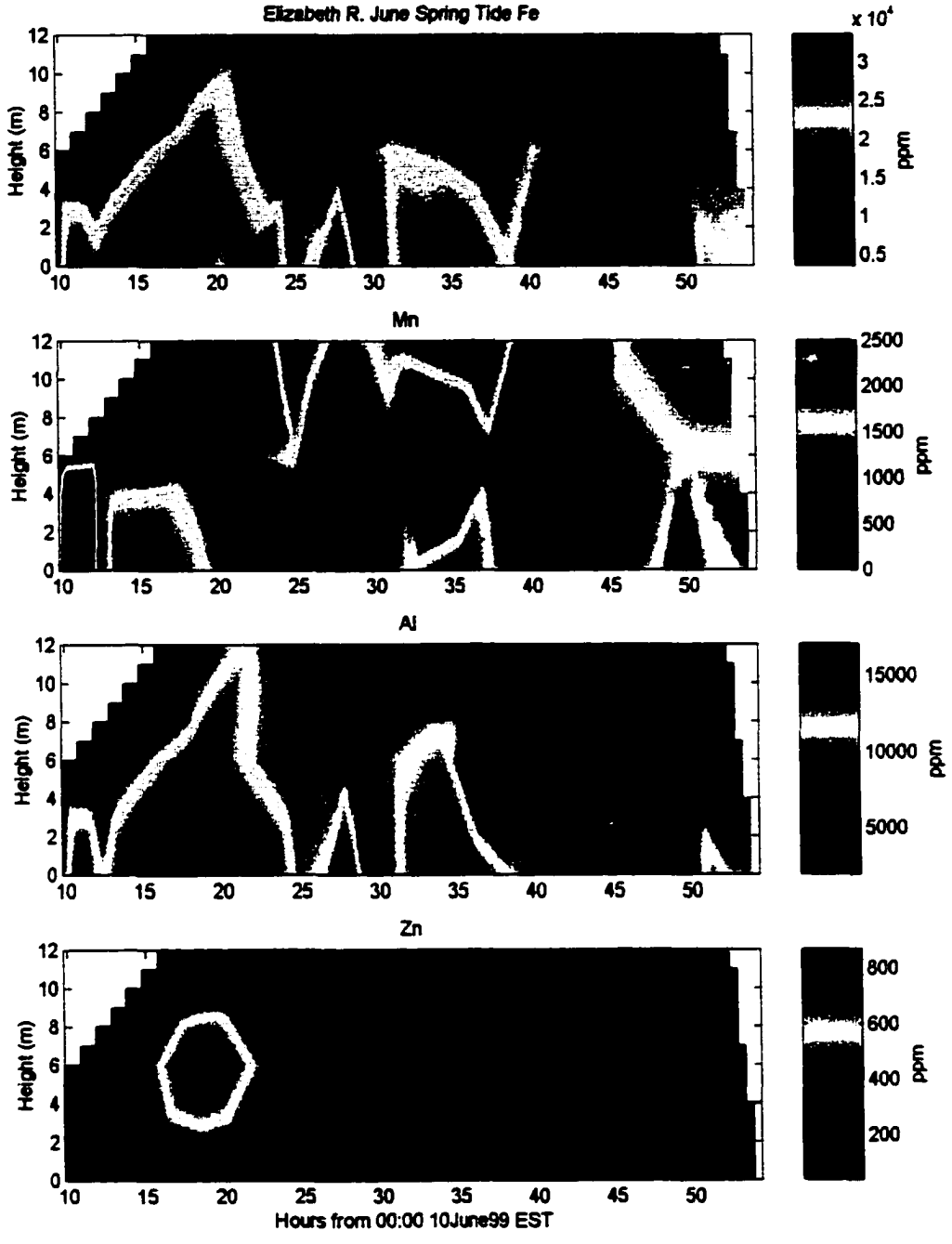

Figure 3-13. Time series of specific metal concentrations for Elizabeth R. June spring tide, (a) Iron, (b) Manganese, (c) Aluminum, (d) Zn.

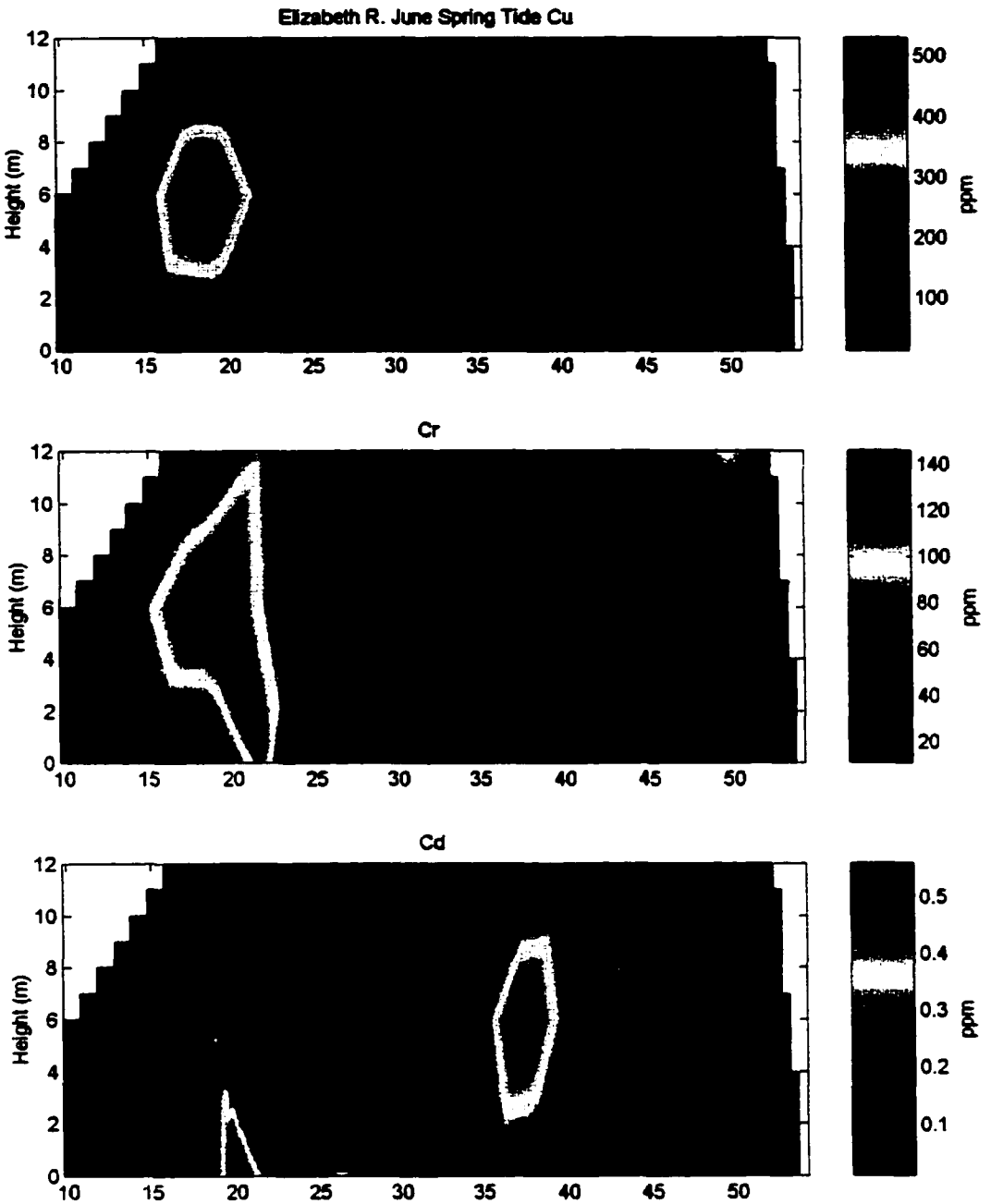

Fig. 3-13 cont. Time series of specific metal concentrations for Elizabeth R. June spring tide, (e) Copper, (f) Chromium, (g) Cadmium

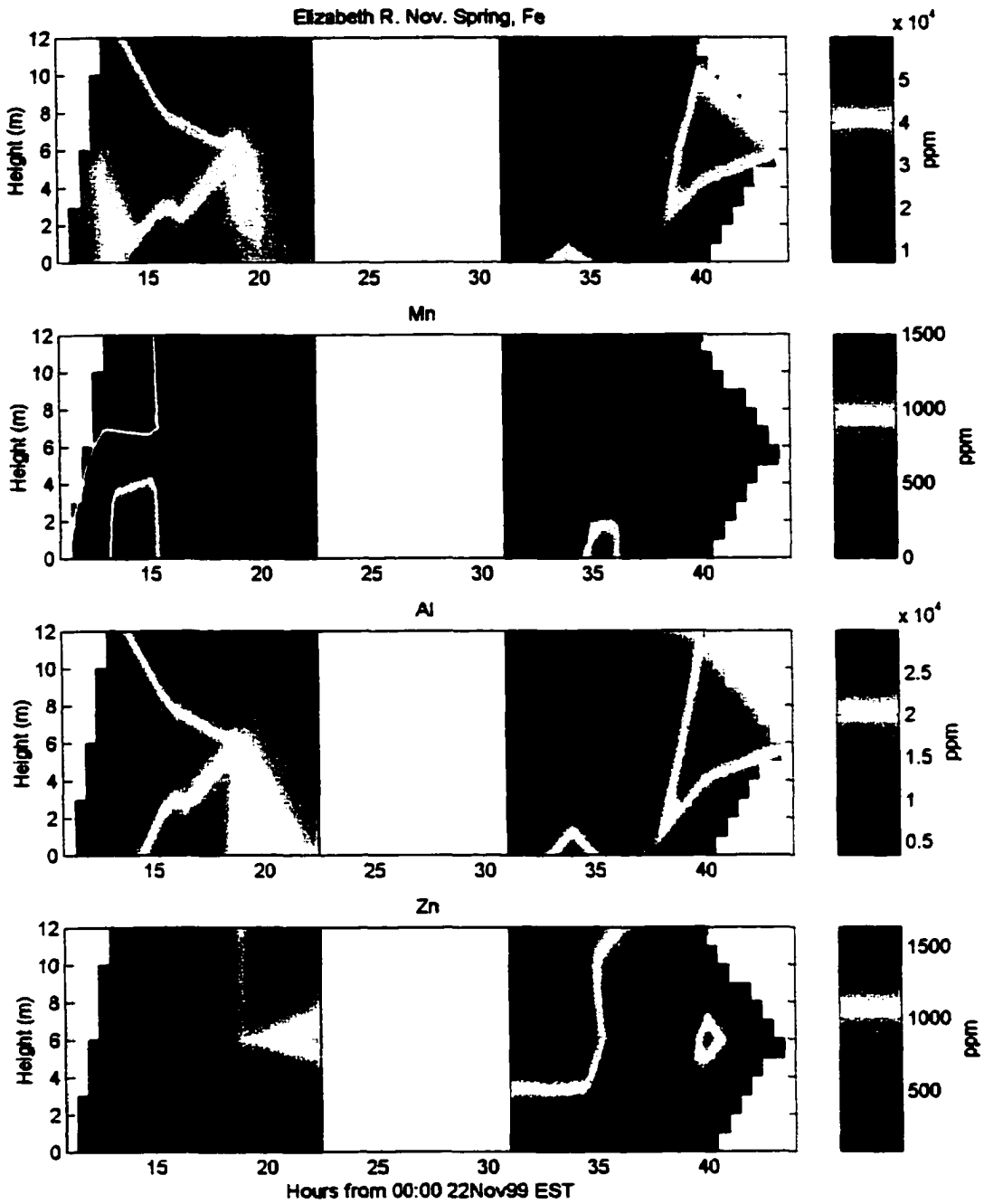

Fig. 3-14. Time series of specific metal concentrations for Elizabeth R. November spring tide, (a) Iron, (b) Manganese, (c) Aluminum, (d) Zn.

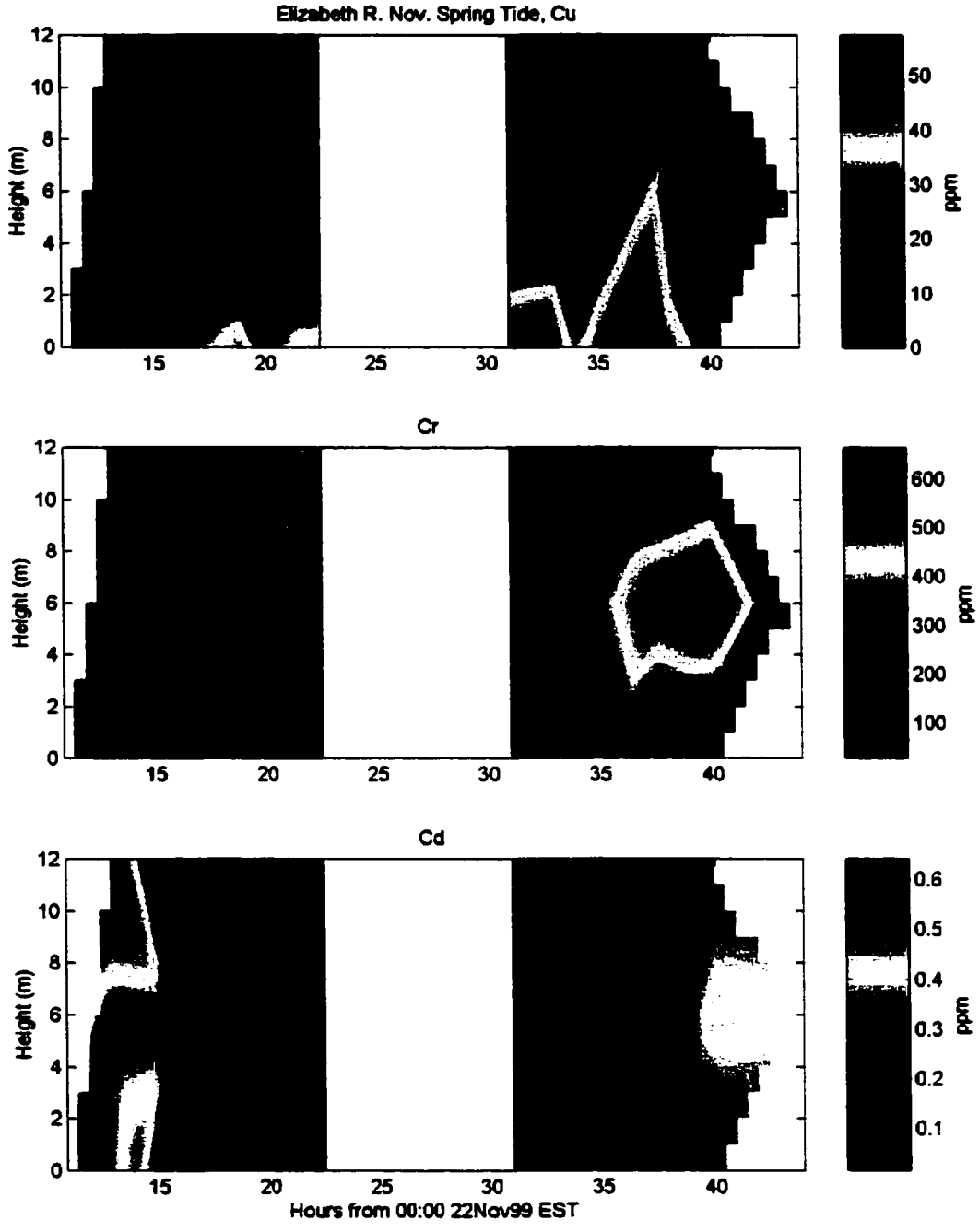

Fig. 3-14 cont. Time series of specific metal concentrations for Elizabeth R. November spring tide, (e) Copper, (f) Chromium, (g) Cadmium

Table 3-2. Elizabeth R. May Neap Tide, Metal Statistics

Fe (ppm)

Mean	Median	Min	Max	Std	n
1644	16789	5274	27328	5274	22
1861	19935	6029	27421	6130	23
17615	18340	3694	25792	4806	29

Corr Coef w/ D50 0.06 n= 69

Mn (ppm)

Mean	Median	Min	Max	Std	n
1218	1106	407	2185	459	22
1028	1005	349	1943	403	23
893	916	213	1483	261	29

Corr Coef w/ D50 -0.30 n= 69

Al (ppm)

Mean	Median	Min	Max	Std	n
7438	6646	2747	17717	3472	22
7431	6646	3001	15550	3253	23
7994	9025	1504	13545	3666	29

Corr Coef w/ D50 0.02 n= 69

Zn (ppm)

Mean	Median	Min	Max	Std	n
246	192	108	696	139	22
218	194	117	451	89	23
176	166	67	307	57	29

Corr Coef w/ D50 -0.06 n= 69

Cu (ppm)

Mean	Median	Min	Max	Std	n
24	17	0	83	27	22
98	53	25	325	91	23
73	63	16	158	30	29

Corr Coef w/ D50 0.23 n= 69

Cr (ppm)

Mean	Median	Min	Max	Std	n
61	60	-6	109	28	22
67	57	33	146	30	23
44	45	24	77	11	29

Corr Coef w/ D50 -0.09 n= 69

Cd (ppm)

Mean	Median	Min	Max	Std	n
0	0	0	1	0	22
0	0	0	2	0	23

Corr Coef w/ D50 -0.12 n= 40

Table 3-2 (cont.). Elizabeth River June Spring Tide, Metal Statistics

Fe (ppm)

Mean	Median	Min	Max	Std	n
13270	13940	2225	19400	4861	12
19147	17655	14935	27317	3740	11
22801	22903	9906	33768	6466	24

Corr Coef w/ D50 0.25 n= 47

Mn (ppm)

Mean	Median	Min	Max	Std	n
1310	1468	0	2667	982	12
1007	1093	0	1583	541	11
1520	1285	432	7791	1424	24

Corr Coef w/ D50 -0.03 n= 47

Al (ppm)

Mean	Median	Min	Max	Std	n
6901	7235	1222	11998	2707	12
9343	8652	3104	14500	3013	11
11597	10868	5069	17175	3447	24

Corr Coef w/ D50 0.21 n= 47

Zn (ppm)

Mean	Median	Min	Max	Std	n
178	158	31	417	108	12
264	232	66	895	234	11
189	193	71	271	53	24

Corr Coef w/ D50 0.06 n= 47

Cu (ppm)

Mean	Median	Min	Max	Std	n
42	46	14	98	26	12
121	61	31	550	157	11
97	98	36	160	31	24

Corr Coef w/ D50 0.09 n= 47

Cr (ppm)

Mean	Median	Min	Max	Std	n
59	54	20	94	22	12
58	52	14	150	35	11
50	48	11	121	22	24

Corr Coef w/ D50 0.02 n= 47

Cd (ppm)

Mean	Median	Min	Max	Std	n
0	0	0	0	0	12
0	0	0	1	0	11
0	0	0	1	0	24

Corr Coef w/ D50 0.15 n= 47

Table 3-2 (cont.). Elizabeth R. Nov. Spring Tide, Metal Statistics

Fe (ppm)

Mean	Median	Min	Max	Std	n
32362	29891	9540	62107	17007	6
37140	41204	7324	56091	17389	7
34868	36880	7959	47474	10295	13

Corr Coef w/ D50 0.30 n= 26

Mn (ppm)

Mean	Median	Min	Max	Std	n
1015	0	0	5859	2375	6
60	0	0	419	158	7
571	350	0	2292	681	13

Corr Coef w/ D50 -0.13 n= 26

Al (ppm)

Mean	Median	Min	Max	Std	n
15545	1324	4742	30670	8984	6
19334	20523	3428	28048	9166	7
18580	20103	3610	25594	5919	13

Corr Coef w/ D50 0.32 n= 26

Zn (ppm)

Mean	Median	Min	Max	Std	n
692	620	74	1449	490	6
717	583	57	1638	603	7
378	344	169	879	179	13

Corr Coef w/ D50 -0.20 n= 26

Cu (ppm)

Mean	Median	Min	Max	Std	n
8	6	0	21	9	6
6	0	0	37	14	7
32	31	8	57	15	13

Corr Coef w/ D50 0.24 n= 26

Cr (ppm)

Mean	Median	Min	Max	Std	n
200	195	27	393	137	6
360	316	84	664	203	7
124	104	33	275	76	13

Corr Coef w/ D50 0.22 n= 26

Cd (ppm)

Mean	Median	Min	Max	Std	n
0	0	0	1	0	6
0	0	0	0	0	7
0	0	0	0	0	13

Corr Coef w/ D50 0.13 n= 26

Table 3-3. Metal Correlation Matrices

Elizabeth R. May Neap, Surface

Fe	Mn	Al	Zn	Cu	Cr	Cd
1.00	0.86	0.35	0.19	0.13	0.15	0.46
0.86	1.00	0.39	0.25	0.22	0.26	0.35
0.35	0.39	1.00	-0.14	0.20	-0.30	0.32
0.19	0.25	-0.14	1.00	0.33	0.23	0.02
0.13	0.22	0.20	0.33	1.00	0.13	0.07
0.15	0.26	-0.30	0.23	0.13	1.00	0.11
0.46	0.35	0.32	0.02	0.07	0.11	1.00

Elizabeth R. May Neap, Mid

1.00	0.92	0.55	0.33	0.52	0.31	0.27
0.92	1.00	0.36	0.30	0.64	0.36	0.21
0.55	0.36	1.00	0.16	-0.30	-0.32	-0.20
0.33	0.30	0.16	1.00	0.24	0.60	0.39
0.52	0.64	-0.30	0.24	1.00	0.70	0.44
0.31	0.36	-0.32	0.60	0.70	1.00	0.57
0.27	0.21	-0.20	0.39	0.44	0.57	1.00

Elizabeth R. May Neap, Bottom

1.00	0.83	0.82	0.40	0.12	0.18
0.83	1.00	0.63	0.31	0.29	0.09
0.82	0.63	1.00	0.38	-0.30	0.26
0.40	0.31	0.38	1.00	0.36	0.26
0.12	0.29	-0.30	0.36	1.00	0.05
0.18	0.09	0.26	0.26	0.05	1.00

Elizabeth R. June Spring, Surface

Fe	Mn	Al	Zn	Cu	Cr	Cd
1.00	0.27	0.96	0.08	0.33	0.90	0.53
0.27	1.00	0.06	0.10	0.33	0.34	0.18
0.96	0.06	1.00	0.05	0.24	0.84	0.50
0.08	0.10	0.05	1.00	0.10	0.00	-0.21
0.33	0.33	0.24	0.10	1.00	0.36	-0.16
0.90	0.34	0.84	0.00	0.36	1.00	0.45
0.53	0.18	0.50	-0.21	-0.16	0.45	1.00

Table 3-3. (cont.)

Elizabeth R. June Spring, Mid

Fe	Mn	Al	Zn	Cu	Cr	Cd
1.00	0.04	0.77	0.86	0.79	0.72	0.10
0.04	1.00	-0.33	0.25	0.17	0.31	0.24
0.77	-0.33	1.00	0.68	0.58	0.50	-0.46
0.86	0.25	0.68	1.00	0.95	0.87	-0.02
0.79	0.17	0.58	0.95	1.00	0.94	0.05
0.72	0.31	0.50	0.87	0.94	1.00	-0.02
0.10	0.24	-0.46	-0.02	0.05	-0.02	1.00

Elizabeth R. June Spring, Bottom

1.00	0.36	0.97	0.63	0.63	0.30	0.25
0.36	1.00	0.36	0.33	0.32	-0.03	0.01
0.97	0.36	1.00	0.62	0.54	0.38	0.30
0.63	0.33	0.62	1.00	0.75	0.38	0.33
0.63	0.32	0.54	0.75	1.00	0.06	0.27
0.30	-0.03	0.38	0.38	0.06	1.00	0.47
0.25	0.01	0.30	0.33	0.27	0.47	1.00

Elizabeth R. Nov. Spring, Surface

1.00	0.86	0.97	0.23	0.28	0.46	0.94
0.86	1.00	0.82	-0.06	0.36	0.43	0.90
0.97	0.82	1.00	0.10	0.47	0.38	0.98
0.23	-0.06	0.10	1.00	-0.69	-0.23	0.03
0.28	0.36	0.47	-0.69	1.00	0.00	0.50
0.46	0.43	0.38	-0.23	0.00	1.00	0.33
0.94	0.90	0.98	0.03	0.50	0.33	1.00

Elizabeth R. Nov. Spring, Mid

1.00	0.48	0.99	-0.25	-0.41	0.00	0.71
0.48	1.00	0.42	-0.24	-0.19	-0.31	0.17
0.99	0.42	1.00	-0.26	-0.42	0.00	0.73
-0.25	-0.24	-0.26	1.00	-0.47	0.24	-0.48
-0.41	-0.19	-0.42	-0.47	1.00	0.49	-0.15
0.00	-0.31	0.00	0.24	0.49	1.00	0.04
0.71	0.17	0.73	-0.48	-0.15	0.04	1.00

Table 3-3. (cont.)

Elizabeth R. Nov. Spring, Bottom

Fe	Mn	Al	Zn	Cu	Cr	Cd
1.00	0.23	0.96	0.47	0.04	0.31	0.05
0.23	1.00	0.27	0.10	-0.07	0.24	0.44
0.96	0.27	1.00	0.53	0.04	0.26	0.19
0.47	0.10	0.53	1.00	-0.46	-0.37	0.51
0.04	-0.07	0.04	-0.46	1.00	0.58	-0.16
0.31	0.24	0.26	-0.37	0.58	1.00	-0.30
0.05	0.44	0.19	0.51	-0.16	-0.30	1.00

at the surface or middepth in the May neap and November spring tides (except for mean Al during May neap), which were stratified, but during the well mixed June spring survey the highest mean and maximum concentrations of these metals occur at the bottom. Contrary to expectations, correlations between all of the specific metal concentrations and log 10 of the median grain size are poor. Correlations among the contaminant metals and between Fe, Mn, and Al are generally poor with the exception of the June spring bottom and middle water column. During this survey Zn and Cu are generally well correlated with Fe, Mn, and Al, as well as with each other. Given that C/N is vertically homogenous, whereas metal concentrations are vertically heterogeneous, there is no apparent relationship between C/N and metal concentrations. The level of PFS also is not related to metal concentrations. PFS is generally higher near the bottom, but not metal concentrations, which tend to peak at middepth. The exception is during the well mixed June spring survey, where the relation of high PFS levels with high metal concentrations near the bed is opposite from what would be expected.

Comparison of these results with the salinity profiles suggests that stratification may be playing a major role in contaminant specific concentrations in the Elizabeth R via its effect on the partition coefficients (K_d) of the contaminants, where $K_d=C_s/C_d$ and C_s is the concentration of the metal in the solid phase and C_d is the metal concentration in the dissolved phase. The water column was well mixed throughout most of the June spring survey, while it was generally stratified during the other two. Figure 3-15a shows pH data collected at depth intervals of a meter and time intervals of one month for the entire year of 1999 in the Elizabeth R. by the Chesapeake Bay Foundation's water quality monitoring program. The pH values range from 6.2 to 7.6 and there appears to be little vertical gradient except in September through November when there was a tendency for lower surface pH. Lu and Allen (2001) found that the K_d for Cu increases sharply at pH 6-7, which is right in the range of values for the Elizabeth R. So minor changes in pH in the Elizabeth R. could have relatively large effects on K_d and consequently on the suspended sediment specific concentrations of Cu. Figure 3-15b shows dissolved oxygen values obtained from the same dataset. There is a clear seasonal signal of hypoxia near bottom. Balls et al. (1994) found Mn and Zn K_d's were positively associated with dissolved oxygen while Cd K_d was negatively associated with dissolved oxygen. Salinity

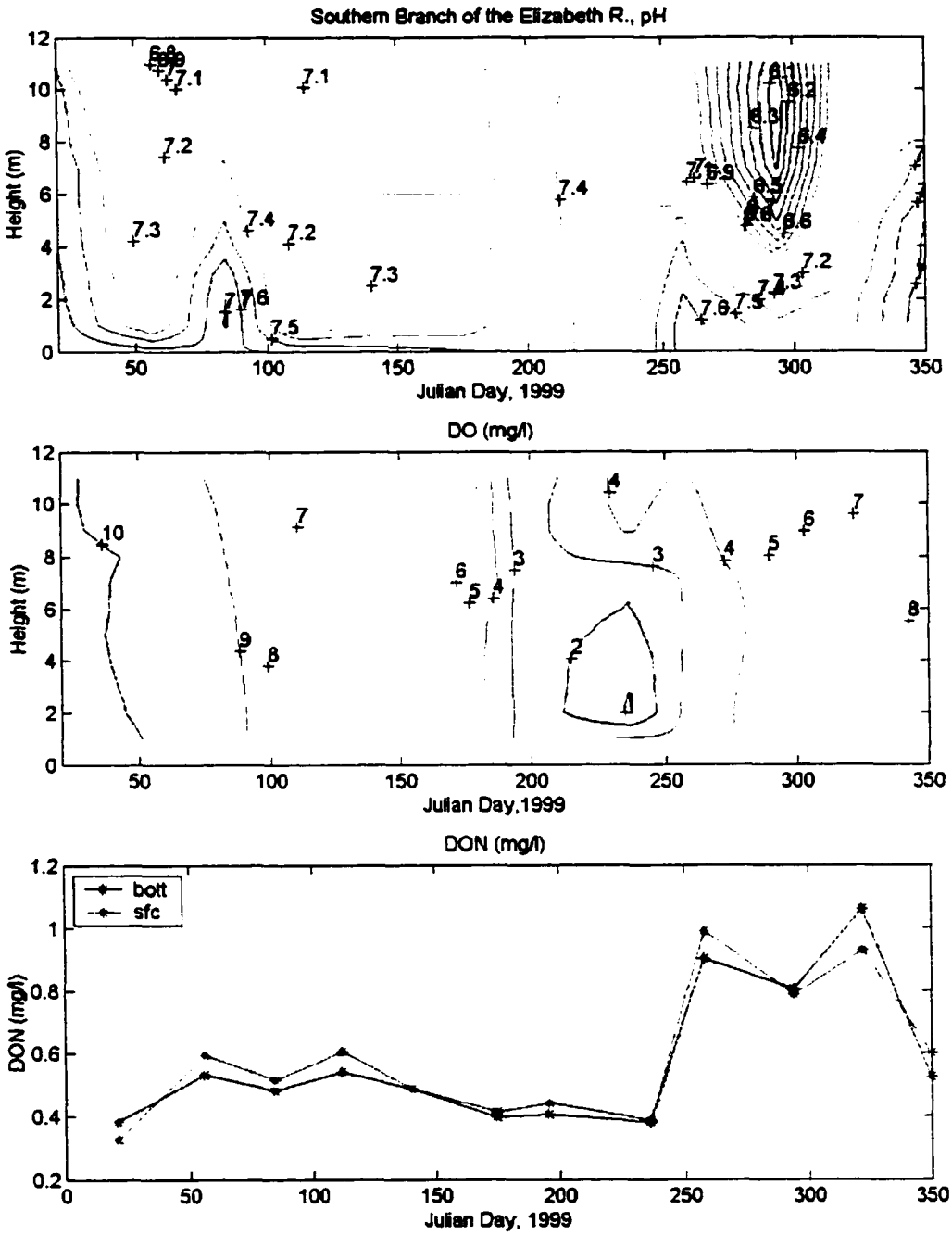

Fig. 3-15. Time series of Southern Branch of the Elizabeth R. data, 1999 from Chesapeake Bay Foundation Water Quality Monitoring Program (a) pH, (b) Dissolved Oxygen (mg/l), (c) Dissolved Organic Nitrogen (DON)

itself affects the K_d of metals. Comber et al. (1995) found Cu K_d to increase with increasing salinity. Ng et al. (1996) found K_d's of Zn and Cd to be positively and negatively correlated with salinity, respectively. Salinity controls K_d of many trace metals through the opposing effects of precipitation with Fe and Mn hydroxides at high salinities and increased desorption of the specific trace metals with higher salinity (Roux et al., 1998).

While suspended particulate trace metal concentrations are conservative in some estuaries (Comber et al., 1995; Roux et al., 1998), this does not appear to be the general case in the Elizabeth River. Peak concentrations in middepth and surface regions probably represent the combined effect of introduction of metals at the surface, and complex changes in the partition coefficients of the respective metals as particles cross the pycnocline into different pH, DO, and salinity environments. High adsorption rates have been measured for Cd, Cu and Zn in river sediments, so rapid adjustments to changes in partition coefficients are expected (Watanabe et al., 1985). During well mixed conditions such as the June spring tide, however, trace metal concentrations are well correlated with Fe, Mn, and Al, reflecting their association with the oxyhydroxide species of those metals. Fe, Mn, and Al concentrations are also higher near the bottom during this survey, where particles are likely to have been in the water column longer and adsorbed more metal than those particles more recently horizontally advected near the surface.

The very low correlations of median grain size and specific metal concentrations may be explained by a combination of factors. Given the very low suspended sediment concentrations in the Elizabeth R., metals going through rapid changes between solid and dissolved phases may not have time to equilibrate with the suspended sediment. In addition, background concentrations as indirectly estimated by the ADV (see chapter 2) near the bed are of the same order of magnitude as the larger rapidly settling and resuspending concentrations. Metal associations with the very fine grained background concentration may dominate specific concentrations of the metals and dilute the size effect within the relatively small portion of larger particles. In addition to the fine grained background concentration, the even smaller colloid fraction may play an important role. Benoit and Rozan (1999) found that a substantial portion of metals occur in the colloidal

fraction in four Connecticut, USA rivers. Other studies have also shown the potential importance of the colloidal fraction to transport of trace metals (Kaplan et al., 1995; Moran and Buesseler, 1993; Myers, 1999) Considering the very low concentrations of suspended solids in the Elizabeth R., much of the trace metal contaminants may be associated with dissolved organics. Sediment-porewater K_d of PAH's may depend on DOC concentrations (Mitra et al., 1999) since contaminants may bond with DOM. Estimates of DOM and DOC are unavailable for the Elizabeth R. during the surveys, but measures of DON are, and may be considered a proxy for the amount of DOM in the water column. Figure 3-15c shows DON data from the Chesapeake Bay Foundation's water quality monitoring program. Note that the concentrations of DON are equal to or higher than the particulate nitrogen concentrations (Table 1). Measurements of dissolved and colloidal metal concentrations are necessary to confirm the hypothesis that this paper has engendered. Namely, most net transport of trace metal concentrations in the Elizabeth R. occurs in the dissolved or colloidal phase and ultimately depends on the hydrodynamics of the system, including stratification and mixing patterns and overall processes of tidal dispersion.

CONCLUSIONS

Standard paradigms of contaminant concentration relationships with particle size and particle constituents were not supported in the low energy, low concentration suspended sediment of the heavily polluted Elizabeth R. estuary. No significant seasonal relationships were found in the PFS values, nor were there any relationships found between PFS and median grain size or metal concentrations. Chlorophyll a values did vary seasonally, but also were not related to grain size or metal concentrations. Chlorophyll a values tended to be higher at the surface and upstream from the study site. C/N was vertically homogenous and varied significantly over timescales longer than the tidal period. C/N was not related to grain size or metal concentrations, or PFS or chlorophyll a values. There is a tendency for higher C/N downstream of the study site, suggesting that the source of the higher organic constituent material downstream is not marine phytoplankton. Metal concentrations were not related to median grain sizes nor to tidally varying hydrodynamics, but showed a strong tendency to be high at surface and middepth during stratified conditions.

Contaminant concentrations are not available in the relatively high energy, high concentration and undisturbed estuary of the York R. In contrast to the Elizabeth R., measures of organic content from PFS levels and C/N were related to aggregate size consistent with standard paradigms. Lower PFS levels and C/N were associated with larger size aggregates.

The major implication of these results to the modeling of contaminant fate and transport in the Elizabeth R. is that the standard paradigms of particle aggregation dynamics and particle size and constituent determined scavenging efficiency are insufficient to describe contaminant behavior in the Elizabeth R. Because of the low suspended sediment concentrations and potentially high DOM concentrations it is speculated that most net transport of trace metals in the Elizabeth R. occurs in the

dissolved or colloidal phase and ultimately depends on the hydrodynamics of the system, including stratification and mixing patterns and overall processes of tidal dispersion.

REFERENCES FOR CHAPTER 3

Alber, M., 2000. Settleable and Non-Settleable Suspended Sediments in the Ogeechee River Estuary, Georgia, U.S.A. Estuarine, Coastal and Shelf Science 50(6): 805-816.

Balls, P.W., Laslett, R.E. and Price, N.B., 1994. Nutrient and trace metal distributions over a complete semi- diurnal tidal cycle in the Forth Estuary, Scotland. Neth. J. Sea Res. 33(1): 1-17.

Benoit, G. and Rozan, T.F., 1999. The influence of size distribution on the particle concentration effect and trace metal partitioning in rivers. Geochimica et Cosmochimica Acta 63(1): 113-127.

Blanton, J., Alexander, C., Alber, M. and Kineke, G., 1999. The mobilization and deposition of mud deposits in a coastal plain estuary. Limnologica 29(3): 293-300.

Brassard, P., Kramer, J.R. and Collins, P.V., 1997. Dissolved metal concentrations and suspended sediment in Hamilton Harbour. J. Great Lakes Res. 23(1): 86- 96.

Comber, S.D.W., Gunn, A.M. and Whalley, C., 1995. Comparison of the partitioning of trace metals in the Humber and Mersey Estuaries. Mar. Pollut. Bull. 30(12): 851-860.

Conrad, C.F., Chisholm-Brause, C.J., Daus, J., Fugate, D.C. and Kuehl, S.A., 2000. Historical trends in trace metal contaminants of the Elizabeth River subestuary, Chesapeake Bay, Virginia, National American Chemical Society Meeting, Washington, D.C.

Cope, W.G., Wiener, J.G. and Steingraeber, M.T., 1996. Test system for exposing fish to resuspended, contaminated sediment. Environ. Pollut. 91(2): 177- 182.

Dauer, D.M. and Llanso, R.J., 2001. Levels of benthic community degradation in the Chesapeake Bay; The use of probability based sampling at various spatial scales, 16th Biennial Conference of the Estuarine Research Federation. Estuarine Research Federation, St. Pete Beach.

Dellapenna, T.M., Kuehl, S.A. and Schaffner, L.C., 1998. Sea-bed mixing and particle residence times in biologically and physically dominated estuarine systems: a Comparison of Lower Chesapeake Bay and the York River Subestuary. Estuarine and Coastal Marine Science, 46: 777-795.

Eisma, D. et al., 1991b. Suspended-matter particle size in some west-European estuaries; Part 2: A review on floc formation and break-up. Neth. J. Sea Res. 28(3): 215-220.

Eisma, D. et al., 1991a. Suspended-matter particle size in some West-European Estuaries; Part I: Particle-size distribution. Netherlands Journal of Sea Research, 28(3): 193-214.

Engel, A., 2000. The role of transparent exopolymer particles (TEP) in the increase in apparent particle stickiness (alpha) during the decline of a diatom bloom. Journal of Plankton Research 22(3): 485-497.

Feng, H., Cochran, J.K., Hirschberg, D.J. and Povinee, P.P., 1999. ^{234}Th and ^{7}Be as tracers for transport and sources of particle-associated contaminants in the Hudson River Estuary. Science of the Total Environment 237-238(1-3): 401-418.

Friedrichs, C.T., Wright, L.D., Hepworth, D.A. and Kim, S.C., 2000. Bottom-boundary-layer processes associated with fine sediment accumulation in coastal seas and bays. Continental Shelf Research 20(7): 807-841.

Gossiaux, D.C., Landrum, P.F. and Fisher, S.W., 1998. The assimilation of contaminants from suspended sediment and algae by the zebra mussel, Dreissena polymorpha. Chemosphere 36(15): 3181- 3197.

Gregg, J.C., Fleeger, J.W. and Carman, K.R., 1997. Effects of suspended, diesel-contaminated sediment on feeding rate in the darter goby, Gobionellus boleosoma (Teleostei: Gobiidae). Mar. Pollut. Bull. 34(4): 269-275.

Hahn, H.H. and Xanthopoulos, C., 1990. Pollutants Attached to Particles from Drainage Areas. The Science of the Total Environment STENDL, Vol. 93, p 441- 448.

Hayes, D.F., Crockett, T.R., Ward, T.J. and Averett, D., 2000. Sediment resuspension during cutterhead dredging operations. Journal of Waterway, Port, Coastal and Ocean Engineering 126(3): 153-161.

Kango, R.A., Dubey, K.P. and Zutshi, D.P., 1987. Environmental geochemistry of iron and manganese in six Himalayan Lakes. Acta Hydrochim. Hydrobiol. 1987, 15(1): 57-64.

Kaplan, D.I., Bertsch, P.M. and Adriano, D.C., 1995. Facilitated transport of contaminant metals through an acidified aquifer. Ground Water 33(5): 708-717.

Ko, F.C. and Baker, J.E., 1995. Partitioning of hydrophobic organic contaminants to resuspended sediments and plankton in the mesohaline Chesapeak Bay. Marine Chemistry, 49: 171-188.

Latimer, J.S., Davis, W.R. and Keith, D.J., 1999. Mobilization of PAHs and PCBs from in-place contaminated marine sediments during simulated resuspension events. Estuarine,Coastal and Shelf Science, 49: 577-595.

Lu, Y. and Allen, H.E., 2001. Partitioning of copper onto suspended particulate matter in river waters. The Science of the Total Environment, 277: 119-132.

Marshall, J.S., Mellinger, D.L. and Parker, J.I., 1981. Combined Effects of Cadmium and Zinc on a Lake Michigan Zooplankton Community. Journal, of Great Lakes Research Vol 7, No 3, p 215-223.

Matson, E.A. and Brinson, M.M., 1990. Stable carbon isotopes and the C : N ratio in the estuaries of the Pamlico and Neuse Rivers, North Carolina. Limnol. Oceanogr. 35(6): 1290- 1300.

Mitra, S., Dellapenna, T.M. and Dickhut, R.M., 1999. Polycyclic Aromatic Hydrocarbon Distribution within Lower Hudson River Estuarine Sediments: Physical Mixing vs Sediment Geochemistry. Estuarine, Coastal and Shelf Science 49(3): 311-326.

Mitra, S., Dickhut, R.M., Kuehl, S.A. and Kimbrough, K., 1998. Polycyclic aromatic hydrocarbon distribution of coefficients in estuarine sediments: The role of sediment geochemistry, submitted to Marine Chemistry.

Moran, S.B. and Buesseler, K.O., 1993. Size-fractionated super(234)Th in continental shelf waters off New England: Implications for the role of colloids in oceanic trace metal scavenging. J. Mar. Res. 51(4): 893-922.

Myers, T.E., 1999. Metals Release from Freshwater and Estuarine Sediments in Thin-Disk Leaching Columns, 2834. pp.

Neal, C., Jarvie, H.P., Whitton, B.A. and Gemmell, J., 2000. The water quality of the River Wear, north-east England. Science of the Total 251-252(1-3): 153-172 # 3 of 123 from Set 40 - ASFA.

Neilson, B.J., 1975. A water quality study of the Elizabeth River: The effects of the army base and Lambert Point STP effluents. VIMS, VIMS.

Nelson, Y.M. et al., 1998. Model for trace metal exposure in filter-feeding flamingos at alkaline Rift Valley Lake, Kenya. Environmental Toxicology and Chemistry 17(11): 2302-2309.

Ng, B., Turner, A., Tyler, A.O., Falconer, R.A. and Millward, G.E., 1996. Modelling contaminant geochemistry in estuaries. Water Res. 30(1): 63-74.

Nichols, M.M. and Howard-Strobel, M.M., 1991. Evolution of an urban estuarine harbor: Norfolk, Virginia. Journal of Coastal Research, 7(3): 745-757.

Nichols, M.M., Kim, S.C. and Brouwer, C.M., 1991. Sediment characterization of the Chesapeake Bay and its tributaries, National Estuarine Inventory: Supplement, NOAA Strategic Assessment Branch, Virginia Province, pp. 88 pp.

Ongley, E.D., Bynoe, M.C. and Percival, J.B., 1981. Physical and Geochemical Characteristics of Suspended Solids, Wilton Creek, Ontario. Canadian, Journal of Earth Sciences Vol 18, No 8, p 1365-1379.

Padmalal, D. and Seralathan, P., 1993. Heavy metal content in suspended particulates and bed sediments of a tropical perennial river and estuary. Central Kerala, India. J. Geol. Soc. India 42(4): 349-355.

Riggs, S.R., 1996. Sediment evolution and habitat function of organic-rich muds within the Albemarle estuarine system, North Carolina. Spagnolo, R.J.;Ambrogio, E.;Rielly, F.J., Jr. (eds.) MARINE AND ESTUARINE SHALLOW WATER SCIENCE AND MANAGEMENT. 1996, pp. 169- 185.

Roux, L.R., le Roux, S. and Appriou, P., 1998. Behaviour and speciation of metallic species Cu, Cd, Mn and Fe during estuarine mixing. Marine Pollution Bulletin, 36(1): 56-64.

Schaffner, L.C. et al., 2001. Physical energy regimes, seabed dynamics, and organism-sediment interactions along an estuarine gradient. In: J.Y. Aller, Woodin, S.A., Aller, R.C. (Editor), Organism-Sediment Interactions. University of South Carolina Press, Columbia, S.C., pp. 159-179.

Schofield, J.S., 1988. Uptake of ^{109}Cd and ^{203}Hg from particulates, dissolved medium, and food by Mysidopsis almyra, a marine hypopelagic mysid. Diss., ABST. INT. PT. B - SCI. & ENG.[S.l.].

Stroemberg, B. and Banwart, S., 1999. Weathering kinetics of waste rock from the Aitik copper mine, Sweden: scale dependent rate factors and pH controls in large column experiments. Journal of Contaminant Hydrology 39(1-2): 59-89.

Titley, J.G., Glegg, G.A., Glasson, D.R. and Millward, G.E., 1987. Surface areas and porosities of particulate matter in turbid estuaries. Continental Shelf Research, 7(11/12): 1363-1366.

Warren, L.A. and Zimmermann, A.P., 1994. Suspended particulate grain size dynamics and their implications for trace metal sorption in the Don River. Aquat. Sci. 1015-1621 1994, 56(4): 348-362.

Watanabe, N., Sato, E. and Ose, Y., 1985. Adsorption and desorption of polydimethylsiloxane, PCBs, cadmium nitrate, copper sulfate, nickel sulfate and

zinc nitrate by rifer surface sediments. The Science of the Total Environment, 41: 153-161.

Williamson, R.B., Van Dam, L.F., Bell, R.G., Green, M.O. and Kim, J.P., 1996. Heavy metal and suspended sediment fluxes from a contaminated, intertidal inlet (Manukau Harbour, New Zealand). Mar. Pollut. Bull. 32(11): 812-822.

Wiltshire, K.H., Geisssler, C.D., Schroeder, E. and Knauth, H.D., 1996. Pigments in suspended matter from the Elbe estuary and the German Bight: Their use as marker compounds for the characterisation of suspended matter and in the interpretation of heavy metal loadings. Kausch, H.;Michaelis, W. (eds.) SUSPENDED PARTICULATE MATTER IN RIVERS AND ESTUARIES. PROCEEDING OF AN INTERNATIONAL SYMPOSIUM. 3510470486 STUTTGART (FRG), SCHWEIZERBART'SCHE VERLAGSBUCHHANDLUNG, 1996 pp. 53-63.

GENERAL SUMMARY AND CONCLUSIONS

This body of work has extensively investigated aggregation dynamics and particle properties in three partially mixed estuaries of the mid-Atlantic bight. In addition, useful methods were developed to measure fall velocity and particle size distributions of estuarine aggregates and turbulent kinetic energy production. Aggregation processes and particle adherent contaminant concentrations patterns were found to be more complex than implied by standard paradigms of aggregation and relations of size to concentration.

The first chapter established the response of various in situ instruments to changes in mass concentration and particle size distributions. The Acoustic Doppler Velocimeter (ADV) was found to be a particularly versatile instrument for measuring suspended sediment properties. The ADV was relatively insensitive to the particle size distribution and so was good at predicting mass concentrations. The high sampling frequency of the ADV allowed indirect estimation of particle fall velocities. The Laser In Situ Scatterer and Transmissometer proved reasonably effective at measuring relative size distributions, despite the problems of measuring organic estuarine aggregates associated with laser diffraction technology. The codeployment of multiple in situ instruments allowed the identification of multiple subpopulations of suspended sediment. Besides the well documented presence of a very slowly settling background subpopulation, two rapidly settling subpopulations were identified, with differing critical shear velocities and settling velocities.

The second chapter investigated the processes and factors that determine particle size distributions in partially mixed estuaries. The physical processes of differential settling, turbulent kinetic energy production, and concentration that are typically invoked to explain particle size distributions proved to vary in importance depending upon the physical and biologic environment as well as the height above the bottom. . For low

energy low concentration estuaries such as the Elizabeth R., stochastic events such as advection, boat wake or other forcings dominate the physical processes conventionally held to be important, although concentration does seem to exert some influence on minimum particle size. Despite the dominance of random events on particle dynamics, vertical profiles tended to be consistent, with the largest particles found in the middle of the water column, the smallest at the surface, and intermediate sizes near the bed. One result important to characterizing particle dynamics in estuaries is that important advective events occur at time scales longer than the tidal period, and surveys intended to measure mean particle parameters such as size or concentration should endure as long as possible. Even in more typical estuaries such as the York R., particle sizes in low concentration surface regions that were expected to respond to changes in concentration were instead dominated by stochastic events. Aggregation dynamics in the middepth region of the York R., a relatively high energy and high concentration estuary, were determined by the combined processes of turbulent shear and differential settling. Particle size distributions near the bed were different in each of the three principle study sites, reflecting their hydrodynamic and benthic environments. Near bed particles in the low energy Elizabeth R. were large porous aggregates, those in the energetic physically dominated York R. were smaller and more dense, while those at the energetic, biologically influenced Cherrystone site were large and denser than the large particles in the Elizabeth R. Depending on the relative energy and biological activity, relations between tidally varying TKE production and tidally varying particle size, concentration and fall velocity also differed systematically among the three sites.

In addition to the methods developed in the first chapter, an alternate measure of turbulent kinetic energy production was developed in the second chapter that can be applied to high frequency velocity ADV data that has inadvertent signals imposed by boat motion or waves or both.

The results from the study on particle constituents in the third chapter showed that standard paradigms of contaminant concentration relationships with particle size and particle constituents were not supported in the low energy, low concentration suspended sediment of the heavily polluted Elizabeth R. estuary. No significant seasonal relationships were found in the PFS values, nor were there any relationships found

between PFS and median grain size or metal concentrations. Chlorophyll a values did vary seasonally, but also were not related to grain size or metal concentrations. Chlorophyll a values tended to be higher at the surface and upstream from the study site. C/N was vertically homogenous and varied significantly over timescales longer than the tidal period. C/N was not related to grain size or metal concentrations, or PFS or chlorophyll a values. There is a tendency for higher C/N downstream of the study site, suggesting that the source of the higher organic constituent material downstream is not marine phytoplankton. Metal concentrations were not related to median grain sizes, nor to tidally varying hydrodynamics, but showed a strong tendency to be high at surface and middepth during stratified conditions.

In contrast to the Elizabeth R., measures of organic content from PFS levels and C/N were related to aggregate size consistent with standard paradigms. Lower PFS levels and C/N were associated with larger size aggregates.

The major implication of these results to the modeling of contaminant fate and transport in the Elizabeth R. is that the standard paradigms of particle aggregation dynamics and particle size and constituent determined scavenging efficiency are insufficient to describe contaminant behavior in the Elizabeth R. Because of the low suspended sediment concentrations and potentially high DOM concentrations it is speculated that most net transport of trace metals in the Elizabeth R. during calm conditions occurs in the dissolved or colloidal phase and ultimately depends on the hydrodynamics of the system, including stratification and mixing patterns and overall processes of tidal dispersion. Because this study has strongly suggested that contaminant solid and dissolved phase are often not at equilibrium, future studies of contaminant research in this and other systems would greatly benefit from measurements of the dissolved phases of the contaminants in order to make better management decisions. The Elizabeth R. has been a low concentration estuary only in the last decade or so, probably due to more recent deeper channels reducing flow velocity. Significant sediment and associated contaminant transport may occur episodically. Future studies should attempt to address this issue by monitoring suspended and dissolved contaminants during storm events, a difficult undertaking.

VITA

David C. Fugate

Born in Chapel Hill, NC on December 18, 1960. Graduated from South Mecklenburg High School, Charlotte, NC in 1978. Obtained B.S. in Biostatistics from University of North Carolina, Chapel Hill in 1983. Worked in population research from 1983 to 1982. Received Masters degree in 1996 in Marine Biology from Virginia Institute of Marine Science. Received Ph.D. in Physical Sciences from Virginia Institute of Marine Science in 2002.